STUDY OF LINEARIZED FLOW PATTERNS
FOR STRATIFIED AND UNSTRATIFIED
RESERVOIRS.

BY

ROBERT BURNS WILSON

STUDY OF LINE DRIVE FLOOD PATTERNS FOR STRATIFIED AND UNSTRATIFIED RESERVOIRS

STUDY OF LINE DRIVE FLOOD PATTERNS FOR STRATIFIED AND UNSTRATIFIED RESERVOIRS

by

ROBERT BURNS WILSON, B.S. M.E.

THESIS

Presented to the Faculty of the Graduate School of

The University of Texas in Partial Fulfillment

of the Requirements

For the Degree of

MASTER OF SCIENCE

In

PETROLEUM ENGINEERING

THE UNIVERSITY OF TEXAS

August, 1964

ABSTRACT

The effect of mobility ratio on areal sweep efficiency and conductance ratio has been made for direct and staggered line drive well patterns. This study was made using miscible fluids, artificially consolidated sandstone models, and a photographic method of data recording. The mobility ratio was varied between 0.1 and 12, which is the range common to water flood operations.

A method of predicting the performance of waterfloods in stratified reservoirs using conductance ratios is treated. This technique is not limited in number of strata and indicates one method of considering a free gas saturation.

ACKNOWLEDGMENTS

The author wishes to acknowledge the assistance and guidance received from others while in the process of acquiring a Petroleum Engineering education at The University of Texas. First appreciation is due Dr. Ben H. Caudle, Dr. Kenneth E. Gray, Dr. Frank Jessen, and Dr. Sylvain J. Pirson for a thorough and comprehensive introduction to Petroleum Engineering in a limited period of time.

Appreciation is due the United States Navy for providing the opportunity and financial support for the postgraduate education of the author.

Many thanks are due my supervising professor, Dr. Ben H. Caudle, for his patient direction and guidance throughout this project. The author is also grateful to Dr. Kermit Brown and Dr. Kenneth E. Gray for their timely assistance as members of the supervising committee.

And finally in token appreciation for all hardships endured, this thesis is dedicated to Pat, Ellen, Eric, and Wendy.

Robert B. Wilson
LT, CEC, USN

Austin, Texas
August, 1964

TABLE OF CONTENTS

TABLE OF CONTENTS (continued)

LIST OF FIGURES

LIST OF FIGURES (continued)

LIST OF TABLES

INTRODUCTION

The importance of secondary recovery techniques in petroleum engineering is continually increasing and is taking an increasing percentage of reservoir research activity. Since primary reservoir depletion normally will leave approximately 75 per cent of the original oil in place, the reason for this increasing role of secondary recovery is obvious.

Perhaps the oldest and most used method of recovering oil by secondary techniques is the waterflood. This involves injection of water into the reservoir to displace the oil. Water injection requires expenditure of energy and funds, therefore, reliable methods for predicting waterflood results are necessary.

Extensive study has gone into conformance factor or sweep efficiency predictions for various well patterns at varying mobility ratios. This permits predictions for single stratum reservoirs.

Most reservoirs are composed of several strata, however, and performance predictions for stratified reservoirs are not feasible with only sweep efficiency data available. In predictions for stratified systems, it is necessary to place performance on a time basis. This requires that flow potential or flow rate for a pressure drop be available for the system under investigation.

Flow potential data (conductance ratios) are available for all regular patterns[7,20,34] with the exception of the line drive. The purpose of this study was to obtain line drive conductance ratios and to test methods for approximating conductance ratios analytically. A method of predicting performance of a stratified system using these data is also presented.

WATER FLOOD PREDICTIONS

In studies of petroleum reservoirs, much qualitative and quantitative use has been made of models to more completely understand the phenomenon of oil production. Since no two reservoirs are exactly the same, model studies are limited in scope. Therefore, in a rigorous interpretation, models can only be used for studies of a particular field; however, by generalizing parameters, study of a reservoir segment will yield data for qualitative application in a number of situations.

A great deal of work has gone into the determination of scaling criteria for model studies.[3,4,10,17,23,29,31] Probably the most complete analysis covering general situations has been presented by Geertsma, Croes, and Schwarz.[17] A strict interpretation of this analysis, however, leads one to the conclusion that the model must be identical to the prototype in every respect. Since this is completely impractical, it is necessary to decide which reservoir factors are of greatest importance and construct the model accordingly. A detailed description and application of model scaling for edgewater drive reservoirs has been presented by Caudle.[4]

The efficiency of a secondary recovery project, in which a fluid (usually water) is injected to displace the oil in the reservoir, can be defined by the volumetric sweep efficiency. In reservoir studies, models are normally two dimensional representations and the displacement efficiency may be defined in terms of areal sweep efficiency. This

is the ratio of the area swept by the injected fluid to the total model area.

Generally, the areal sweep efficiency is determined by the well pattern geometry and the mobility ratio. This assumes that the reservoir is homogeneous and that gravitational forces are not present. The mobility ratio is defined as the ratio of the sum of the mobilities of the fluids behind the front to the sum of the mobilities of the fluids ahead of the front. The mobility (λ) of a fluid in a porous media is expressed as the effective rock permeability (k) to the fluid of interest at its saturation divided by the fluid viscosity (μ).

$$M = \frac{(k/\mu) \text{ swept}}{(k/\mu) \text{ unswept}} = \frac{\lambda_s}{\lambda_u} = \text{Mobility Ratio} \qquad (1)$$

Early model studies utilized the electrolytic model to represent waterfloods. This model uses the principle of ionic flow to simulate fluid flow. Use of this model is limited to mobility ratios of one. Muskat, Wyckoff, and Botset[27] were among the first to utilize this method to determine breakthrough sweep efficiencies for various well patterns. In a later publication, Muskat and Wyckoff[26] analyzed the previous electrolytic model results[27] and concluded that the shape of the flood front and the breakthrough areal sweep efficiency were dependent on the geometry of the system and not on pressure differential, well spacing, or rock properties. It is noted that Muskat[24, 25, 26] indicates

that the results obtained in the electrolytic models do not consider the effects of two fluids with different viscosities. In other words, the electrolytic model is valid for a mobility ratio of one only.

The electrolytic model and the similar but more sophisticated potentiometric model have since been used in the study of various reservoir conditions. Limited use has also been made of heat flow models to simulate fluid flow with a mobility ratio of one.[22]

Sweep Efficiency

Early studies on the effect of mobility ratio on areal sweep efficiency utilized potentiometric models. Aronofsky[1] reported results of a potentiometric model study of mobility ratio effects. A stepwise procedure was utilized to vary the ratio of the depth of the electrolyte behind the front to that ahead of the front. This variation in depth made the electrical conductivity ahead of the front different from that behind the front, thereby simulating fluids of different mobilities flowing in a porous media. After computing a new frontal position, the electrolyte depth was changed to fit the new frontal position and the process was repeated. In this iterative manner, sweep efficiencies for mobility ratios other than one were approximated by advancing the front in a series of steady-state steps.

The effect of mobility ratio on areal sweep efficiency has also been studied with an electric analog model by Nobles and Janzen.[28]

This study utilized a resistance network and an iterative process similar to Aronofsky's[1] to simulate frontal movement.

Cheek and Menzie[8] studied the effects of mobility ratio on areal sweep through the use of a fluid mapper. This model uses fluid flow between two closely spaced parallel plates to simulate fluid flow in a porous media. Results are reported for five spot and direct line drive well patterns.

Slobod and Caudle[32] introduced the X-ray shadowgraph technique to study fluid flow phenomenon. This new technique used a porous plate and fluid flow with one of the fluids containing an X-ray absorbing material so that a contrast between displaced and displacing fluid could be observed on X-ray shadowgraphs taken during the experiment. By taking successive X-ray exposures, a complete history of the flood was obtained.

Dyes, Caudle, and Erickson[13] used the X-ray shadowgraph method to illustrate that a significant amount of production could take place after initial breakthrough. The results of this study demonstrated that, with most water floods, an ultimate areal sweep efficiency of 85-100 per cent could be obtained for various mobility ratios at an economic water-oil ratio. The only previous reports which indicated consideration of production after breakthrough were made by Hurst[21] for a mobility ratio of one and Fay and Prats[15] for a mobility ratio of 4.0 using numerical techniques.

The X-ray shadowgraph has been used extensively to study a variety of reservoir conditions at varying mobility ratios.[5,6,7,11,13,14,16] Included among these studies are five-spot pattern floods, stratified five-spot floods, and the effect of fractures on flood performance.

Habermann[18] utilized a method similar to the X-ray shadowgraph for studying fluid flow. This method consisted of artificially consolidated sand models covered with clear plastic. One of the fluids, either displaced or displacing, contained a dye which permitted visual observation of the front as it progressed. Photographs taken during the flood permitted calculation of areal sweep efficiency.

Conductance Ratio

The use of areal sweep efficiency data permits ultimate recovery predictions for single stratum reservoirs. In order to predict performance of stratified reservoirs and also to predict recovery of single stratum reservoirs on a time basis, it is necessary to know the change in the flow potential or flow rate per unit pressure drop for the system under study.

Prediction of flow potential was first discussed by Muskat[24] in terms of conductivity (production rate per well per unit-pressure differential). This permitted predictions for systems with mobility ratios of one.

Aronofsky and Ramey[2] first introduced the concept of conductance

ratio in a potentiometric study of mobility ratio effects on a five-spot water flood. The conductance ratio (γ) is defined as the flow rate (q) per unit pressure drop (ΔP) between the injection and production wells at a specified time to that conductivity with only the original fluid present.

$$\gamma = \frac{(q/\Delta P) \text{ time } t}{(q/\Delta P) \text{ initial}} = \text{Conductance Ratio} \qquad (2)$$

Analytical methods of studying the change in flow potential has been presented in terms of dimensionless injectivity by various methods. Prats, Matthews, Jewett, and Baker[30] have computed injectivity for five-spot systems by considering that the reservoir consists of several layers, each having a uniform but different permeability. Hauber[19] presented another approximate method which considers that flow utilizes the stream tubes and iso-potential lines obtained by the solution of differential equations for a mobility ratio of one.

Deppe[12] presented a method to approximate conductivity for varying mobility ratios and for varying well patterns. In the five-spot pattern used as an example, Deppe[12] essentially divided the pattern into two regions of radial flow. The first region was around the injection well and covered almost one-half of the area. The second radial flow region was the same except that it was around the production well.

The results of Deppe's[12] study provided injectivity (conductance ratio) curves which were not too unreasonable for five-spot and nine-spot well patterns. Closer agreement was obtained for unfavorable mobility ratios, which is normally true when using this type of approximation methods.

In an attempt to improve on the work of Deppe, this study has divided the pattern into 3 regions as illustrated by Figure 1 for a staggered line drive pattern. The first region surrounds the injection well where the largest pressure drop is encountered. This region is considered to have radial flow and has a radius equal to one-fourth the well row spacing. The second region is considered to be linear, with only slight pressure change, and extends to the areal sweep at breakthrough. The third region is one of radial flow around the production well where the pressure drop is considered to be a function of fractional flow from the swept region.

Conductance ratio for the system is computed by considering a constant flow rate which reduces the equation to

$$\gamma = \frac{\Delta P_i}{\Delta P_t} \tag{3}$$

Pressure drop across the system is obtained by summing the pressure drops in the three regions at the time of interest.

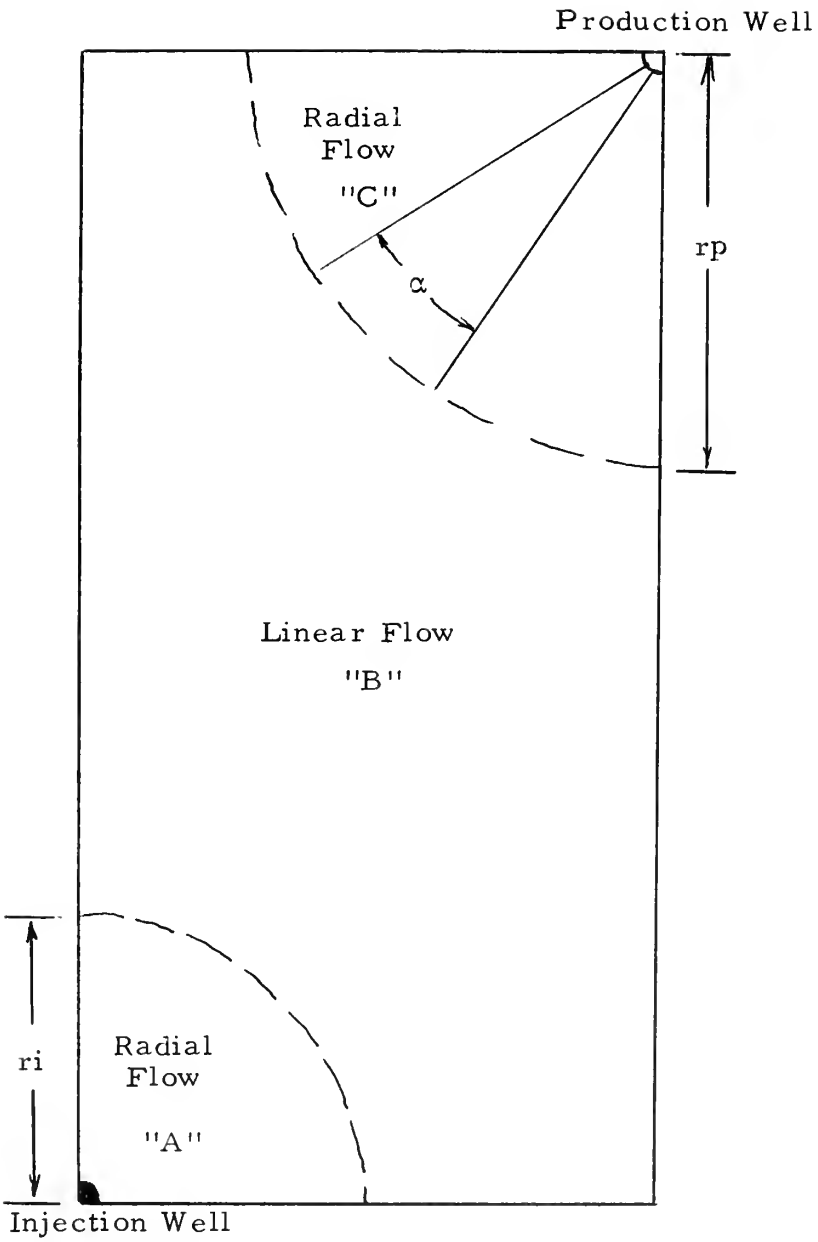

ri	Radius of radial flow area surrounding injection well
rp	Radius of radial flow area surrounding producing well
α	Angle open to flow from swept region after breakthrough

FIGURE 1. STAGGERED LINE DRIVE -- ASSUMED FLOW REGIONS

With only single fluid flow in the system (or at initial conditions) the pressure drop in each region can be represented by modifications of Darcy's Law as

$$\Delta P_{Ai} = \frac{q \ln ri/rw}{\lambda_u 7.08h} \tag{4}$$

$$\Delta P_{Bi} = \frac{q\, L/w}{\lambda_u 1.127h} \tag{5}$$

$$\Delta P_{Ci} = \frac{q \ln rp/rw}{\lambda_u 7.08h} \tag{6}$$

which when added, gives an initial pressure drop for the system of

$$\Delta P_i = \frac{q}{\lambda_u 7.08h} \left(\ln ri/rw + 6.28\, L/w + \ln rp/rw\right) \tag{7}$$

After the flood has started and two fluids are flowing in the model, the pressure drop can be represented as a summation of the pressure drop in each fluid region. When the front is in the first region the pressure drop therein can be represented as

$$\Delta P_{At} = \frac{q \ln rf/rw}{\lambda_s 7.08h} + \frac{q \ln ri/rf}{\lambda_u 7.08h} \tag{8}$$

$$= \frac{q\,(1/M) \ln rf/rw + \ln ri/rf}{\lambda_u 7.08h}$$

When the front is in the second region the pressure drop therein is

$$\Delta P_{Bt} = \frac{q\ell}{\lambda_s 1.127hw} + \frac{q(L-\ell)}{\lambda_u 1.127hw}$$

$$= q\frac{\left[\frac{1}{M} - 1\right]\ell/w + L/w}{\lambda_u 1.127h} \qquad (9)$$

After breakthrough, the flow rate in the third region must be summed for parallel flow since two fluids are flowing into the producing well. Consider that portion of the well illustrated in Figure 1 or one-quarter of the well. Let α equal the angle open to flow from the swept region and $(\pi/2-\alpha)$ equal the angle open to flow from the unswept region. Then the fractional flow from the swept region is[30]

$$fs = \frac{\lambda_s \alpha}{\lambda_s \alpha + \lambda_u(\pi/2-\alpha)} \qquad (10)$$

then

$$\alpha = \frac{fs\ \pi/2}{M-fs(M-1)} \qquad (11)$$

The pressure drop in the swept and unswept region is

$$\Delta P_{Cs} = \frac{fs\ q\ \ln\ rp/rw\ \pi/2}{7.08h\ \lambda_s\ \alpha} \tag{12}$$

$$\Delta P_{Cu} = \frac{(1-fs)\ q\ \ln\ rp/rw\ \pi/2}{7.08h\ \lambda_u\ (\pi/2-\alpha)} \tag{13}$$

For parallel flow, the pressure drop given by equation (12) must equal that of equation (13). Therefore, the pressure drop in the third region may be obtained from either the equation for the swept or the unswept portion. By substituting equation (11) into (13) we obtain

$$\Delta P_{Ct} = \frac{(1-fs)\ q\ \ln\ rp/rw}{7.08h\ \lambda_u\ \left[1-fs/[M-fs(M-1)]\right]} \tag{14}$$

In summing equations (8), (9), and (14) the following conditions apply:

1. When $Es<Es_A$: $\ell/w = 0$, $fs = 0$, and $rf = f(Es)$.
2. When $Es_A<Es<Es_{BT}$: $rf = ri$, $fs = 0$, and $\ell/w = f(Es)$.
3. When $Es>Es_{BT}$: $rf = ri$, $\ell/w = L/w$, and $fs = f(Es)$.

The total pressure drop at any time is then

$$\Delta P_t = \frac{q}{\lambda_u 7.08h} \Big\langle (1/M) \ln rf/rw + \ln ri/rf + 6.28 \left[\frac{1}{M} - 1\right] \ell/w + 6.28\ L/w + \frac{(1-fs) \ln rp/rw}{1-fs/[M-fs(M-1)]} \Big\rangle \tag{15}$$

The conductance ratio from equation (3) becomes the ratio of equation (7) to equation (15) or

$$\gamma = \Delta P_i/\Delta P_t = (\ln ri/rw + 6.28\ L/w + \ln rp/rw)/ \Big\langle (1/M) \ln rf/rw + \ln ri/rf + 6.28 \left[\frac{1}{M} - 1\right] \ell/w + 6.28\ L/w + \frac{(1-fs) \ln rp/rw}{1-fs/[M-fs(M-1)]} \Big\rangle \tag{16}$$

Values for L/w were obtained by using both arbitrary values and by assuming that the pressure drop across a linear system is equal to that across a line drive with well radius equal to ri. Muskat's equation for flow rate in a line drive is:

$$\Delta P = \frac{q\mu}{kh} \frac{d/a - 1.17 + 0.637 \log a/ri}{2.254} \tag{17}$$

Setting equation (17) equal to (5) and solving for L/w yields

$$L/w = \frac{d/a - 1.17 + 0.637 \log a/ri}{2.0} \qquad (18)$$

which is valid when $d/a \geq 1$. Calculations were performed by programming the above for the Controlled Data Corporation 1604 digital computer. Appendix D contains the flow diagram and FORTRAN language program utilized in these computations. A conversion table for the FORTRAN symbols is also provided in Appendix D.

In the calculations for conductance ratios, various values of L/w were assumed in an attempt to match the model study results. Using equation (18), L/w was 0.357. Other values used for L/w were 0 and 0.1. As can be seen from the plots of Appendix D, varying L/w made only small changes in the conductance ratio. Comparison plots for L/w of 0.1 and as obtained from the model studies, indicate results similar to those obtained by Deppe.[12] Agreement is fair for unfavorable mobility ratios and not too good for favorable mobility ratios.

This method can be used for rough approximation of conductance ratios for varying well patterns by modifying the initial values in the program to correspond to those of the pattern under study. However, it is believed that fluid flow model study results would be more reliable.

The effect of mobility ratio on conductance ratio has been studied for various well patterns using fluid flow models. Caudle and

Witte[7] have published data for the five-spot, the inverted skewed seven-spot has been studied by Hickman,[20] and the inverted nine-spot was studied by Watson.[34] This study provides data for line drive well patterns.

Stratified Reservoirs

In a reservoir composed of strata of varying permeabilities and porosities, performance prediction becomes more complex than for a single stratum. To illustrate, consider a two strata system of equal characteristics with fluids of equal viscosity and with the permeability in the first stratum twice that of the second. From Darcy's Law

$$v = -\frac{k}{\mu}\frac{\Delta P}{\Delta \ell} \tag{19}$$

it can readily be seen that the first stratum will have a frontal advance twice that of the second strata and that at breakthrough for the first stratum the second stratum will have a volumetric sweep of only half of the breakthrough sweep efficiency. In this simple example, a miscible system was assumed in order that mobility ratios of one could be used for each strata. For mobility ratios other than one, the linear relationship of flow velocity to permeability no longer exists in a stratified system and then becomes a function of distance traveled or area swept.

In order to apply the data obtained in this study to a stratified reservoir, it is necessary to put the performance of each strata on an equal time basis. This is most easily done through the use of the conductance ratios obtained in this and other studies. It is noted that this method is developed and accurate for separated strata or for strata without cross flow. When cross flow between strata exists and the mobility ratio is greater than one, this method provides a good approximation for predicting water flood results. A similar method using theoretical dimensionless injectivities has been presented by Pratts, et al.[30] The method developed herein permits performance prediction as accurately but more simply than the method described by Prats, et al.[30]

To develop this time relationshlp, consider Darcy's Law (19) and let

$$v = q/A$$

and

$$A = Vd/\ell$$

Darcy's Law can then be written in terms of conductance as

$$q/\Delta P = -\frac{k}{\mu}\frac{Vd}{\ell}\frac{1}{\Delta \ell} = \text{conductance} \qquad (20)$$

Consider now two adjacent parallel strata in a reservoir with single fluid flowing; the variables between these two strata are permeability (k)

and displaceable volume (Vd).

Therefore the conductance between a stratum 1 and any stratum j will vary as their permeability and displaceable volume ratios vary or

$$\frac{q_j}{\Delta P_j} = \frac{k_j Vd_j}{k_1 Vd_1} \frac{q_1}{\Delta P_1} \tag{21}$$

By definition,

$$\gamma = (q/\Delta P)_t \; / \; (q/\Delta P)_i \tag{22}$$

then

$$\left[q_j/\Delta P_j\right]_t = \gamma_j \frac{k_j Vd_j}{k_1 Vd_1} \left[\frac{q_1}{\Delta P_1}\right]_i \tag{23}$$

and

$$q_j = \frac{dWi}{dt} = \Delta P_j \, \gamma_j \frac{k_j Vd_j}{k_1 Vd_1} \left[\frac{q_1}{\Delta P_1}\right]_i \tag{24}$$

solving for dt, integrating, and letting c equal $\Delta P_j \left[\frac{q_1}{\Delta P_1}\right]_i$

$$ct = \frac{k_1 Vd_1}{k_j Vd_j} \int 1/\gamma_j \; dWi \tag{25}$$

Other equations needed to express stratified reservoir performance are for total flow from the swept region (fs) and total conductance ratio (γ).

By definition,

$$f_s = qs/q = \Sigma\, qs_j \;/\; \Sigma\, q_j \tag{26}$$

then

$$qs_j = fs_j\; q_j \tag{27}$$

and

$$q_j = \gamma_j\; [q_j]_i\; \frac{\Delta P_j}{[\Delta P_j]_i} \tag{28}$$

from (7)

$$[q_j]_i = \frac{k_j Vd_j}{k_1 Vd_1}\; [q_1]_i \tag{29}$$

then by substituting into (26) we have

$$fs = \frac{\Sigma\, \gamma_j\, fs_j\, k_j\, Vd_j}{\Sigma\, \gamma_j\, k_j\, Vd_j} \tag{30}$$

The expression for overall conductance ratio can be derived in this same manner as

$$\gamma = \frac{\Sigma\, \gamma_j\, k_j\, Vd_j}{\Sigma\, k_j\, Vd_j} \tag{31}$$

An example performance prediction for a stratified reservoir using this method is described in Appendix E. A possible method of considering an initial free gas saturation is also mentioned in Appendix E.

EXPERIMENTAL APPARATUS

Model Theory

The majority of oil reservoirs are drilled with a regular pattern of wells. Probably the most common pattern utilized in this country is a square array of wells on a 40 acre spacing. This well pattern, illustrated by Figure 2, readily lends itself to secondary recovery operations normally referred to as the Direct Line Drive, which is obtained by converting alternate rows of wells to injection wells.

The Staggered Line Drive is also obtained by converting alternate rows of wells to injection wells; however, the wells are not drilled in a square array but rather in an offset fashion. The well pattern for the Staggered Line Drive system is shown by Figure 3.

With the regular well systems shown by Figures 2 and 3, it can readily be seen that there will exist numerous mirrow images divided by lines of symmetry. These lines or planes of symmetry represent invarient streamlines or boundaries across which no flow will occur, as long as production and injection quantities are uniform.[9] Since the planes of symmetry are in effect flow boundaries in a homogeneous system, it is apparent that only the smallest segment bounded by symmetry planes need be considered. Figures 4 and 5 show enlarged views of the model and its relationship to the line drive systems studied. As can be seen, the model utilized represents a line drive pattern wherein the row spacing equals the well spacing.

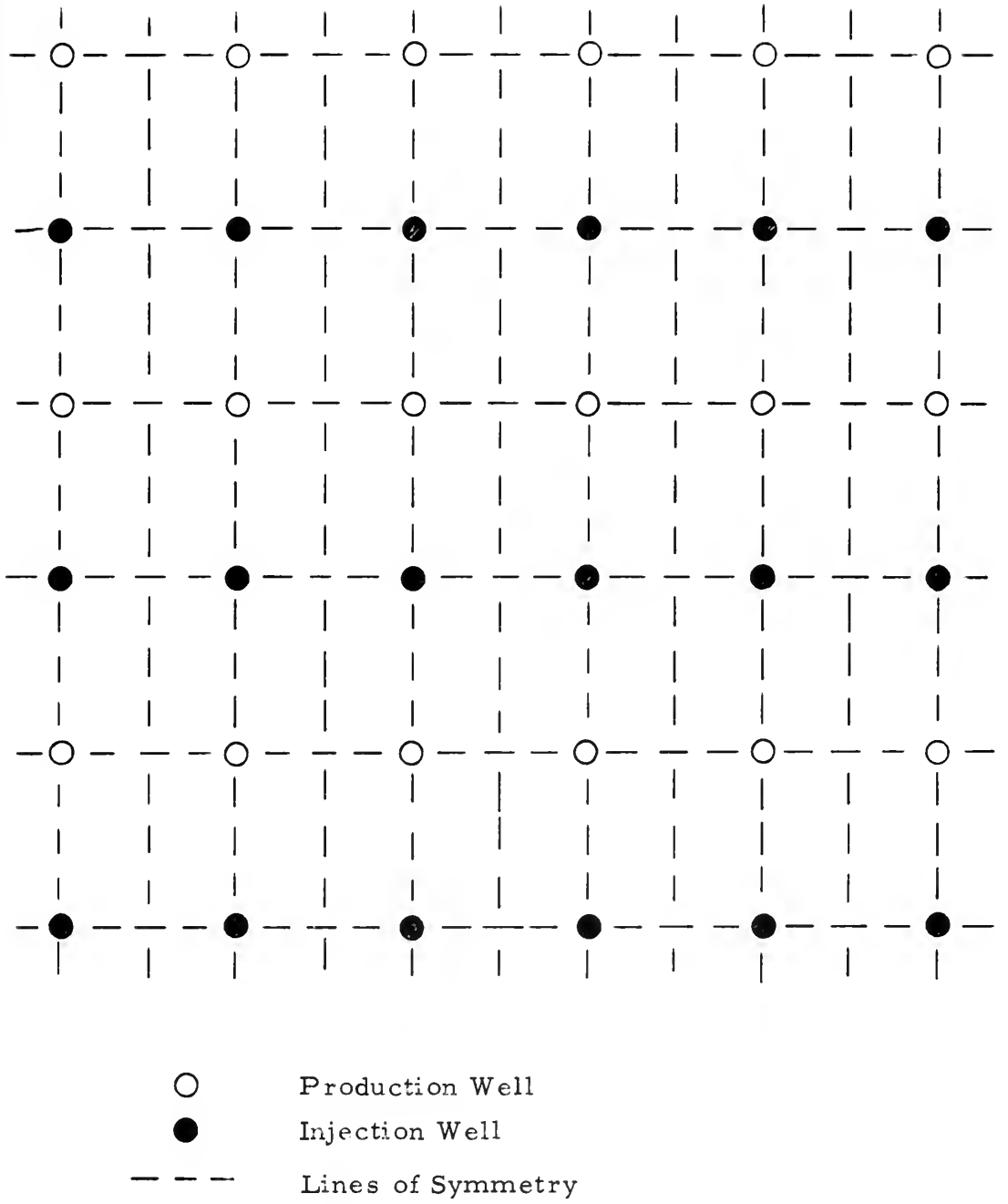

FIGURE 2. DIRECT LINE DRIVE WELL ARRAY

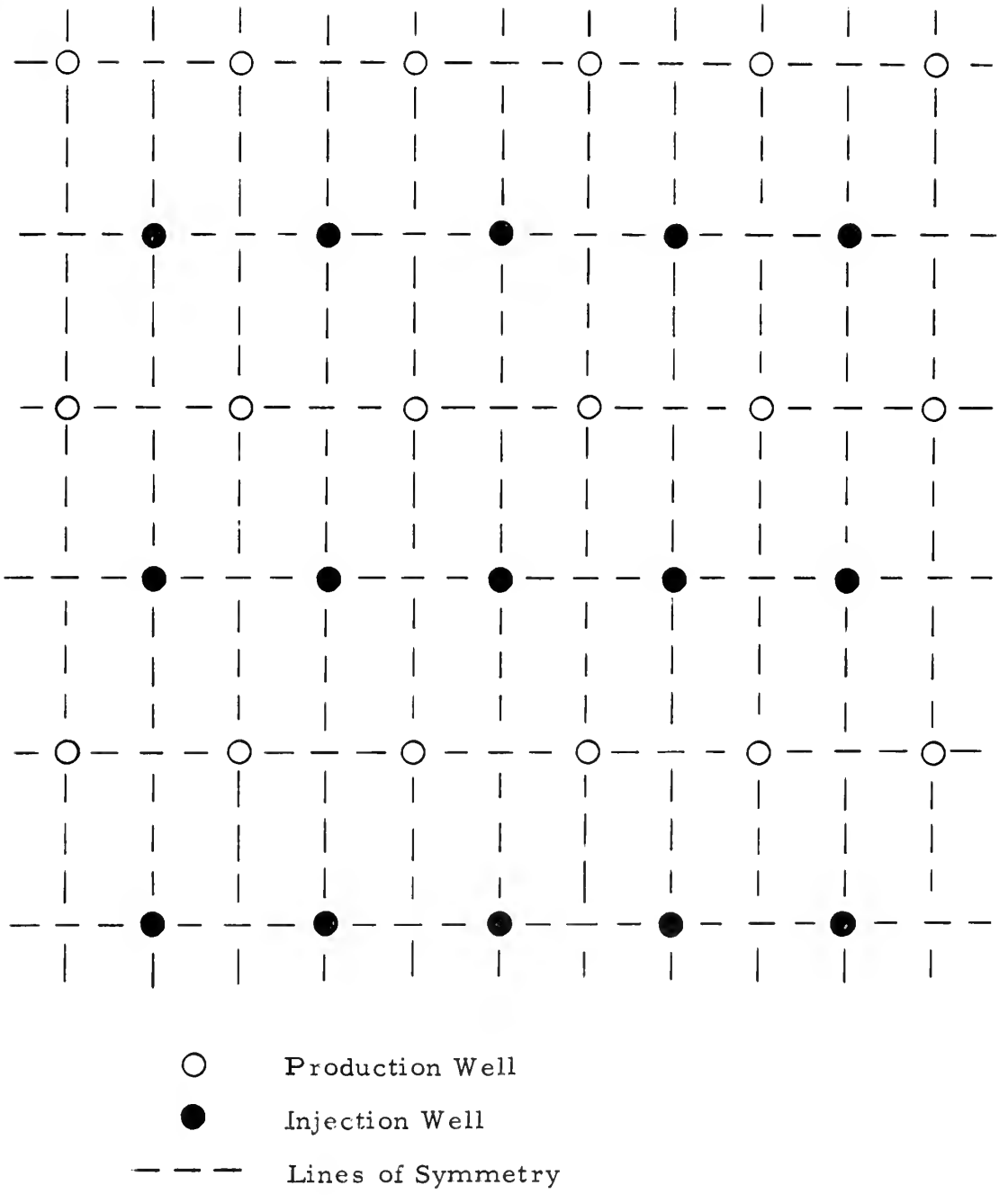

FIGURE 3. STAGGERED LINE DRIVE WELL ARRAY

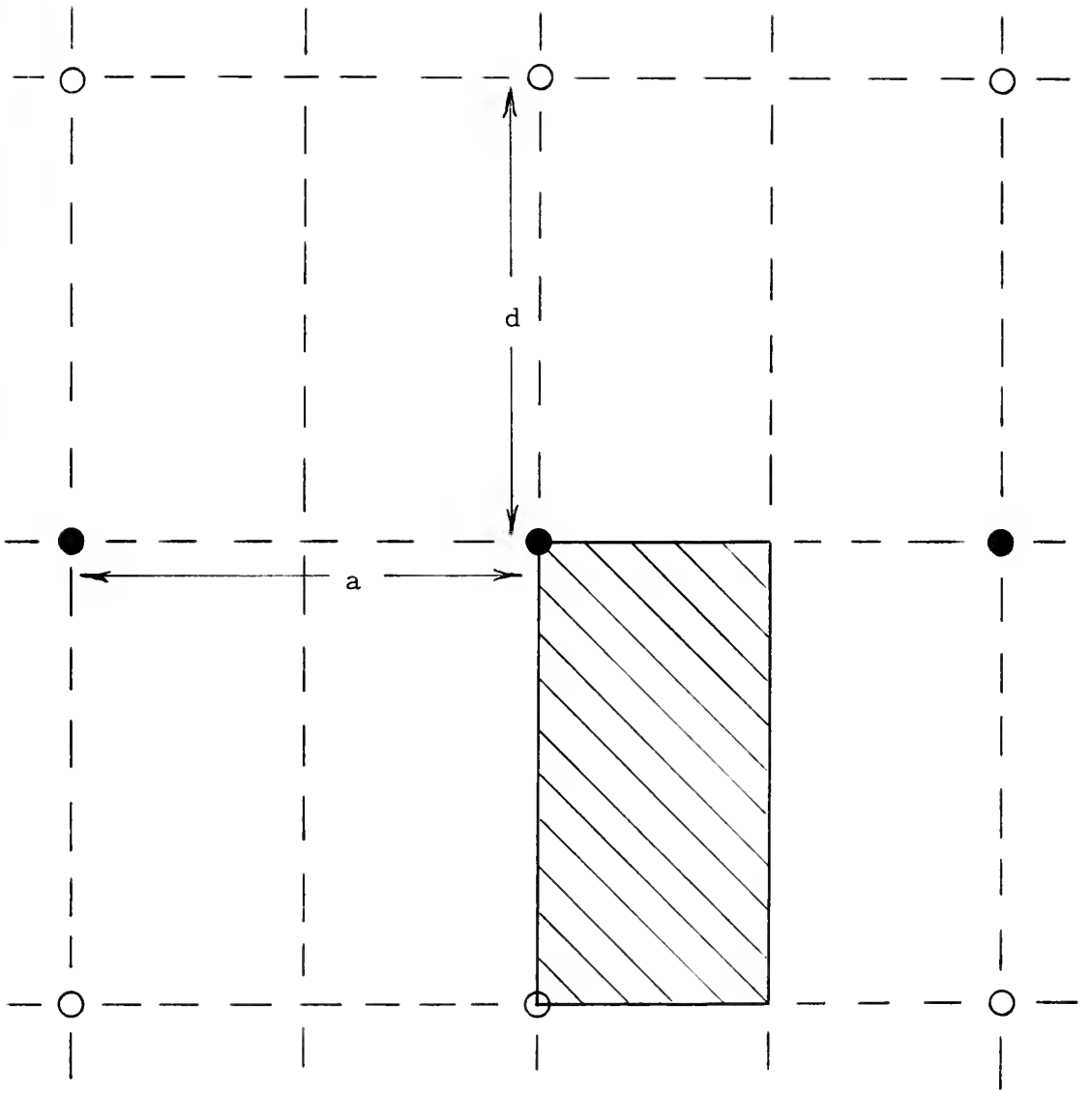

○ Production Well

● Injection Well

— — — Lines of Symmetry

▨ Model Used

d Distance Between Rows

a Distance Between Wells

FIGURE 4. DIRECT LINE DRIVE PATTERN

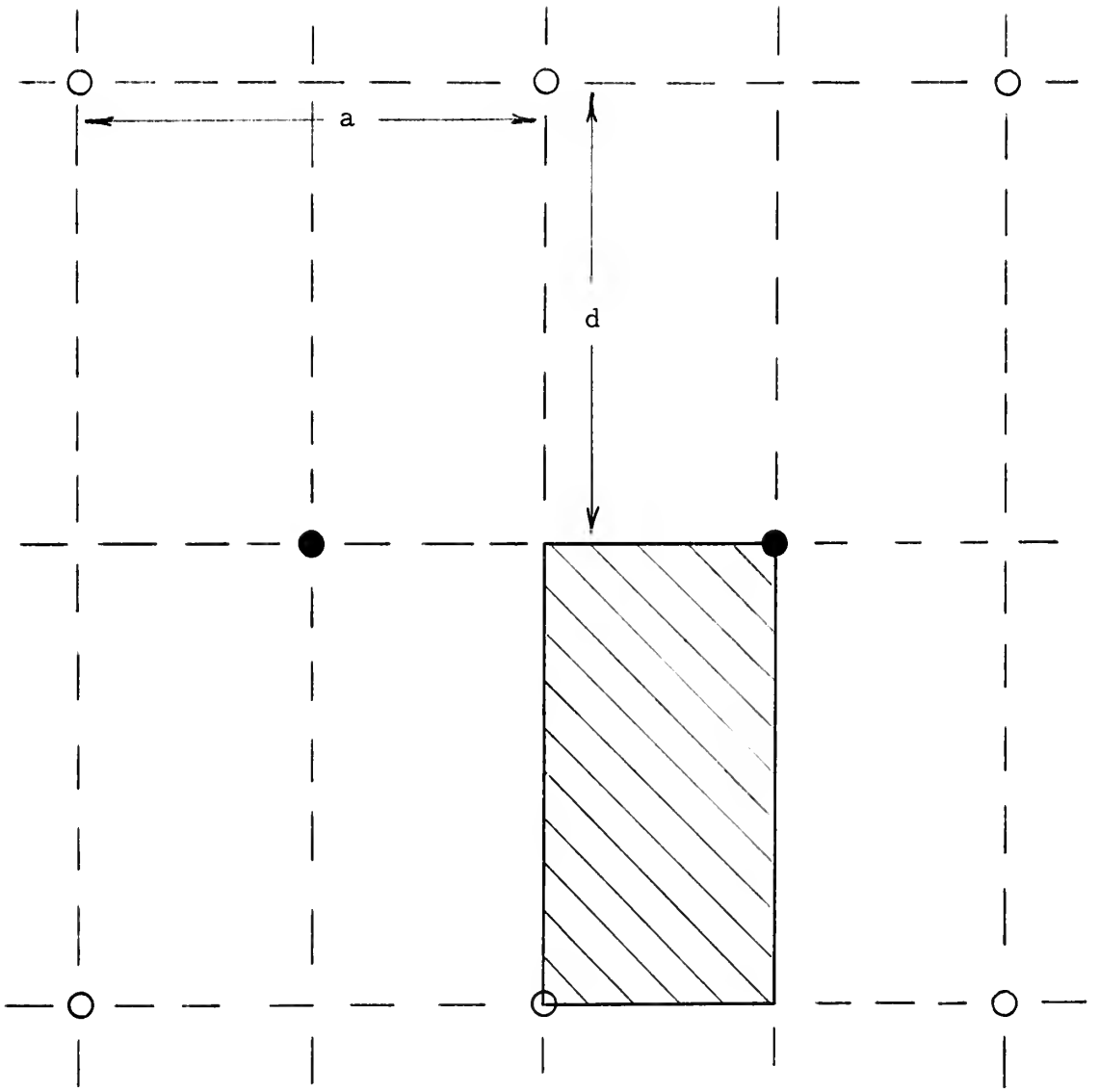

○ Production Well

● Injection Well

— — — Lines of Symmetry

▨ Model Used

d Distance Between Rows

a Distance Between Wells

FIGURE 5. STAGGERED LINE DRIVE PATTERN

Model Construction

The model utilized in this study was an artificially consolidated sand plate constructed generally as described by Watson[34] and Hickman.[20]

The artificial sandstone was composed of a clear epoxy resin and 60-100 mesh Ottawa sand. Actual construction of the artificial sandstone has been reported in detail by Watson,[34] Hickman,[20] and Caudle.[4] In order to avoid any possible loose streaks which may have occurred during packing of the artificial sand a minimum of 2 inches was cut from the model sides by using a diamond saw. To seal the model, an extremely viscous epoxy resin was spread over all exposed sand faces. The high viscosity of the epoxy resin was necessary to prevent imbibition of the coating into the model and was obtained by applying the coating just prior to it being completely "set-up."

Injection and producing "wells" were constructed from 1/2 inch thick acrylic plastic plate as shown by Figure 6. Swagelok fittings for 1/8 inch tubing were utilized to connect the "wells" to the injection systems. Prior to attaching the plastic plates to the model, well bores were reamed out at the well corners.

As seen from Figure 6, the model utilized was 32 cm in length, 16 cm in width, 0.6 cm thick, and had a well bore diameter of 0.2 cm. This represents a d/rw ratio of 320.

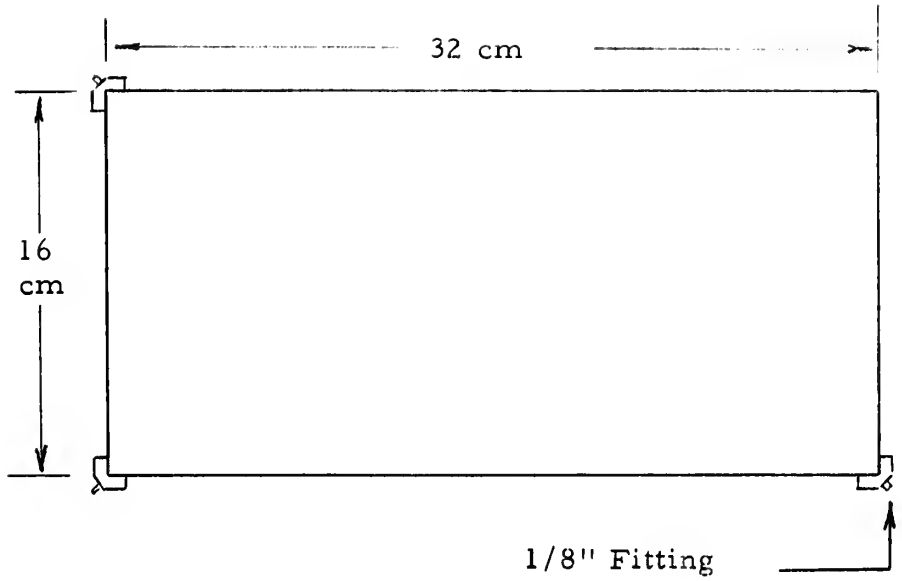

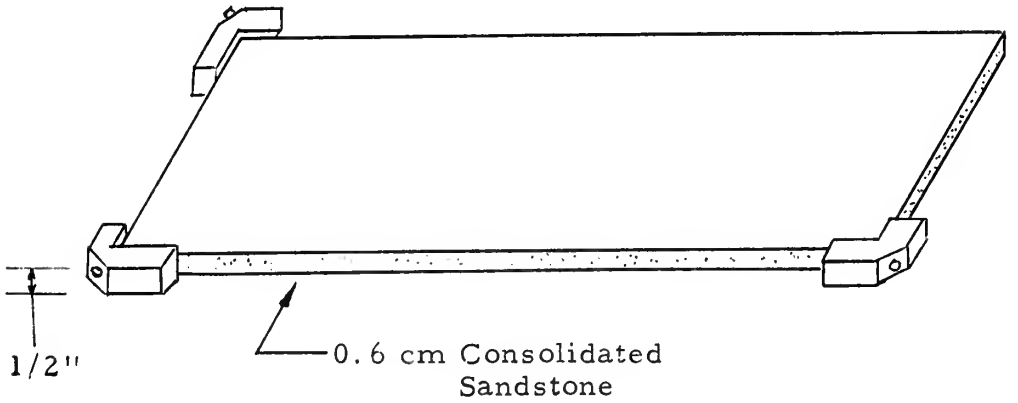

FIGURE 6. LINE DRIVE MODEL

Fluids

The fluids utilized in this study were miscible in all proportions. The use of miscible fluids to simulate reservoir fluids in model studies of mobility ratio effects has been well established with experimental data by Slobod and Caudle[32] and in other publications.[5,6,7,13,14,33]

By using miscible fluids in this study, there are no effects of capillary forces as will be found in immiscible systems. The absence of capillary effects eliminates the problem of saturation gradients in determining the effective mobility ratio. Also by utilizing miscible fluids, the effective permeability to each fluid is the same, thereby eliminating the need to determine relative permeabilities. This system therefore models a water flood with little or no flow of oil behind the water front. The mobility ratio, $\frac{(k/\mu)\ \text{swept}}{(k/\mu)\ \text{unswept}}$, then reduces to the viscosity ratio of $\frac{(\mu)\ \text{unswept}}{(\mu)\ \text{swept}}$. Therefore, only the viscosity of the fluids needed to be changed in order to vary the mobility ratio of the system.

To obtain fluids of the desired viscosities, a mixture of glycerine and water was used. The quantity of glycerine added for the desired viscosity was determined on a weight per cent basis through the use of standard chemical tables and checked with an Ostwald viscosimeter.

In the photographic technique used in this study, one of the fluids

contained a dye to establish a contrast between the displacing and the displaced fluids. Since the epoxy used to consolidate the sand renders the grains oil wet, oil soluble dyes could not be used. It was found that an ordinary household food coloring used in about 5 per cent volumetric proportions with the water obtained the desired contrast.

Injection System

The constant rate pumps, utilized and described by Hickman[20] and Watson[34] were used in this study. This pump is basically a hydraulic cylinder using a screw type mechanism to move the piston. It is driven by a gear and chain arrangement from an electric motor through a variable speed reduction gear. By changing the gears in the drive mechanism and/or the speed output of the reduction gear, the desired injection rate could be obtained.

A pressure gauge was located at the injection well. The producing well was permitted to discharge at atmospheric pressure, thereby permitting the gauge to indicate the pressure drop across the model.

Data Recording

A 35 mm camera was used to record the frontal position, pressure reading, and time during the runs. The camera was actuated by a D. C. timing motor which advanced the film and made one exposure per minute. Exposures could be made at longer intervals by using a "sign flasher" to interrupt current flow to the timing motor. This was done during the

slower runs. A red filter was used to obtain better contrast between the blue and clear fluids on black and white medium speed panchromatic film. A more complete description of the photographic and developing technique has been previously written by Caudle.[4]

Figure 7 is a schematic diagram of the equipment used in this study.

Typical photographs are shown in Figures 8 and 9. Figure 8 is an exposure of a direct line drive at a mobility ratio of one and Figure 9 is for a staggered line drive at a mobility ratio of twelve. Both exposures indicate frontal positions shortly before breakthrough.

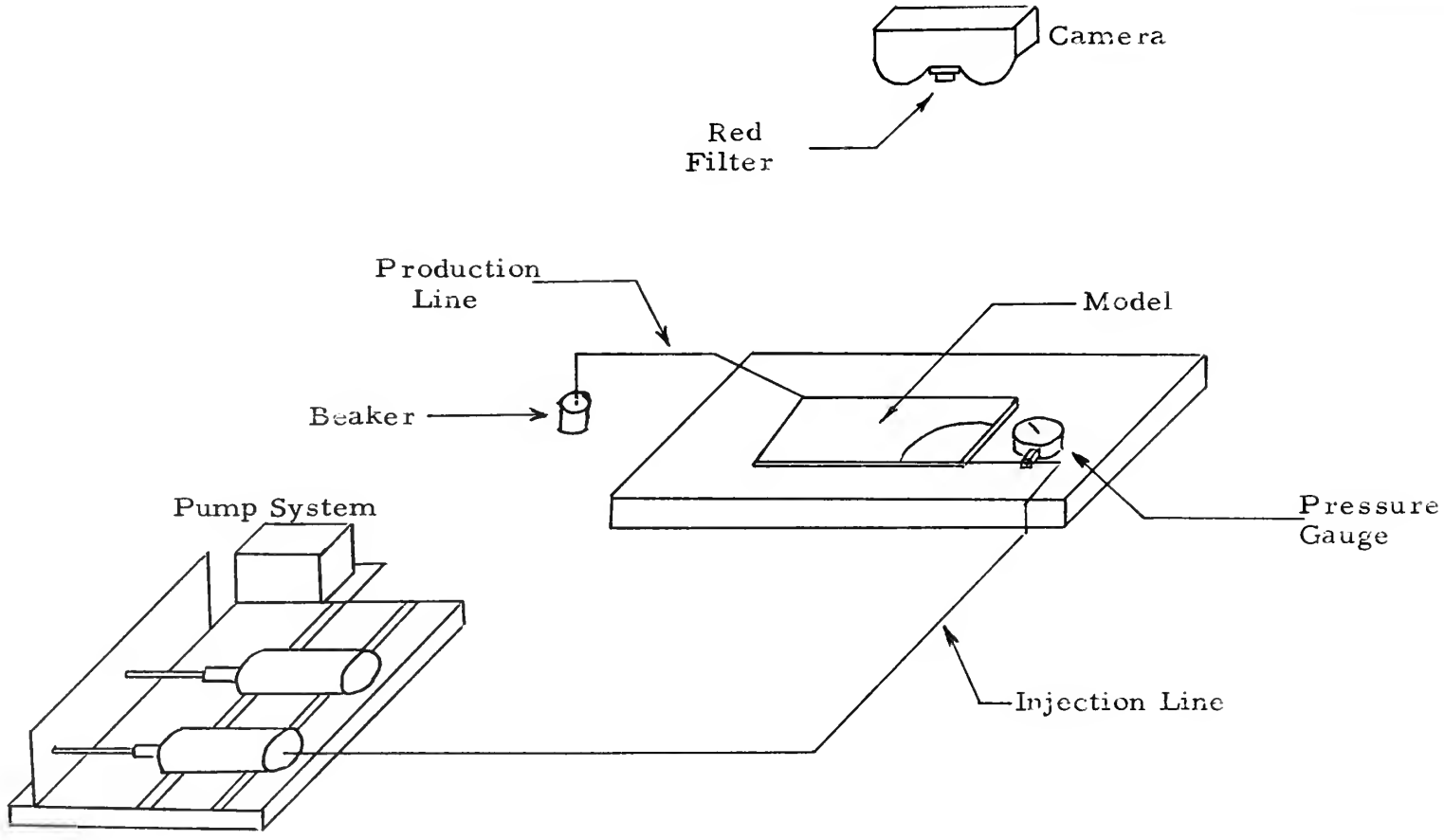

FIGURE 7. SCHEMATIC DIAGRAM OF EQUIPMENT

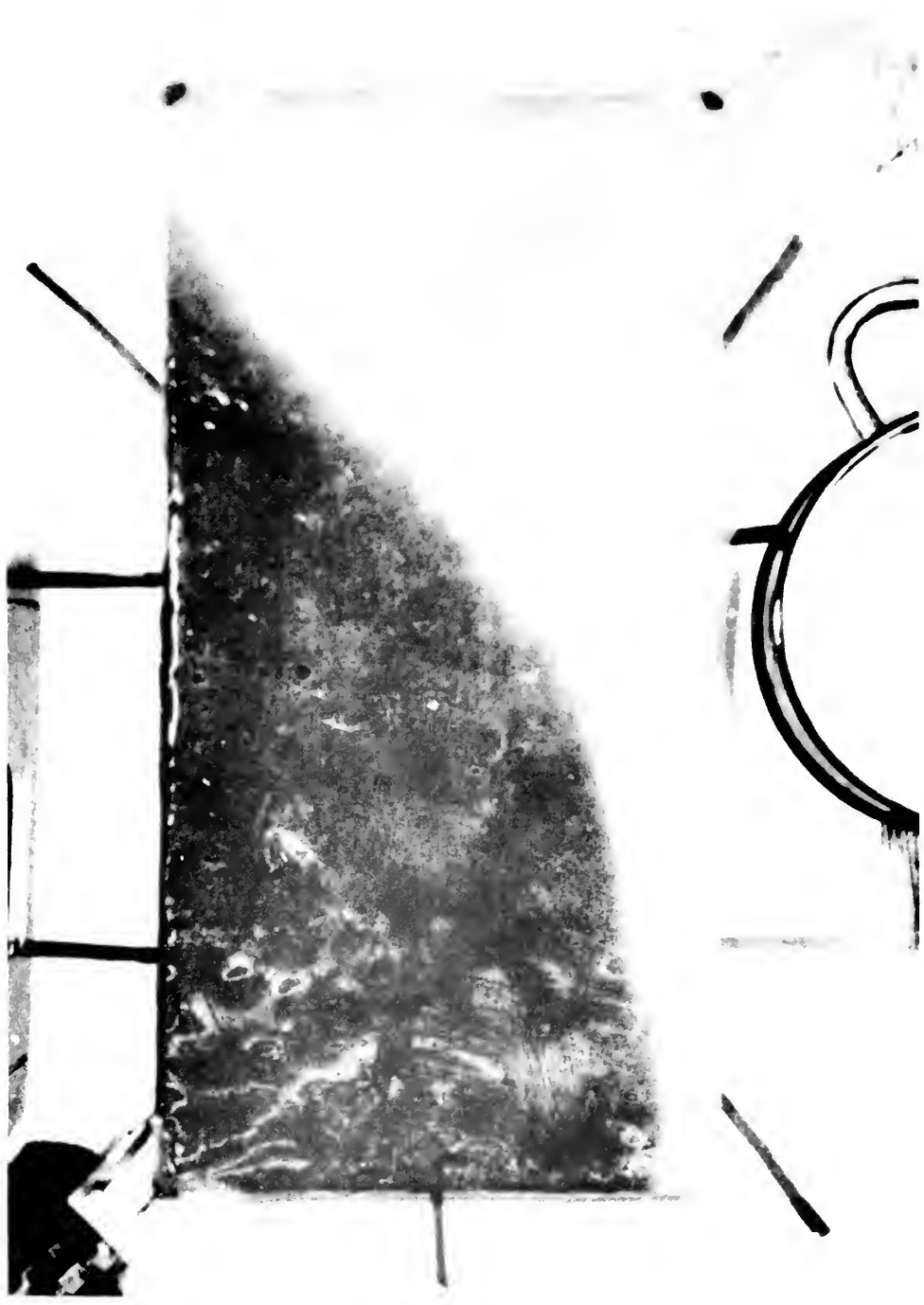

FIGURE 8. PHOTOGRAPH OF MODEL DURING A DIRECT LINE DRIVE RUN, M = 1.

FIGURE 9. PHOTOGRAPH OF MODEL DURING A STAGGERED LINE DRIVE RUN, M = 12.

EXPERIMENTAL PROCEDURE

The performance of both direct and staggered line drive patterns were studied for mobility ratios between 0.1 and 12 to determine the effect on areal sweep efficiency, fractional flow, and conductance ratio.

The model was initially evacuated by means of a vacuum pump. After complete evacuation, the model was saturated with water. At this time, all lines and the pressure gauge were connected to the model and the injection pump (Figure 7). The injection pump was loaded with dyed water as the initial displacing fluid, the model, pressure gauge, and clock were placed on a light table beneath the 35 mm camera and the direct line drive runs were started.

As injected fluid moved into the model, the automatic camera recorded the advancing front positions and injection pressures at regular intervals. The camera was stopped after approximately 95 per cent of the model had been swept. In either case, injection was continued until complete displacement of the "oil analog" had occurred.

In the second run, the injection system was loaded with fluid of higher viscosity and the above process was repeated with the clear viscous fluid displacing the dyed fluid. By alternating injection between clear fluid of varying viscosity and the dyed fluid, the range of mobility ratios from 0.1 to 12.0 was covered in five runs.

After completion of a set of runs covering the range of mobility

ratios under study, the roles of the injection and producing wells were reversed and the five runs were repeated. This procedure was then followed for the staggered line drive system. The two runs at the same conditions were made in opposite directions to average out any difference in the pressure drop around the individual wells.

The flow rate was set prior to the start of each run and was maintained constant throughout the run. The rate was chosen so that the injection pressure would not exceed the gauge scale and so that a sufficient number of photographic exposures would be made during the run to permit interpretation. The areal sweep efficiency is independent of flow rate in the line drive floods. Since the conductance ratio (Equation 2) is a dimensionless ratio, the actual rate utilized is of no concern. It is important, however, to ensure that the flow rate remains constant during each run so that the time scale can later be converted to pore volumes of water injected and the conductance ratio computed on the ratio of pressure drop.

ANALYSIS OF DATA

Areal Sweep Efficiency

All data was recorded on film during each run. After developing the film, a microfilm reader was used to enlarge the recorded image. Tracings were then made of the model and the frontal positions during sweepout. Appendix A contains typical tracings of frontal positions at various mobility ratios for both the direct line drive and the staggered line drive. The area of the model and the area behind the frontal position were obtained with a polar planimeter. The areal sweep efficiency was then obtained for each frontal position by dividing the area swept by the area of the model. Tables of data are contained in Appendix B.

Areal sweep efficiencies were plotted versus an elapsed time scale. Since runs at the same mobility ratio, but in opposite directions, were not necessarily made at the same rate, a time correction factor was obtained by plotting areal sweep data for the second run on the first curve obtained and then noting the time correction necessary which would make the curves most closely coincide. This permitted easy correlation of data for runs of the same mobility ratio made in opposite directions.

Since each run was made at a constant rate, it is easily seen that the time scale of the basic data plots is directly related to the volume of displacing fluid injected by a constant ratio for each particular rate.

Prior to breakthrough of injected fluid, a plot of areal sweep versus volume injected is a straight line. By noting the area swept and the elapsed time at breakthrough, all subsequent time values may be converted to displaceable volumes of injected fluid by the ratio of area swept to elapsed time at breakthrough. Appendix B contains plots of all mobility ratios studied for the two well patterns considered, with tables of data derived from these plots.

Plots of areal sweep versus displaceable volumes injected can be found in Appendix C. The displaceable volume injected is a more useful term than actual volume (or time at constant injection rate) due to its dimensionless nature. Dyes, et al[13] has defined displaceable volume as the product of the hydrocarbon pore volume of the unit pattern and the volumetric displacement efficiency.

It is noted that areal sweep data from the first 5 runs did not correspond to other runs for the direct line drive made in the opposite direction as regards areal sweep efficiency. After study of the photographed flood front shapes, it was noted that an air pocket had been present near the production well during these runs, thereby distorting streamlines and causing invalid areal sweep data. This error was noted after completion of all runs and an attempt was then made to remake these runs. However, the injection well became "plugged" during these "reruns" and areal sweep data for the direct line drive for mobility

ratios of 3.13, 0.106, and 12.1 is based on one run only. The cause of this "well plugging" is attributed to impurities in the injected fluid, which could have been prevented by installing a filter on the injection line. This air pocket did not interfere with runs subsequent to run 5 since a number of days elapsed between run 5 and 6 and the model was routinely evacuated before making run 6.

Conductance Ratio

The conductance ratio is defined by Aronofsky and Ramey[2] $(q/\Delta P)_t \Big/ (q/\Delta P)_i$ which reduces to $\Delta P_i \Big/ \Delta P_t$ when the flow rate is maintained constant. Pressure data taken from the injection well provides ΔP at a particular areal sweep efficiency and permits direct calculation of the conductance ratio.

From the above equation, it can be seen that if the pressure increases during a run, the conductance ratio will decrease and a decreasing pressure will cause an increasing conductance ratio. The conductance ratio decreases if the mobility ratio is favorable and increases if the mobility ratio is unfavorable. At a mobility ratio of one, the conductance ratio will remain constant during a flood.

Plots of conductance ratio versus areal sweep can be found in Appendix C.

The ratio of the distance between injection and production wells to the wellbore radius d/rw has been shown by Aronofsky and Ramey[2]

to effect the conductance ratio. Although the model was constructed with a d/rw ratio of 320, slight differences in the well bore radius and plugging around the well bore will tend to change this ratio.

The steady state flow equation for single phase flow in line drive patterns was derived by Muskat[24] and presented by Deppe[12] in practical units as

$$q = \frac{0.001538\ k/\mu\ h\ \Delta P}{0.682\ d/a\ -0.798 + \ln d/rw} \qquad (32)$$

This equation is valid for both direct and staggered line drive well patterns with $d/a \geq 1$.

Using the information obtained from the model runs, the effective d/rw ratio for the direct line drive was found to be 922. The effective d/rw ratio for the staggered line drive was calculated as 1110. These values for d/rw are somewhat smaller than those normally encountered in the field. However, it is considered that reasonable accuracy will be obtained by using the conductance ratios obtained in this study without correction.

If it is desired to correct the conductance ratios obtained in this study to the correct value for other d/rw ratios, using the method presented by Aronofsky and Ramey[2] for line drives yields the following relationship:

$$\gamma_f = \frac{0.682(d/a)_f - 0.798 + \ln(d/rw)_m + 0.434 \ln \frac{(rw)_m}{(rw)_f}}{1/\gamma_m [0.682(d/a)_f - 0.798 + \ln(d/rw)_m] + \frac{1+M-fs(M-1)}{4.6M} \ln \frac{(rw)_m}{(rw)_f}} \quad (33)$$

where the subscripts f and m denote field and model respectively.

Fractional Flow

Up to the time of breakthrough, the fractional flow from the unswept region (oil cut) is one. Also up to the time of breakthrough, a plot of areal sweep versus displaceable volumes injected yields a straight line at a slope of one. It can also be seen that a plot of areal sweep versus elapsed time, with injection at a constant rate, will yield a straight line prior to breakthrough. After breakthrough, the areal sweep curve deviates from a straight line.

Previous publications[13, 20] have shown that the fractional flow from the producing well can be obtained from the slope of the areal sweep efficiency curve versus displaceable volumes injected. Since elapsed time and displaceable volumes are directly proportional, the fractional flow from the unswept region can be obtained by the ratio of the slope of the areal sweep efficiency curve at the time of interest to the slope of the straight line portion. Tables of fractional flow are given with the basic data plots in Appendix B and are plotted versus areal sweep efficiency in Appendix C.

INTERPRETATION OF RESULTS

Tables of basic data from the model runs are presented in Appendix B. Appendix B also includes curves of areal sweep efficiency versus elapsed time. Each figure also includes tables of displaceable volumes injected and fractional flow data as derived from these curves. Plots of displaceable volumes injected, fractional flow, and conductance ratio versus areal sweep efficiency for the mobility ratios studied are provided in Appendix C.

Results of this study were compared with those obtained by the X-ray shadowgraph technique[13] and were found to have a maximum deviation of 7% and an average difference of less than 2%. Comparison of areal sweep efficiencies at breakthrough and at 95% fractional flow from the swept region as obtained by Dyes, et al[13] and as obtained in this study are listed in Table I for the direct line drive and in Table II for the staggered line drive.

In order to make the results of this study useful for mobility ratios other than those specifically used here, Figures 10 through 15 indicate the effect of mobility ratio on performance.

In comparing the results obtained for the direct line drive and the staggered line drive, Figure 16 shows that areal sweep efficiencies are significantly higher for the staggered line drive at breakthrough. However, at a fractional flow from the swept region of 95 per cent (assumed economic limit) the areal sweep efficiencies are similar for the two patterns at abandonment up to a mobility ratio of approximately 10. At mobility ratios above 10, previous studies have shown that the

areal sweep efficiencies decrease rapidly in this region for a given fractional flow.

TABLE I

COMPARISON OF AREAL SWEEP EFFICIENCIES
FOR DIRECT LINE DRIVE

Mobility Ratio	Breakthrough Sweep Efficiency		95% Fractional Water Flow Sweep Efficiency	
	Dyes, et al[13]	This Study	Dyes, et al[13]	This Study
0.106	0.92	0.85	0.995	0.98
0.274	0.76	0.76	0.99	0.97
1.0	0.55	0.55	0.98	0.96
3.13	0.46	0.46	0.97	0.95
12.1	*	0.41	*	0.77

*Not available

TABLE II

COMPARISON OF AREAL SWEEP EFFICIENCIES
FOR STAGGERED LINE DRIVE

Mobility Ratio	Breakthrough Sweep Efficiency		95% Fractional Water Flow Sweep Efficiency	
	Dyes, et al[13]	This Study	Dyes, et al[13]	This Study
0.106	0.91	0.89	0.995	0.99
0.274	0.85	0.87	0.99	0.98
1.0	0.75	0.77	0.98	0.98
3.13	0.61	0.66	0.95	0.96
12.1	*	0.55	*	0.89

*Not available

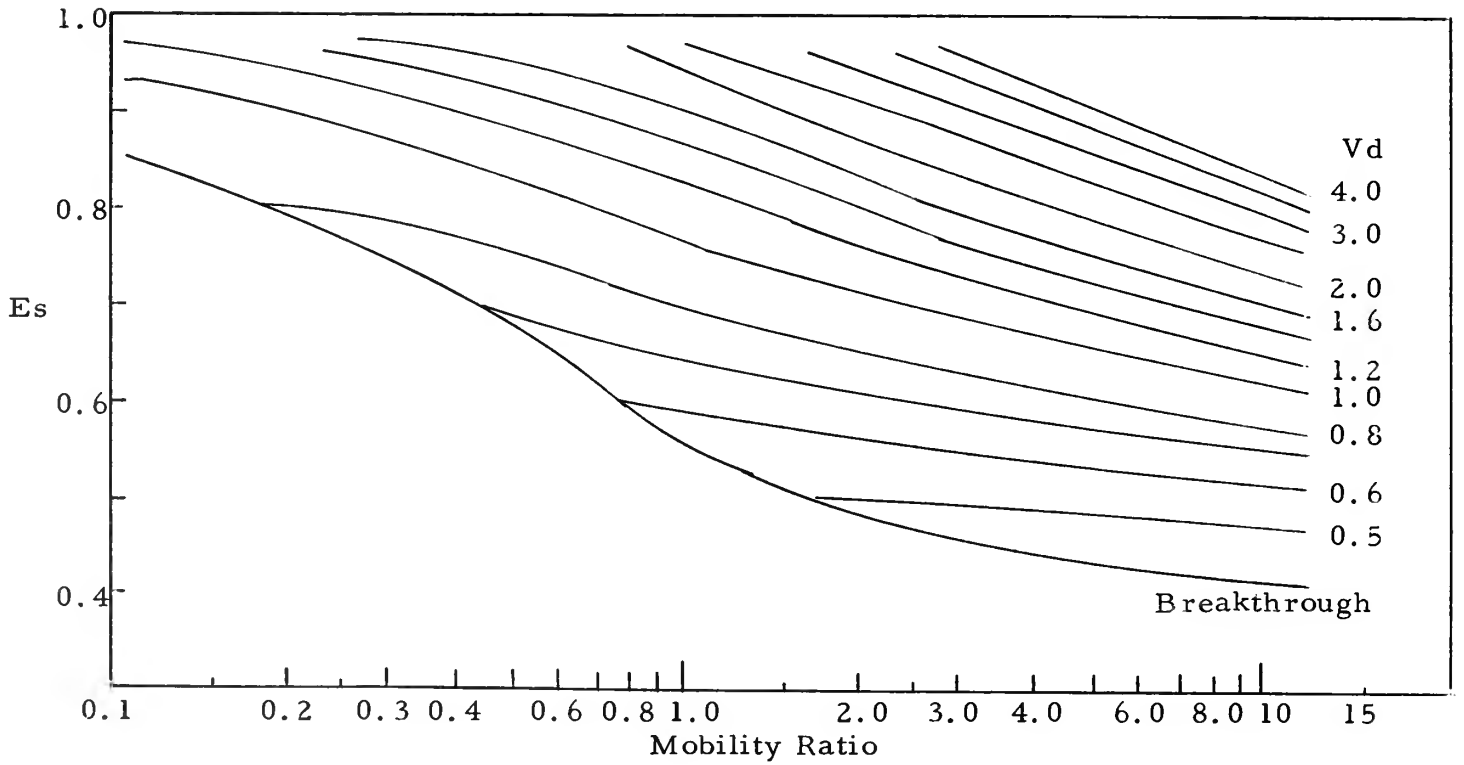

FIGURE 10. DIRECT LINE DRIVE -- VARYING DISPLACEABLE VOLUMES for AREAL SWEEP versus MOBILITY RATIO

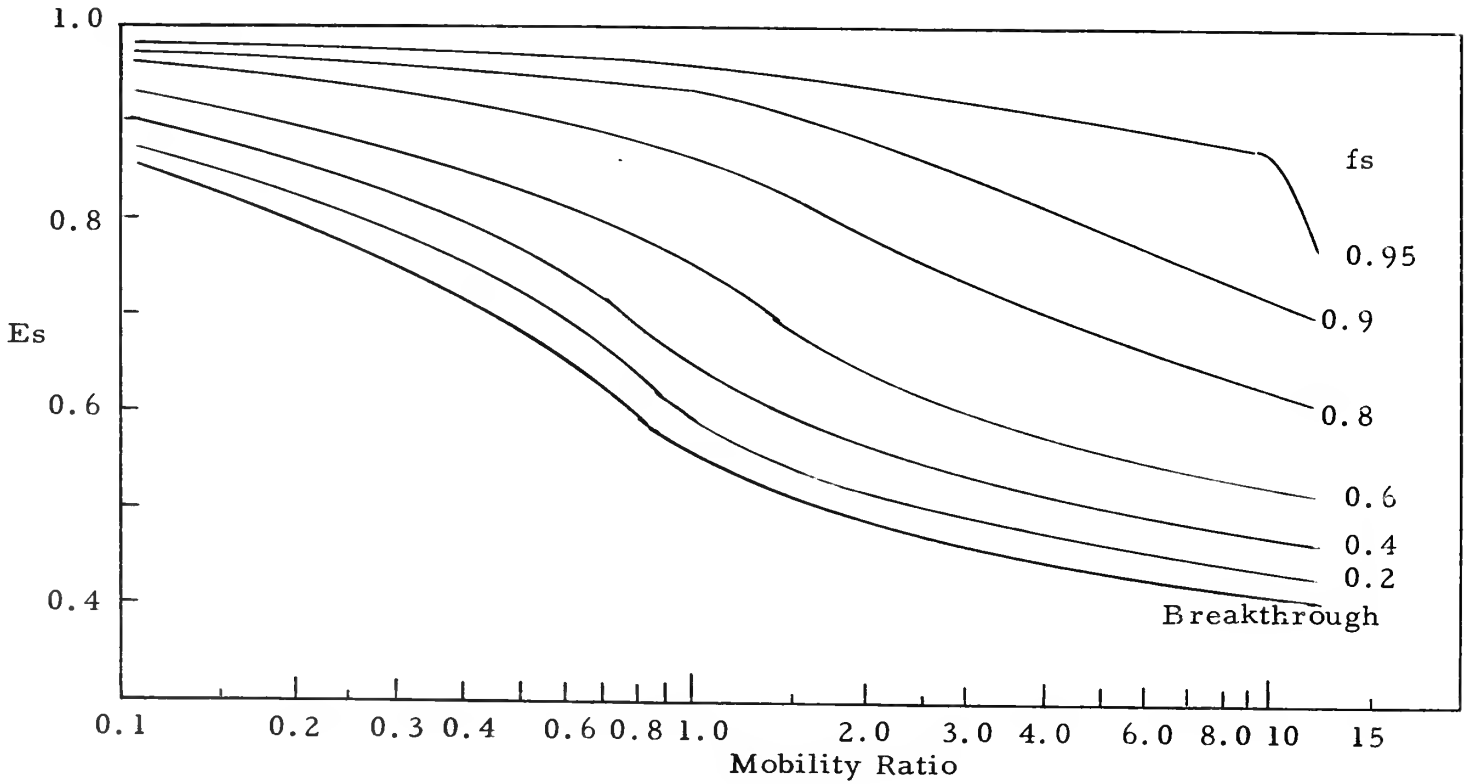

FIGURE 11. DIRECT LINE DRIVE -- VARYING FRACTIONAL FLOWS for AREAL SWEEP versus MOBILITY RATIO

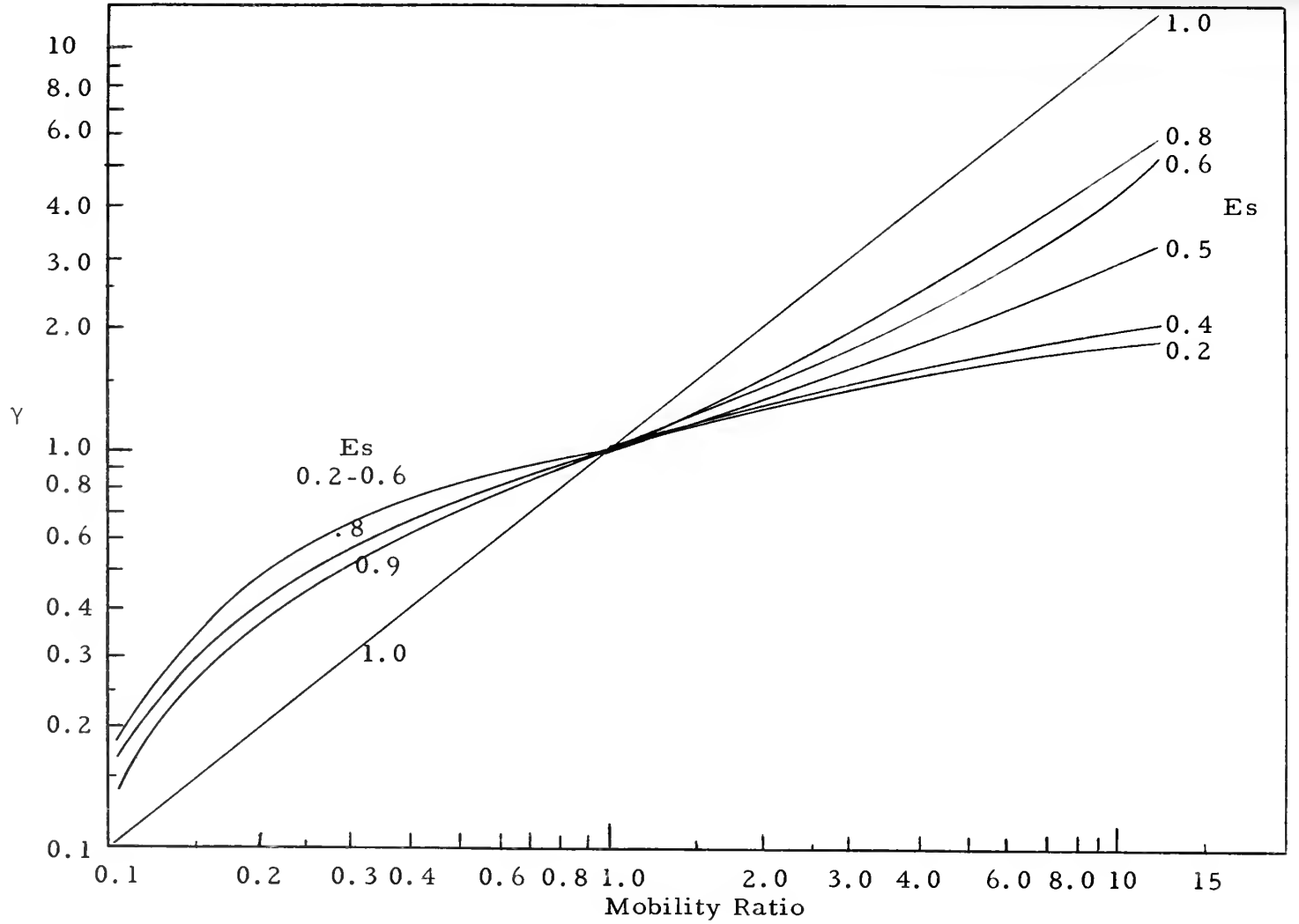

FIGURE 12. DIRECT LINE DRIVE -- VARYING AREAL SWEEP for CONDUCTANCE RATIO versus MOBILITY RATIO

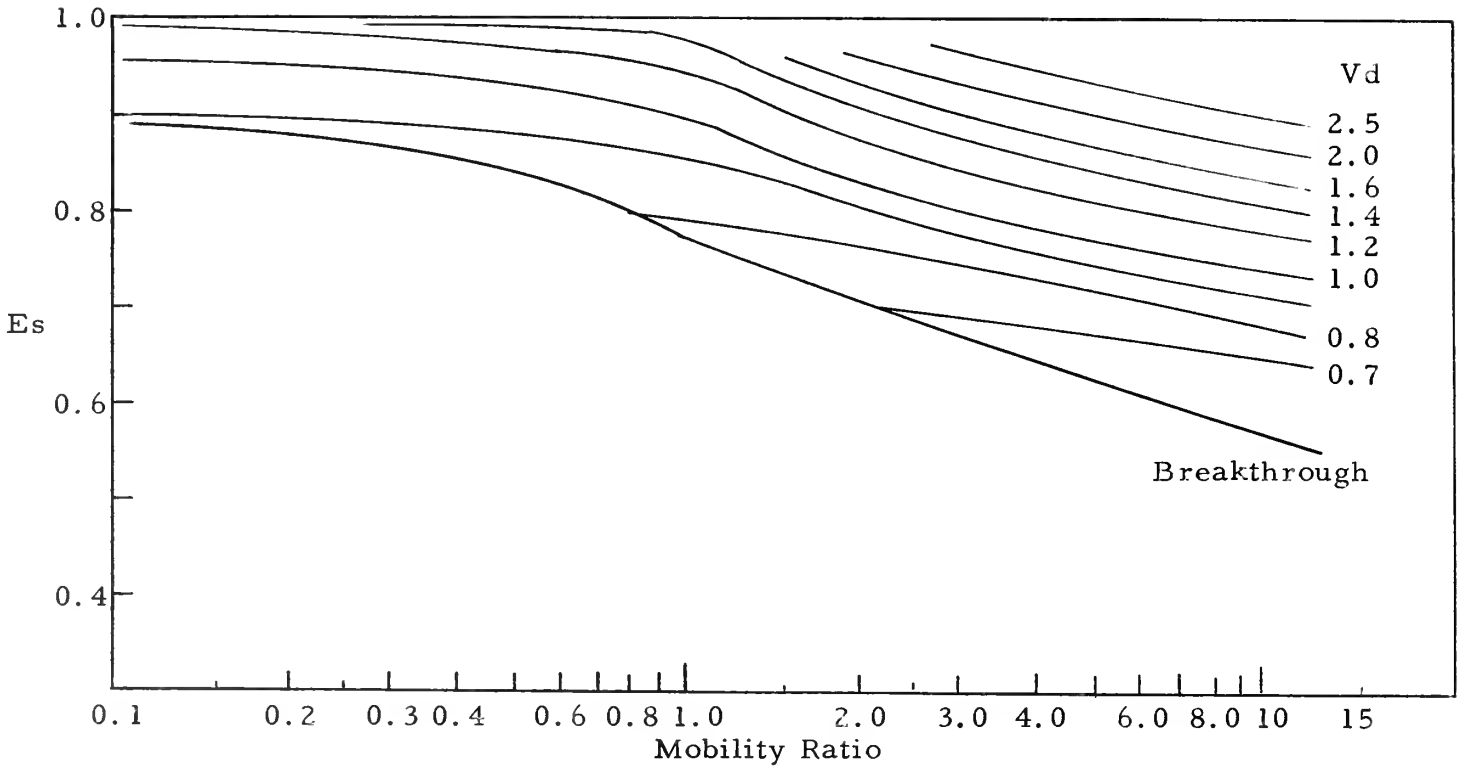

FIGURE 13. STAGGERED LINE DRIVE -- VARYING DISPLACEABLE VOLUMES for AREAL SWEEP versus MOBILITY RATIO

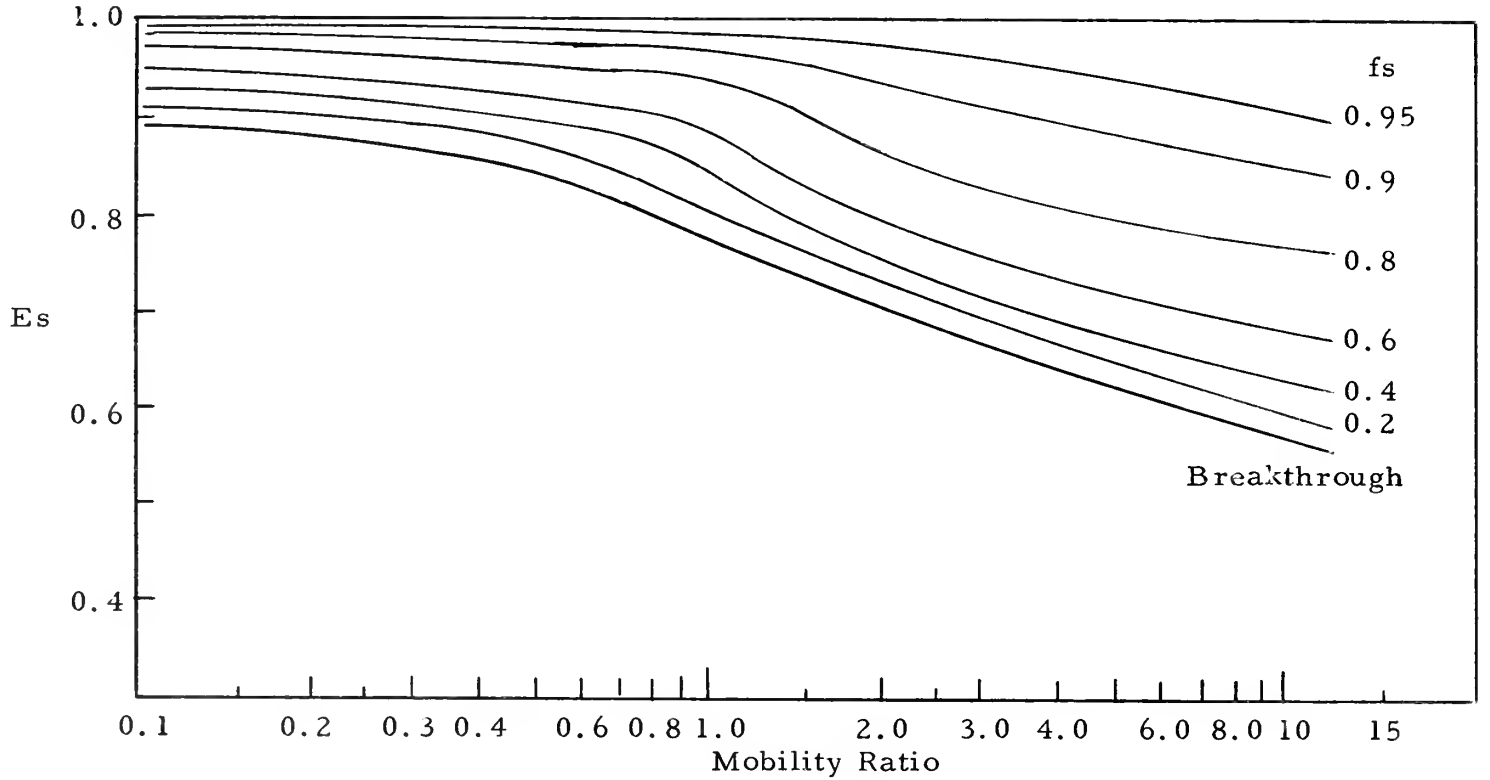

FIGURE 14. STAGGERED LINE DRIVE -- VARYING FRACTIONAL FLOWS for AREAL SWEEP versus MOBILITY RATIO

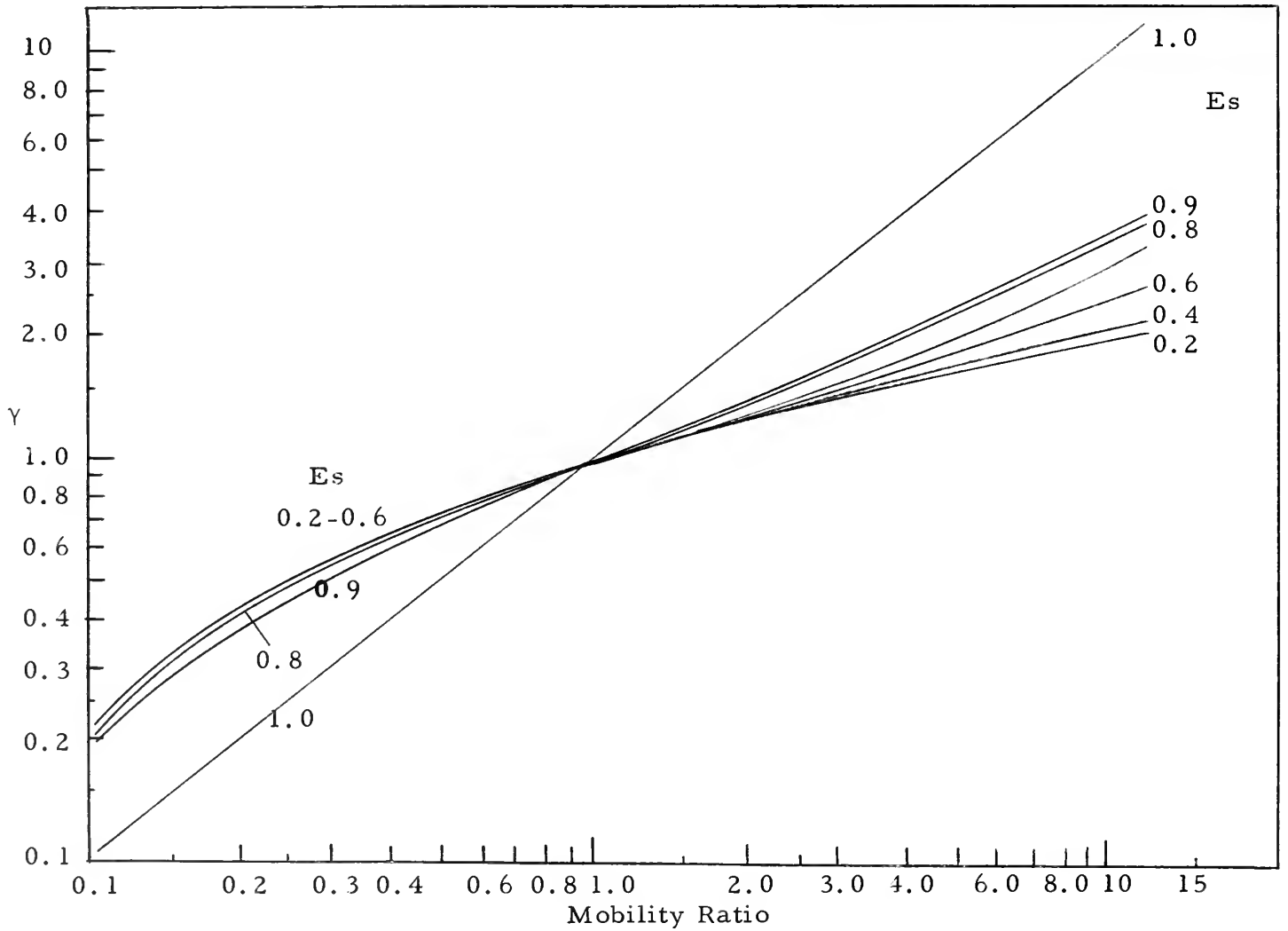

FIGURE 15. STAGGERED LINE DRIVE -- AREAL SWEEPS for CONDUCTANCE RATIO versus MOBILITY RATIO

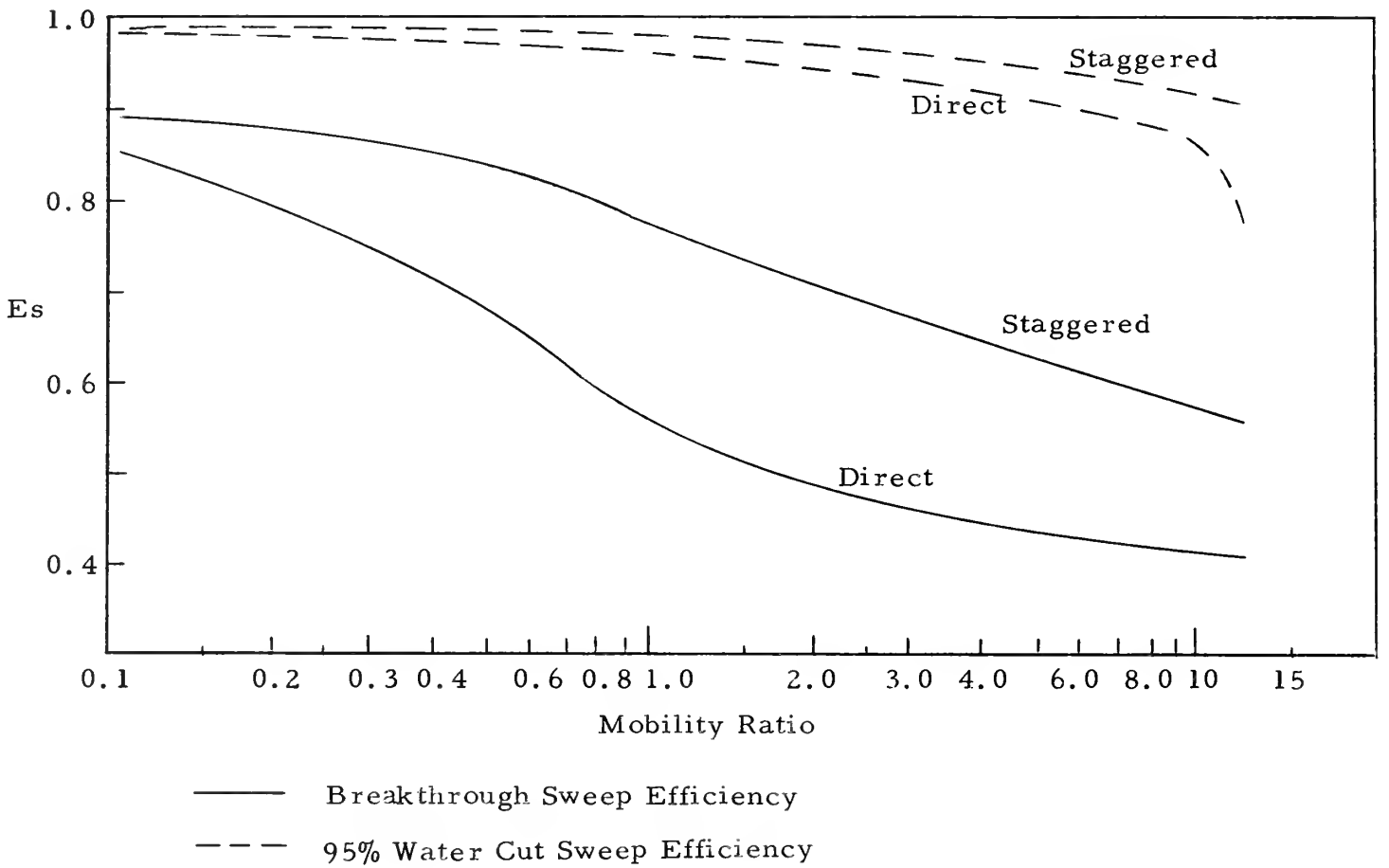

FIGURE 16. SWEEP EFFICIENCY COMPARISON FOR DIRECT AND STAGGERED LINE DRIVES

CONCLUSIONS

The results of this study of line drive flood patterns indicate that mobility ratio has a definite effect on the areal sweep efficiencies at time of breakthrough. At abandonment conditions, the effect of mobility ratio on areal sweep is observable, but not to the pronounced extent as at breakthrough conditions.

The conductance ratios show that the majority of the flow potential change takes place when the front is near the injection well for favorable mobility ratios and near the production well for unfavorable mobility ratios. At time of breakthrough, an apparent change in conductance ratio is noted.

The staggered line drive gave breakthrough sweep efficiencies from 4 to 14 per cent higher than those obtained by the direct line drive. At abandonment conditions, only small differences existed in areal sweep efficiencies for the direct and staggered line drive. However, for very poor mobility ratios, over one additional displaceable volume of injected fluid was required to reach abandonment conditions with the direct line drive.

The method described for predicting performance of stratified reservoirs can be used for any well pattern for which conductance ratios and areal sweep efficiencies are available. This data is available for the five-spot[7], the inverted skewed seven-spot[20], and the inverted nine-spot[34] patterns. This study allows similar predictions for the direct and staggered line drive patterns.

The effect of a free gas saturation on areal sweep efficiency and conductance ratio has not been sufficiently studied. Accurate performance prediction for stratified reservoirs requires additional study on the effect of free gas saturations.

NOMENCLATURE

a	well spacing
c	constant
d	row spacing of wells
Es	fractional area swept
fs	fractional flow from swept region
fw	fractional water flow
h	height or thickness
k	permeability
L	length
ℓ	partial length
M	mobility ratio
Np	fractional oil produced
ΔP	pressure drop
q	total flow
qw	water flow
rf	frontal radius
ri	radius of radial flow region around injection well
rp	radius of radial flow region around production well
rw	radius of well bore
Scw	saturation of connate water
Sro	saturation of residual oil
t	time
Vb	bulk volume
Vd	displaceable volume - Vb ϕ (1 - Scw - Sro)

v	velocity
Wi	water injected
w	width
α	angle open to flow into wellbore from swept region
γ	conductance ratio
ϕ	porosity
λ	mobility - k/μ
μ	viscosity

Subscripts

A	radial flow area around injection well
B	linear flow area between radial flow areas
C	radial flow area around production well
BT	breakthrough
f	field
i	initial
j	any stratum
m	model
o	oil
s	swept region
t	time
u	unswept region
w	water

BIBLIOGRAPHY

1. Aronofsky, J. S.: "Mobility Ratio--Its Influence on Flood Patterns During Water Encroachment", Trans. AIME (1952) 195, 15.

2. Aronofsky, J. S., and Ramey, H. J.: "Mobility Ratio--Its Influence on Injection or Production Histories in Five-Spot Waterflood", Trans. AIME (1956) 207, 205.

3. Carpenter, C. W., Jr., Bail, P. T., and Bobek, J. E.: "A Verification of Waterflood Scaling in Heterogeneous Communicating Flow Models", Trans. AIME (1962) 225, Part II 9.

4. Caudle, B. H.: "Laboratory Models of Oil Reservoirs Produced by Natural Water Drive", Ph.D. Dissertation, The University of Texas (1963).

5. Caudle, B. H., and Dyes, A. B.: "Improving Miscible Displacement by Gas-Water Injection", Trans. AIME (1958) 213, 281.

6. Caudle, B. H., and Loncaric, I. G.: "Oil Recovery in Five-Spot Pilot Floods", Trans. AIME (1960) 219, 132.

7. Caudle, B. H., and Witte, M. D.: "Production Potential Changes During Sweepout In A Five-Spot System", Trans. AIME (1959) 216, 446.

8. Cheek, R. E., and Menzie, D. E.: "Fluid Mapper Model Studies of Mobility Ratio", Trans. AIME (1955) 204, 278.

9. Collins, R. E.: Flow of Fluids Through Porous Media, Reinhold Publishing Corporation, New York, N.Y. (1961).

10. Collins, R. E. and Perkins, F. M.: "Scaling Laws for Laboratory Flow Models of Oil Reservoirs", Trans. AIME (1960) 219, 383.

11. Craig, F. F., Jr., Geffen, T. M., and Morse, R. A.: "Oil Recovery Performance of Pattern Gas or Water Injection Operations from Model Tests", Trans. AIME (1955) 204, 7.

12. Deppe, J. C.: "Injection Rates--The Effect of Mobility Ratio, Area Swept, and Pattern", Trans. AIME (1961) 222, Part II 81.

13. Dyes, A. B., Caudle, B. H., and Erickson, R. A.: "Oil Production After Breakthrough--As Influenced by Mobility Ratio", Trans. AIME (1954) 201, 81.

14. Dyes, A. B., Kemp, C. E., and Caudle, B. H.: "Effect of Fractures on Sweep-out Pattern", Trans. AIME (1958) 213, 245.

15. Fay, C. H., and Prats, M.: "The Application of Numerical Methods of Cycling and Flooding Problems", Proc. Third World Petroleum Congress, Section II (1951), 555.

16. Gaucher, D. H., and Lindley, D. C.: "Waterflood Performance in a Stratified, Five-Spot Reservoir--A Scaled Model Study", Trans. (1960) 219, 208.

17. Geertsma, J., Croes, G. A., and Schwarz, W.: "Theory of Dimensionally Scaled Models of Petroleum Reservoir", Trans. AIME (1952) 207, 118.

18. Habermann, B.: "The Efficiency of Miscible Displacements as a Function of Mobility Ratio", Trans. AIME (1960) 219, 264.

19. Hauber, W. C., "Prediction of Waterflood Performance for Arbitrary Well Patterns and Mobility Ratios", Jour. Pet. Tech. (Jan., 1964), 95.

20. Hickman, B. M.: "Performance of the Inverted Skewed Seven-Spot Injection Pattern", M.S. Thesis, The University of Texas (1963).

21. Hurst, W.: "Determination of Performance Curve in Five-Spot Water-Flood", Petroleum Engineer (April, 1953) 25, B40.

22. Landrum, B. L., Flanagan, D. A., Norwood, B. C., and Crawford, P. B.: "A New Experimental Model for Studying Transient Phenomena", Trans. (1959) 216, 33.

23. Murphy, G.: Similitude in Engineering, Ronald Press, New York, N.Y.

24. Muskat, M.: The Flow of Homogeneous Fluids Through Porous Media, McGraw-Hill Book Co. (1937).

25. Muskat, M.: Physical Principals of Oil Production, McGraw-Hill Book Co. (1949).

26. Muskat, M., and Wyckoff, R. D.: "Theoretical Analysis of Waterflooding Networks", Trans. AIME (1934) 107, 62.

27. Muskat, M., Wyckoff, R. D., and Botset, H. G.: "The Mechanics of Porous Flow Applied to Water-Flooding Problems", Trans. AIME (1933) 103, 219.

28. Nobles, M. A., and Janzen, H. B.: "Application of a Resistance Network for Studying Mobility Ratio Effects", Trans. AIME (1958) 213, 356.

29. Odeh, A. S., Bradley, H. B., and Heller, J. P.: "Scale Limitations in Potentiometric Model Construction", Trans. AIME (1956) 207, 200.

30. Prats, M., Matthews, C. S., Jewett, R. L., and Baker, J. D.: "Prediction of Injection Rate and Production History for Multi-fluid Five-Spot Floods", Trans. AIME (1959) 216, 98.

31. Rappoport, L. A., and Leas, W. J.: "Properties of Linear Water Floods", Trans. AIME (1953) 198, 139.

32. Slobod, R. L., and Caudle, B. H.: "X-Ray Shadowgraph Studies of Areal Sweepout Efficiencies", Trans. AIME (1953) 195, 265.

33. Slobod, R. L., Erickson, R. A., and Caudle, B. H.: "The Encroachment of Injected Fluids Beyond the Normal Well Pattern", Trans. AIME (1955) 204, 84.

34. Watson, R. E.: "Study of The Inverted Nine-Spot Flood Pattern", M.S. Thesis, The University of Texas (1963).

APPENDIX A

FLOOD FRONT TRACINGS

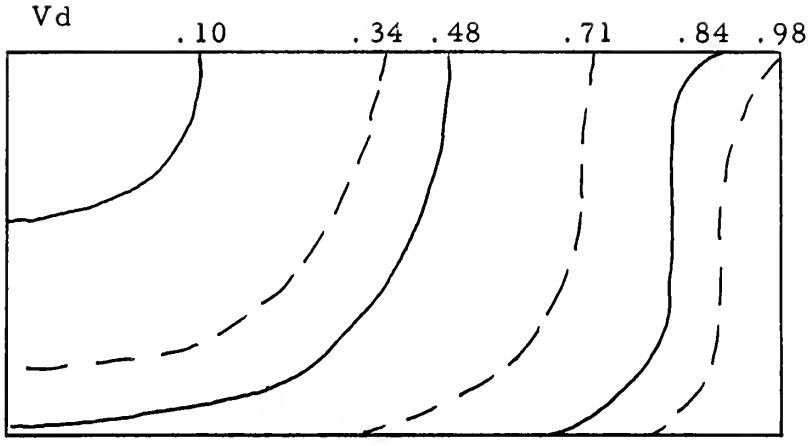

Direct Line Drive

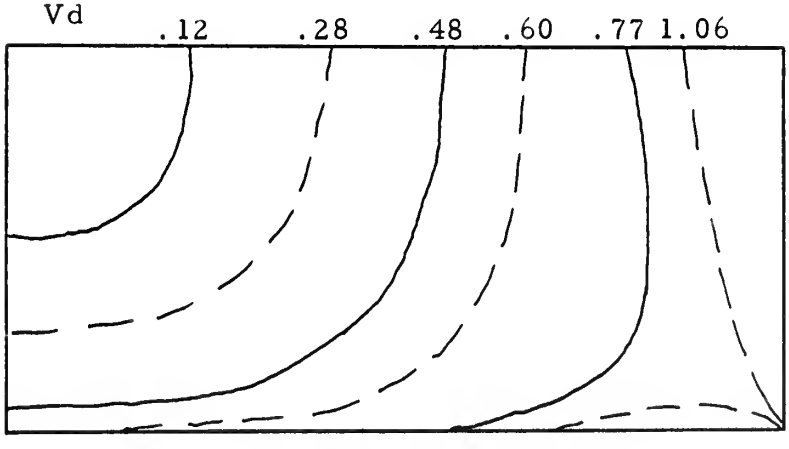

Staggered Line Drive

FIGURE 17. FLOOD FRONT TRACINGS, M = 0.106

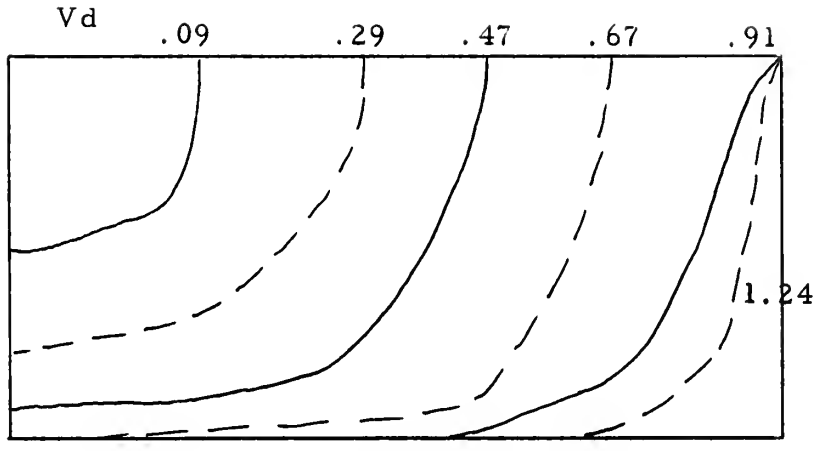

Direct Line Drive

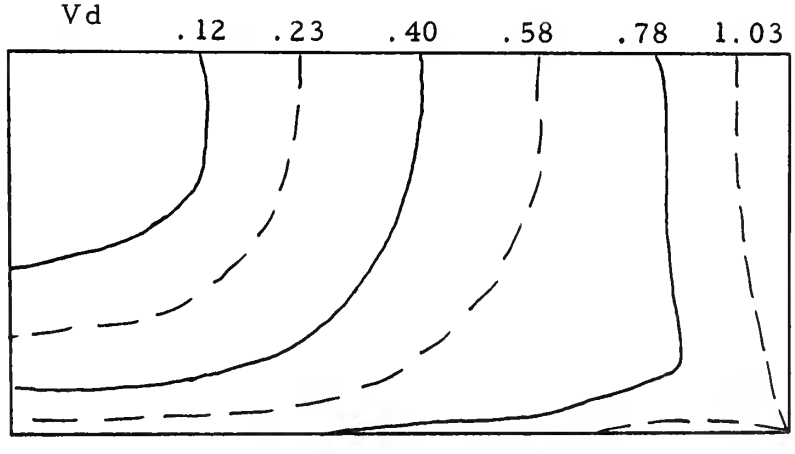

Staggered Line Drive

FIGURE 18. FLOOD FRONT TRACINGS, M = 0.274

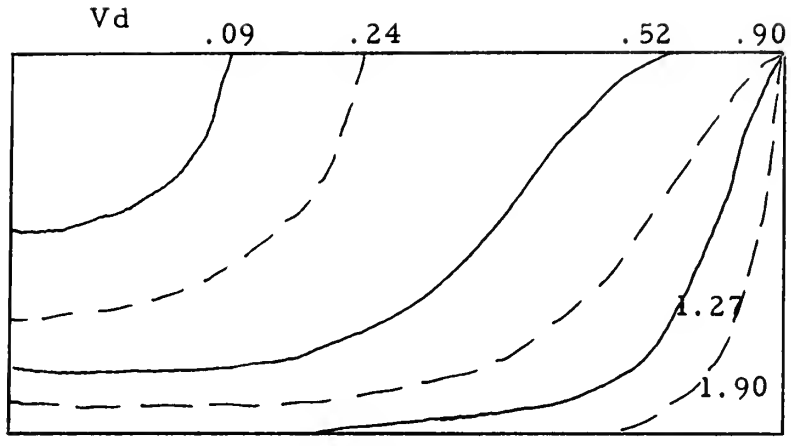

Direct Line Drive

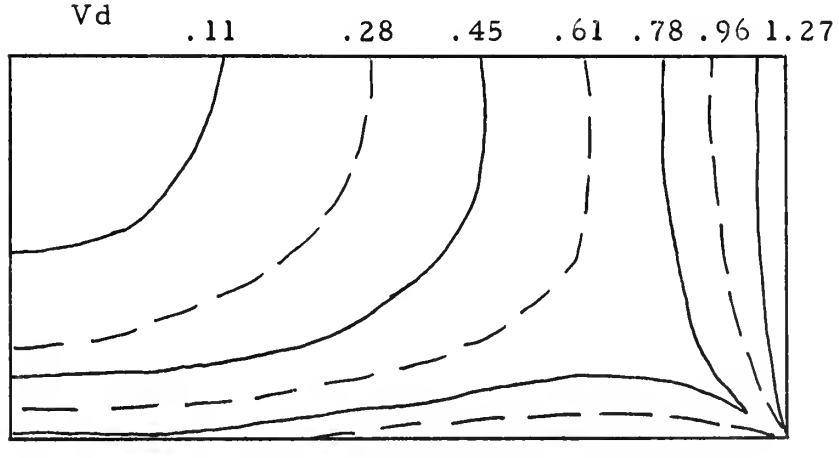

Staggered Line Drive

FIGURE 19. FLOOD FRONT TRACINGS, M = 1

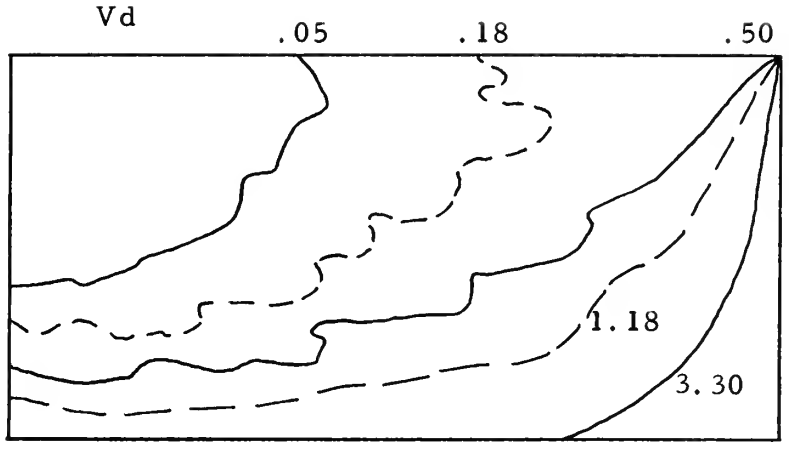

Direct Line Drive

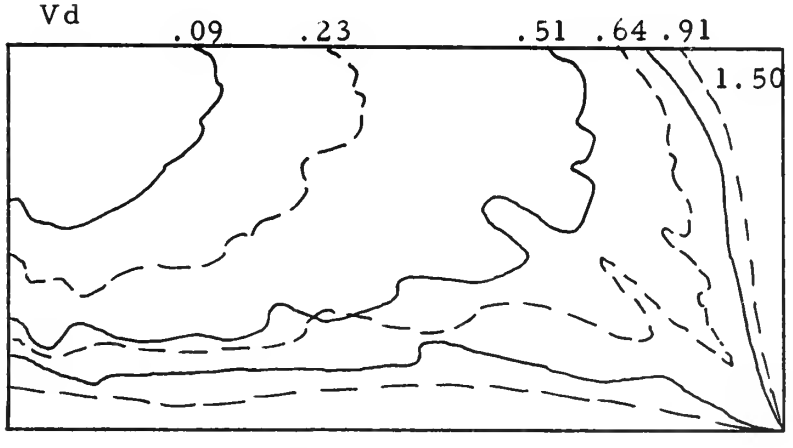

Staggered Line Drive

FIGURE 20. FLOOD FRONT TRACINGS, M = 3.13

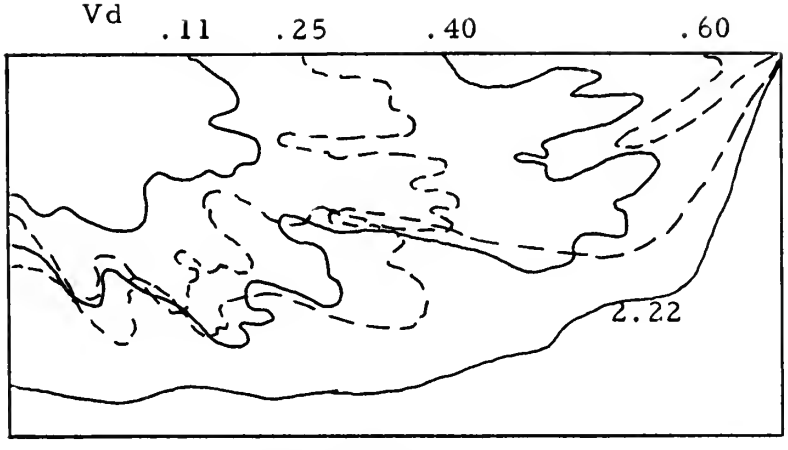

Direct Line Drive

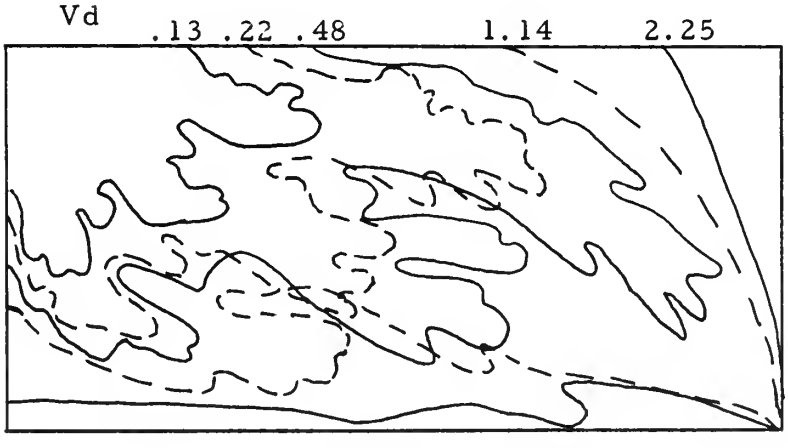

Staggered Line Drive

FIGURE 21. FLOOD FRONT TRACINGS, M = 12.1

APPENDIX B

TABLES AND FIGURES OF BASIC DATA

TABLE III

DIRECT LINE DRIVE

Run	Initial Pressure	Mobility Ratio
4	1.7	0.106

Elapsed Time	Corrected Time	Fractional Area Swept	Pressure	Conductance Ratio
0	-	0.025	8.6	0.198
1.0	-	0.057	9.8	0.174
2.0	-	0.094	10.1	0.168
3.0	-	0.135	10.2	0.166
5.0	-	0.181	10.3	0.165
19.27	-	0.672	11.2	0.152
21.27	-	0.741	11.6	0.146
24.27	-	0.809	12.9	0.132
27.27	-	0.855	13.6	0.125
29.27	-	0.915	14.5	0.117
31.27	-	0.937	14.9	0.114
37.27	-	0.954	15.3	0.111

Note: Areal sweep data is invalid.

TABLE IV

DIRECT LINE DRIVE

Run	Initial Pressure	Mobility Ratio
9	2.2	0.106

Elapsed Time	Corrected Time	Fractional Area Swept	Pressure	Conductance Ratio
0	-	0.039	-	-
1.00	-	0.104	10.4	0.216
2.16	-	0.143	10.6	0.208
9.75	-	0.340	10.8	0.204
13.50	-	0.479	10.9	0.202
20.08	-	0.712	11.4	0.193
23.41	-	0.844	11.9	0.185
24.41	-	0.870	12.6	0.175
25.41	-	-	13.5	0.163
26.41	-	0.926	14.2	0.155
27.41	-	-	14.7	0.150
29.08	-	0.949	15.3	0.144
35.91	-	0.974	15.4	0.143

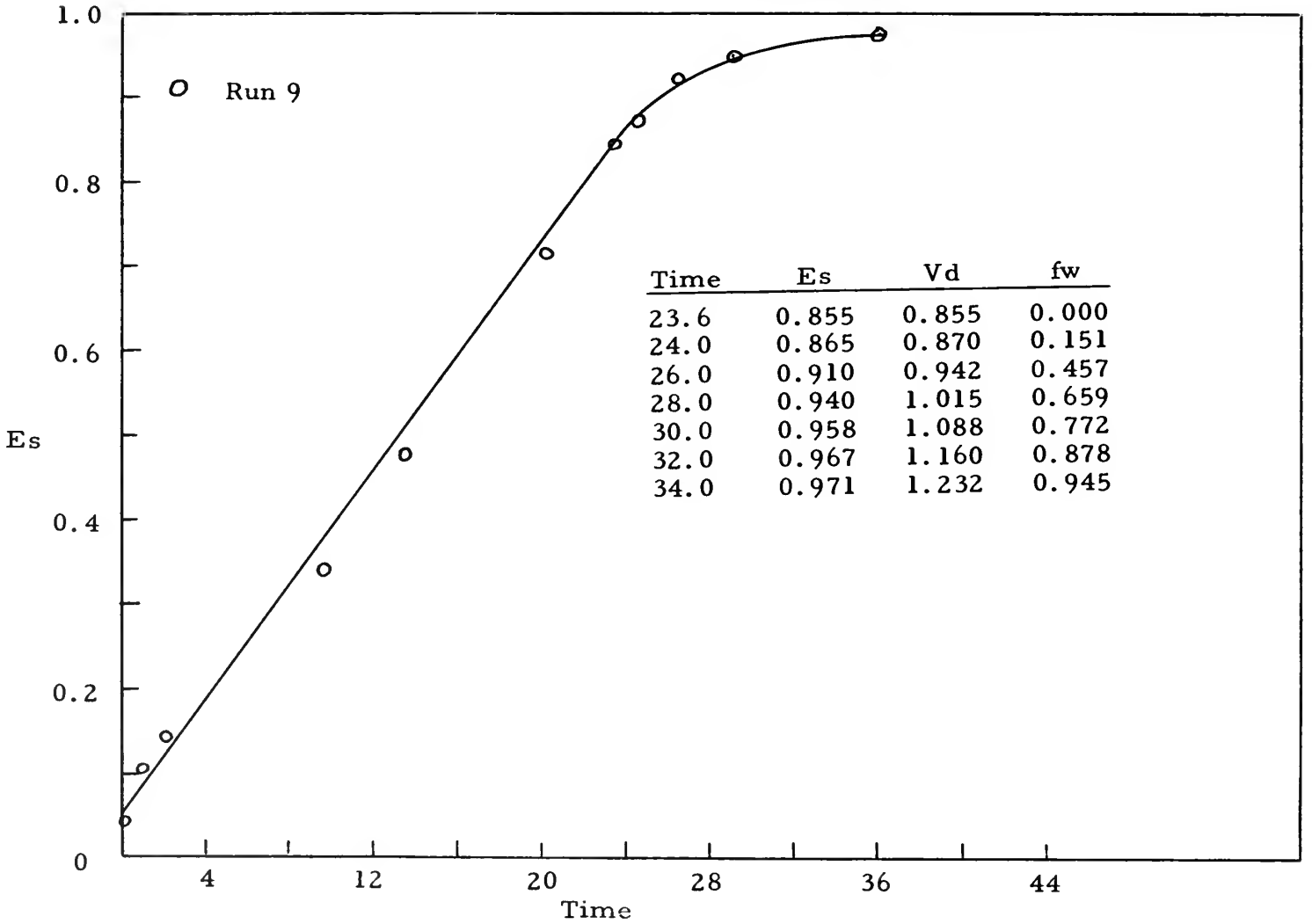

Time	Es	Vd	fw
23.6	0.855	0.855	0.000
24.0	0.865	0.870	0.151
26.0	0.910	0.942	0.457
28.0	0.940	1.015	0.659
30.0	0.958	1.088	0.772
32.0	0.967	1.160	0.878
34.0	0.971	1.232	0.945

FIGURE 22. DIRECT LINE DRIVE -- AREA SWEPT versus ELAPSED TIME
M = 0.106

TABLE V

DIRECT LINE DRIVE

Run	Initial Pressure	Mobility Ratio
2	6.5	0.274

Elapsed Time	Corrected Time	Fractional Area Swept	Pressure	Conductance Ratio
0	-	0.107	10.7	0.607
3.33	-	0.277	11.1	0.586
6.67	-	0.453	11.5	0.565
10.00	-	0.697	12.5	0.520
13.25	-	0.860	14.1	0.461
16.58	-	0.925	14.9	0.436
23.08	-	0.945	15.0	0.433
26.33	-	-	15.3	0.425
29.67	-	0.970	15.4	0.422

Note: Rerun as run 22.

TABLE VI

DIRECT LINE DRIVE

Run	Initial Pressure	Mobility Ratio
9	4.8	0.274

Elapsed Time	Corrected Time	Fractional Area Swept	Pressure	Conductance Ratio
0	0	0.194	7.3	0.658
1.0	1.9	0.288	7.3	0.658
2.0	3.8	0.372	7.3	0.658
3.0	5.7	0.467	7.3	0.658
4.0	7.6	0.558	7.3	0.658
5.0	9.5	0.665	7.3	0.658
7.0	13.3	0.848	8.5	0.565
8.0	15.2	-	9.0	0.533
9.0	17.1	0.897	9.2	0.522
10.0	19.0	-	9.5	0.505
11.0	20.9	0.930	-	

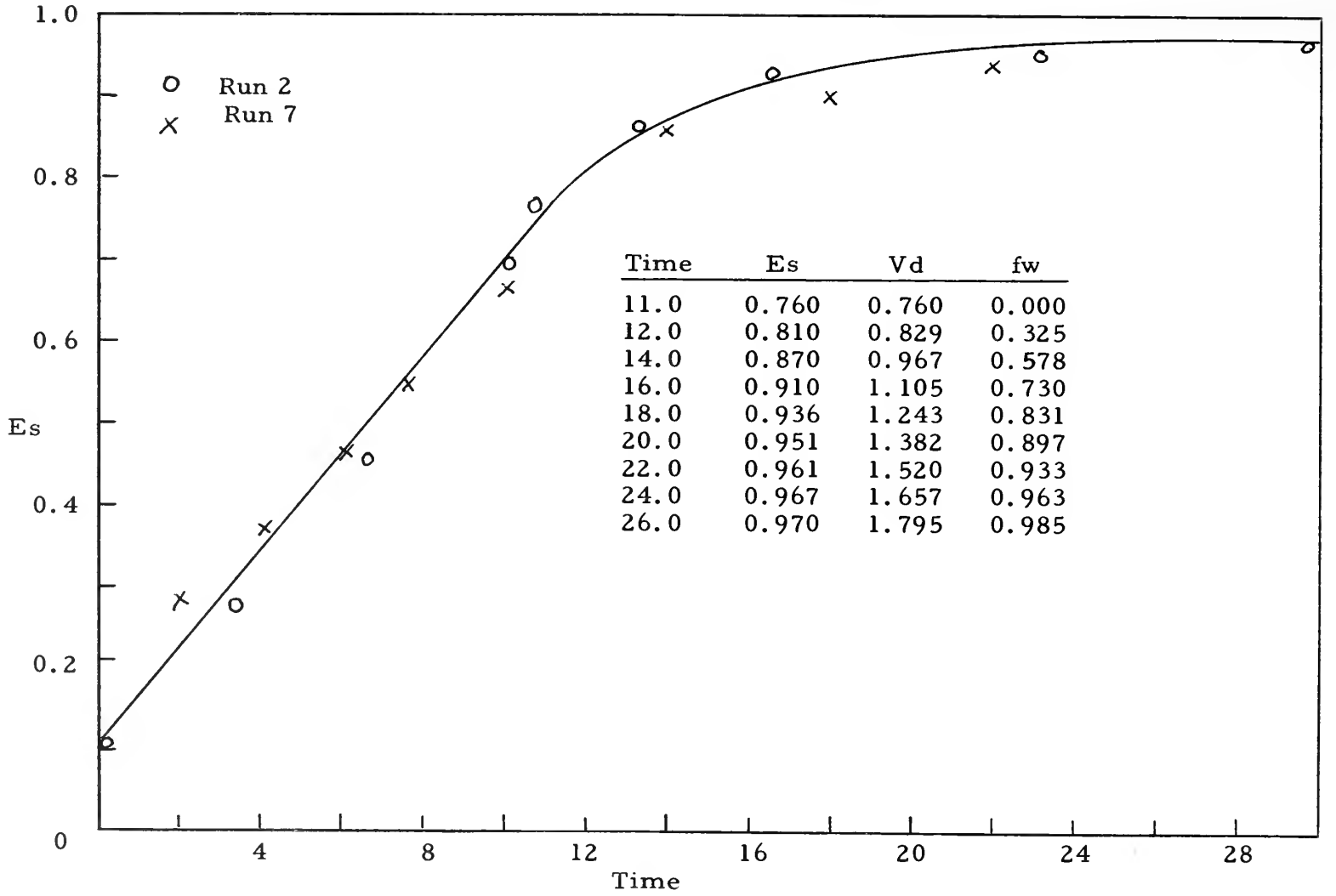

Time	Es	Vd	fw
11.0	0.760	0.760	0.000
12.0	0.810	0.829	0.325
14.0	0.870	0.967	0.578
16.0	0.910	1.105	0.730
18.0	0.936	1.243	0.831
20.0	0.951	1.382	0.897
22.0	0.961	1.520	0.933
24.0	0.967	1.657	0.963
26.0	0.970	1.795	0.985

FIGURE 23. DIRECT LINE DRIVE -- AREA SWEPT versus ELAPSED TIME
M = 0.274

TABLE VII

DIRECT LINE DRIVE

Run
1

Mobility Ratio
1.0

Elapsed Time	Corrected Time	Fractional Area Swept	Pressure	Conductance Ratio
0	-	0.0944		1.0
1.0	-	0.240	C	1.0
2.0	-	0.385	O	1.0
3.0	-	0.519	N	1.0
4.0	-	0.639	S	1.0
5.0	-	0.726	T	1.0
6.33	-	0.791	A	1.0
7.33	-	0.840	N	1.0
10.58	-	0.939	T	1.0
17.08	-	0.973		1.0

Note: Rerun as run 21.

TABLE VIII

DIRECT LINE DRIVE

Run
6

Mobility Ratio
1.0

Elapsed Time	Corrected Time	Fractional Area Swept	Pressure	Conductance Ratio
0	0	0.271		1.0
1.0	0.84	0.356	C	1.0
2.0	1.68	0.450	O	1.0
3.0	2.52	0.546	N	1.0
4.0	3.36	0.605	S	1.0
5.0	4.21	0.667	T	1.0
6.0	5.05	0.724	A	1.0
8.0	6.72	0.790	N	1.0
10.0	8.42	0.845	T	1.0
15.59	13.10	0.934		1.0
18.59	15.60	0.960		1.0

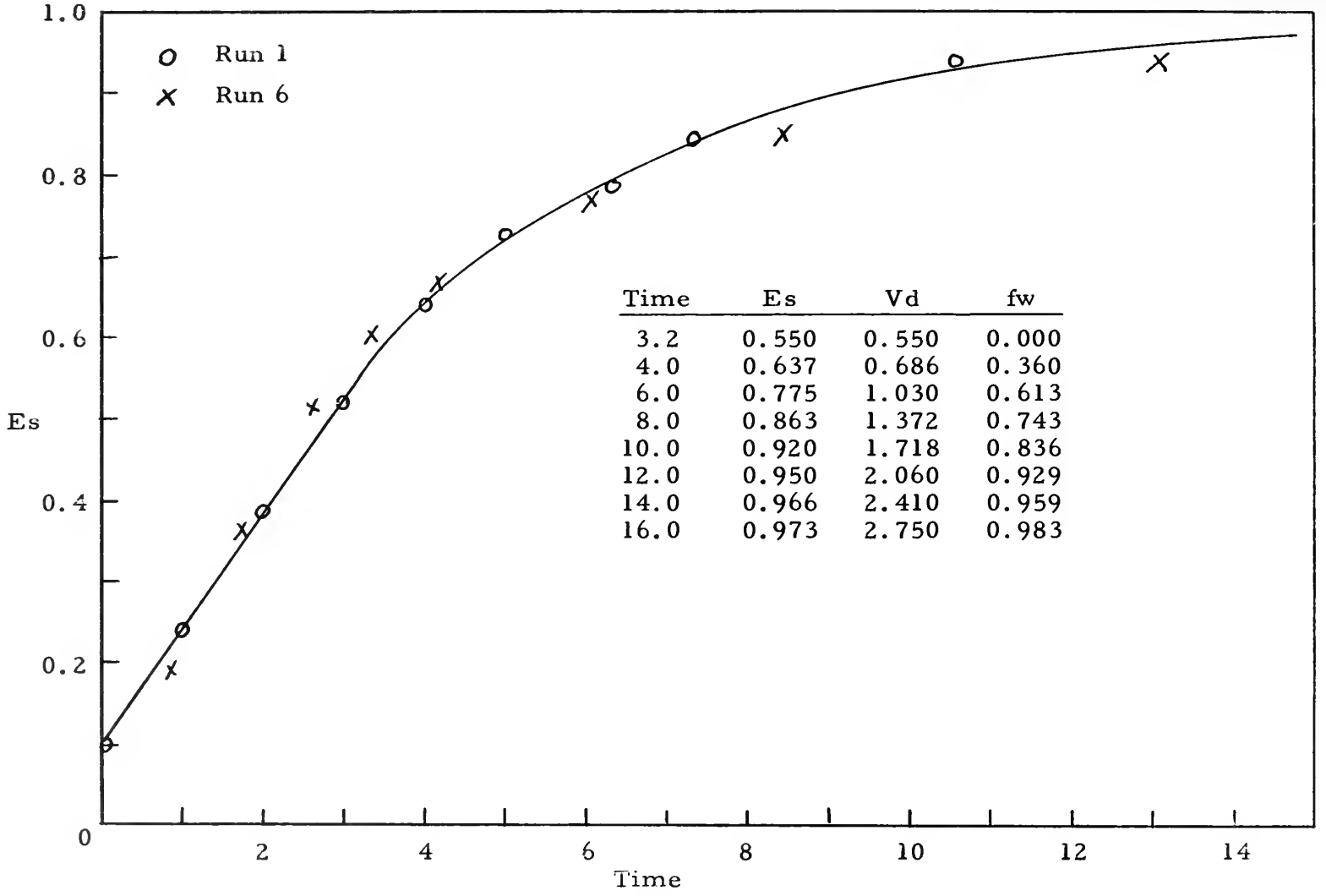

Time	Es	Vd	fw
3.2	0.550	0.550	0.000
4.0	0.637	0.686	0.360
6.0	0.775	1.030	0.613
8.0	0.863	1.372	0.743
10.0	0.920	1.718	0.836
12.0	0.950	2.060	0.929
14.0	0.966	2.410	0.959
16.0	0.973	2.750	0.983

FIGURE 24. DIRECT LINE DRIVE -- AREA SWEPT versus ELAPSED TIME
M = 1

TABLE IX

DIRECT LINE DRIVE

Run	Initial Pressure	Mobility Ratio
3	13.3	3.13

Elapsed Time	Corrected Time	Fractional Area Swept	Pressure	Conductance Ratio
0	-	0.099	-	-
1.0	-	0.210	-	-
2.0	-	0.327	9.1	1.46
3.0	-	0.432	9.1	1.46
4.0	-	0.482	8.1	1.64
5.0	-	0.530	7.3	1.83
10.78	-	0.654	7.0	1.90
17.40	-	0.750	7.0	1.90
21.25	-	0.798	7.0	1.90
28.00	-	0.862	7.0	1.90
34.00	-	0.896	7.0	1.90
35.00	-	0.913	7.0	1.90

Note: Areal sweep data is invalid.

TABLE X

DIRECT LINE DRIVE

Run	Initial Pressure	Mobility Ratio
8	12.4	3.13

Elapsed Time	Corrected Time	Fractional Area Swept	Pressure	Conductance Ratio
0	-	0.051	-	-
1.0	-	0.179	9.4	1.32
2.0	-	0.358	8.5	1.46
3.0	-	-	8.1	1.53
4.0	-	0.580	7.0	1.77
5.0	-	0.642	6.5	1.91
6.0	-	-	6.3	1.97
7.0	-	0.720	6.2	2.00
12.08	-	0.829	6.0	2.07
18.58	-	0.920	6.0	2.07
22.42	-	0.952	6.0	2.07
25.50	-	0.965	6.0	2.07

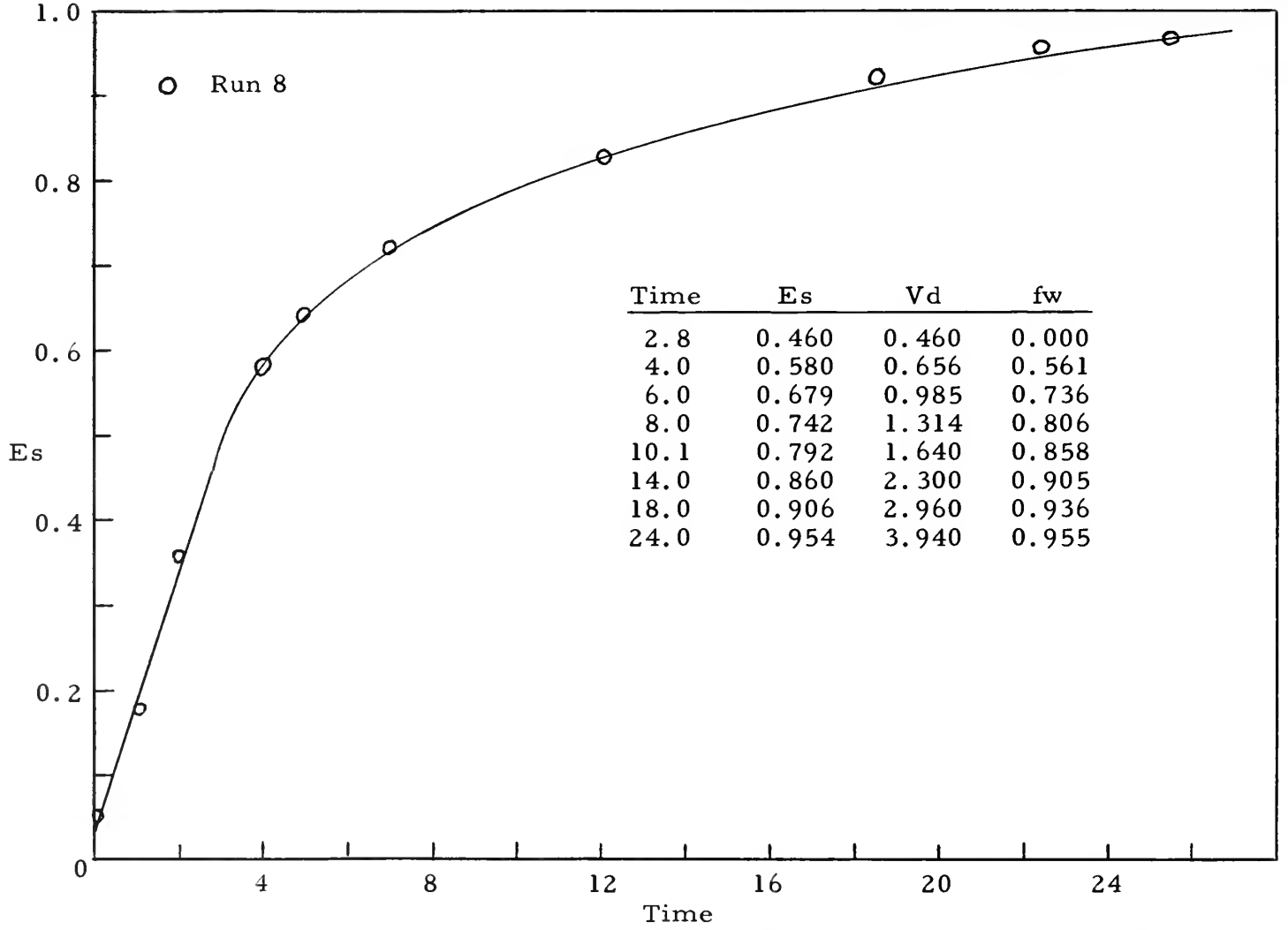

Time	Es	Vd	fw
2.8	0.460	0.460	0.000
4.0	0.580	0.656	0.561
6.0	0.679	0.985	0.736
8.0	0.742	1.314	0.806
10.1	0.792	1.640	0.858
14.0	0.860	2.300	0.905
18.0	0.906	2.960	0.936
24.0	0.954	3.940	0.955

FIGURE 25. DIRECT LINE DRIVE -- AREA SWEPT versus ELAPSED TIME
M = 3.13

TABLE XI

DIRECT LINE DRIVE

Run	Initial Pressure	Mobility Ratio
5	14.7	12.1

Elapsed Time	Corrected Time	Fractional Area Swept	Pressure	Conductance Ratio
0	-	0.065	-	-
1.0	-	0.101	-	-
2.0	-	0.157	6.7	2.19
3.0	-	0.207	6.7	2.19
4.0	-	0.259	6.7	2.19
6.0	-	0.354	6.7	2.19
7.0	-	0.410	6.6	2.23
8.0	-	-	5.9	2.49
9.0	-	0.496	5.0	2.94
10.0	-	-	4.4	3.34
11.0	-	0.525	3.5	4.20
12.0	-	-	2.9	5.07
13.0	-	0.545	2.8	5.26
18.62	-	0.586	2.7	5.45
22.93	-	-	2.6	5.65
29.13	-	0.616	2.3	6.40
39.67	-	0.670	2.3	6.40
56.93	-	0.709	2.3	6.40
74.25	-	0.742	2.3	6.40
91.55	-	0.778	2.3	6.40
119.38	-	0.812	2.3	6.40

Note: Areal sweep data is invalid.

TABLE XII

DIRECT LINE DRIVE

Run	Initial Pressure	Mobility Ratio
10	15.0	12.1

Elapsed Time	Corrected Time	Fractional Area Swept	Pressure	Conductance Ratio
0	-	0.038	-	-
1.0	-	0.107	9.1	1.65
2.0	-	0.173	9.1	1.65
3.0	-	0.247	8.8	1.70
4.0	-	0.323	8.5	1.77
5.0	-	0.401	8.3	1.81
6.0	-	-	7.0	2.14
7.0	-	0.507	4.2	3.57
8.0	-	-	3.6	4.17
9.0	-	0.551	3.4	4.41
10.0	-	-	3.4	4.41
18.0	-	0.654	3.0	5.00
24.59	-	0.706	2.8	5.36
28.34	-	-	2.8	5.36
34.92	-	0.740	2.8	5.36
41.50	-	0.789	2.8	5.36
51.92	-	0.807	2.8	5.36
62.25	-	0.833	2.8	5.36

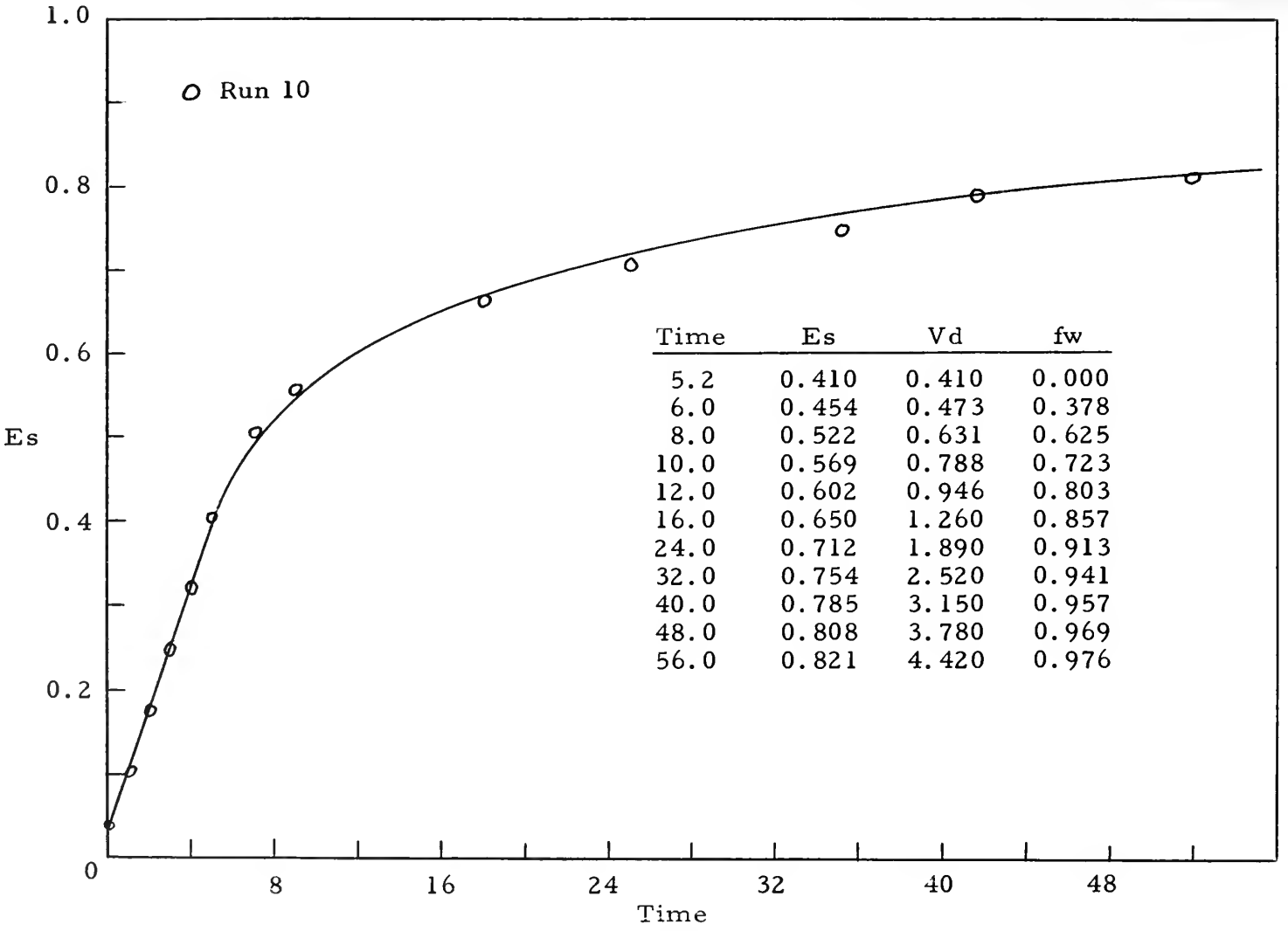

Time	Es	Vd	fw
5.2	0.410	0.410	0.000
6.0	0.454	0.473	0.378
8.0	0.522	0.631	0.625
10.0	0.569	0.788	0.723
12.0	0.602	0.946	0.803
16.0	0.650	1.260	0.857
24.0	0.712	1.890	0.913
32.0	0.754	2.520	0.941
40.0	0.785	3.150	0.957
48.0	0.808	3.780	0.969
56.0	0.821	4.420	0.976

FIGURE 26. DIRECT LINE DRIVE -- AREA SWEPT versus ELAPSED TIME
M = 12.1

TABLE XIII

STAGGERED LINE DRIVE

Run	Initial Pressure	Mobility Ratio
14	2.7	0.106

Elapsed Time	Corrected Time	Fractional Area Swept	Pressure	Conductance Ratio
0	-	0.122	11.7	0.230
6.08	-	0.282	11.8	0.229
13.08	-	0.482	12.0	0.225
16.66	-	0.598	12.1	0.223
23.16	-	0.768	12.5	0.216
26.16	-	0.918	13.7	0.197
27.16	-	-	14.2	0.190
28.16	-	0.955	14.7	0.184
29.16	-	0.969	15.0	0.180
30.16	-	-	15.2	0.178
31.16	-	-	15.4	0.175
32.16	-	0.978	15.6	0.173
37.16	-	0.989	15.7	0.171

TABLE XIV

STAGGERED LINE DRIVE

Run	Initial Pressure	Mobility Ratio
19	2.8	0.106

Elapsed Time	Corrected Time	Fractional Area Swept	Pressure	Conductance Ratio
0	0	0.0086	9.8	0.284
1.87	0.505	0.032	12.1	0.231
5.20	2.21	0.074	12.5	0.224
12.12	5.17	0.174	12.5	0.224
18.62	7.94	0.279	12.5	0.224
25.37	10.80	0.384	12.5	0.224
32.03	13.65	0.503	12.5	0.224
38.62	16.45	0.630	12.5	0.224
45.20	19.20	0.717	12.5	0.224
51.78	22.10	0.822	12.5	0.224
55.12	23.50	0.867	13.0	0.215
58.45	24.90	0.900	14.0	0.200
61.70	26.30	0.932	15.0	0.187
64.95	27.60	0.948	15.8	0.177
74.70	31.80	0.975	16.3	0.172
84.37	35.90	0.990	16.8	0.170

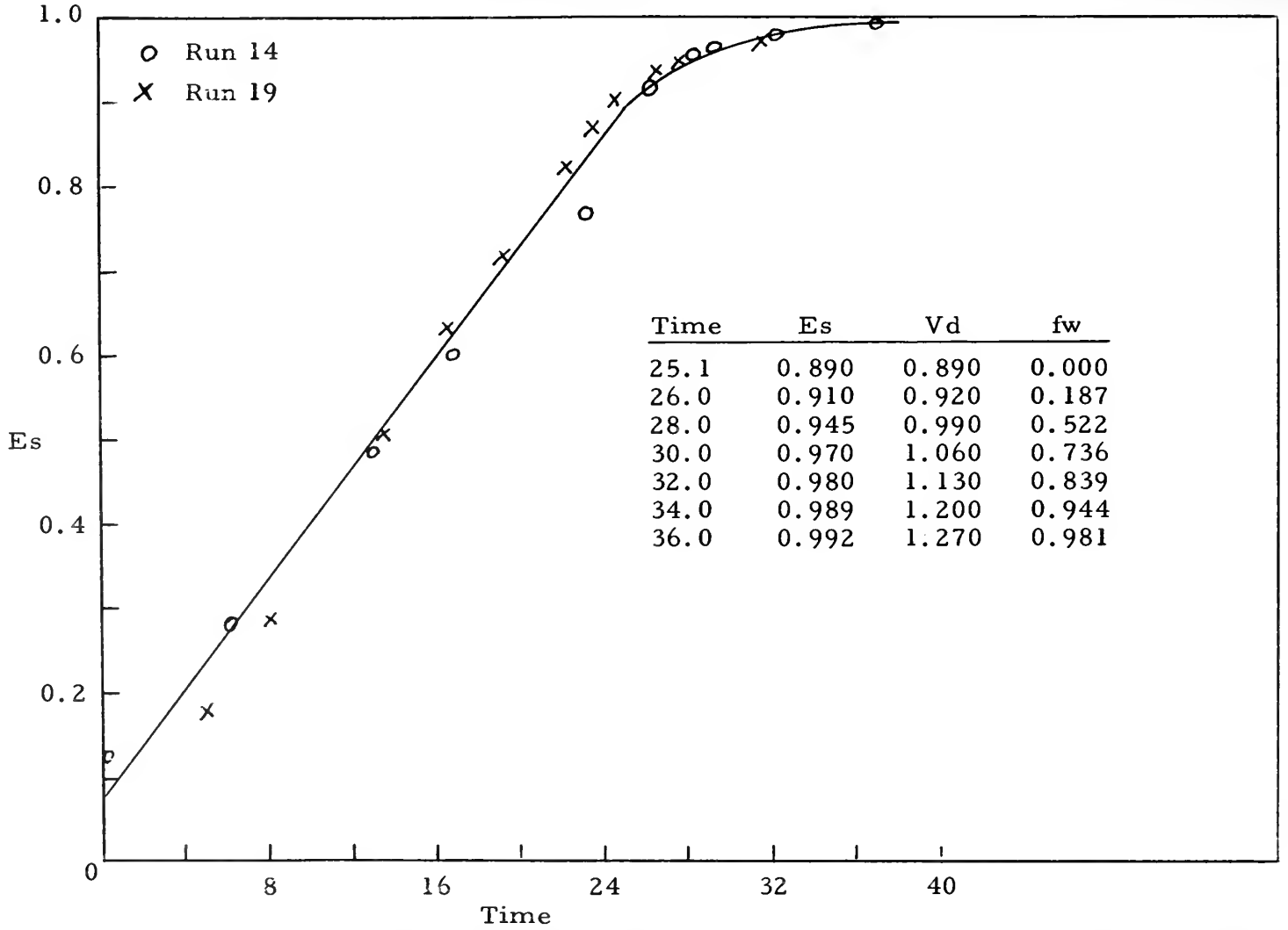

Time	Es	Vd	fw
25.1	0.890	0.890	0.000
26.0	0.910	0.920	0.187
28.0	0.945	0.990	0.522
30.0	0.970	1.060	0.736
32.0	0.980	1.130	0.839
34.0	0.989	1.200	0.944
36.0	0.992	1.270	0.981

FIGURE 27. STAGGERED LINE DRIVE -- AREA SWEPT versus ELAPSED TIME
M = 0.106

TABLE XV

STAGGERED LINE DRIVE

Run	Initial Pressure	Mobility Ratio
12	5.5	0.274

Elapsed Time	Corrected Time	Fractional Area Swept	Pressure	Conductance Ratio
0	-	0.066	-	-
2.0	-	0.187	-	-
4.0	-	0.275	-	-
5.0	-	0.347	-	-
6.0	-	0.396	10.7	0.514
7.0	-	0.461	10.7	0.514
9.0	-	0.584	10.7	0.514
11.0	-	0.718	10.7	0.514
13.0	-	0.842	11.3	0.486
14.0	-	0.923	11.8	0.466
15.0	-	0.950	12.0	0.458
17.0	-	0.971	12.2	0.451
21.0	-	0.980	12.2	0.451
25.0	-	0.988	12.2	0.451

TABLE XVI

STAGGERED LINE DRIVE

Run	Initial Pressure	Mobility Ratio
17	5.1	0.274

Elapsed Time	Corrected Time	Fractional Area Swept	Pressure	Conductance Ratio
0	0	0.414	9.1	0.560
1.0	0.934	0.871	9.5	0.537
2.0	1.88	0.143	9.5	0.537
3.0	2.80	0.196	9.6	0.531
4.0	3.74	0.257	9.6	0.531
6.0	5.60	0.372	9.6	0.531
8.0	7.47	0.481	9.6	0.531
10.0	9.34	0.597	9.6	0.531
12.0	11.20	0.703	9.7	0.526
13.0	12.10	-	9.8	0.520
14.0	13.10	0.793	10.1	0.505
15.0	14.00	0.884	10.6	0.481
16.0	14.94	-	11.0	0.464
17.0	15.88	0.951	11.3	0.451
19.0	17.75	0.976	11.5	0.443
20.0	18.68	-	11.6	0.440
21.0	19.60	0.987	11.7	0.436

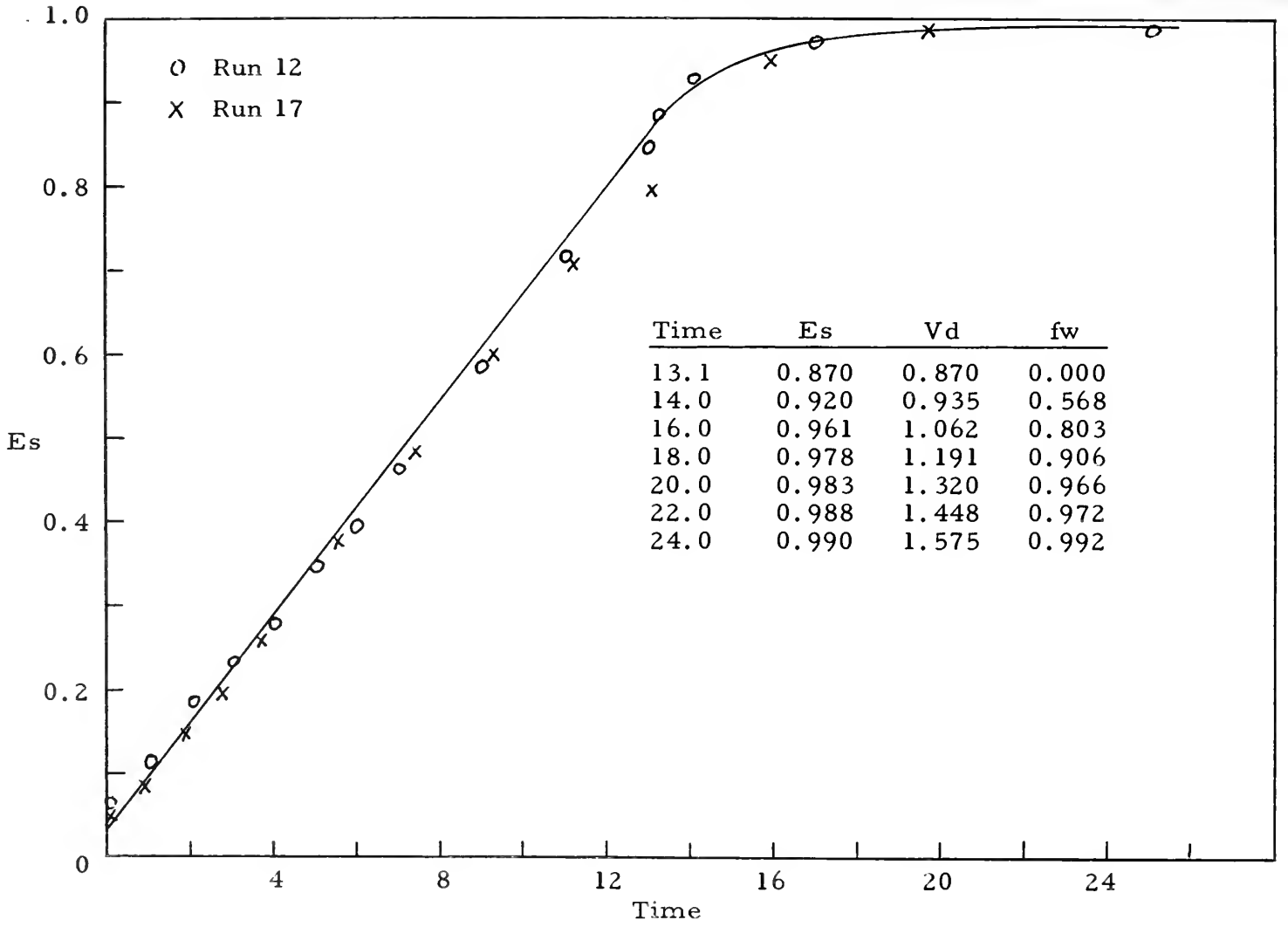

Time	Es	Vd	fw
13.1	0.870	0.870	0.000
14.0	0.920	0.935	0.568
16.0	0.961	1.062	0.803
18.0	0.978	1.191	0.906
20.0	0.983	1.320	0.966
22.0	0.988	1.448	0.972
24.0	0.990	1.575	0.992

FIGURE 28. STAGGERED LINE DRIVE -- AREA SWEPT versus ELAPSED TIME
M = 0.274

TABLE XVII

STAGGERED LINE DRIVE

Run
11

Mobility Ratio
1.0

Elapsed Time	Corrected Time	Fractional Area Swept	Pressure	Conductance Ratio
0	0	0.083	C	1.0
1.0	1.05	0.272	O	1.0
2.0	2.10	0.473	N	1.0
3.0	3.15	0.685	S	1.0
4.0	4.20	0.823	T	1.0
5.0	5.25	0.904	A	1.0
6.0	6.30	0.951	N	1.0
8.0	8.45	0.987	T	1.0

TABLE XVIII

STAGGERED LINE DRIVE

Run
16

Mobility Ratio
1.0

Elapsed Time	Corrected Time	Fractional Area Swept	Pressure	Conductance Ratio
0	-	0.113	C	1.0
1.0	-	0.281	O	1.0
2.0	-	0.450	N	1.0
3.0	-	0.611	S	1.0
4.0	-	0.775	T	1.0
5.0	-	0.876	A	1.0
6.0	-	0.940	N	1.0
7.0	-	0.967	S	1.0
8.0	-	0.992	T	1.0

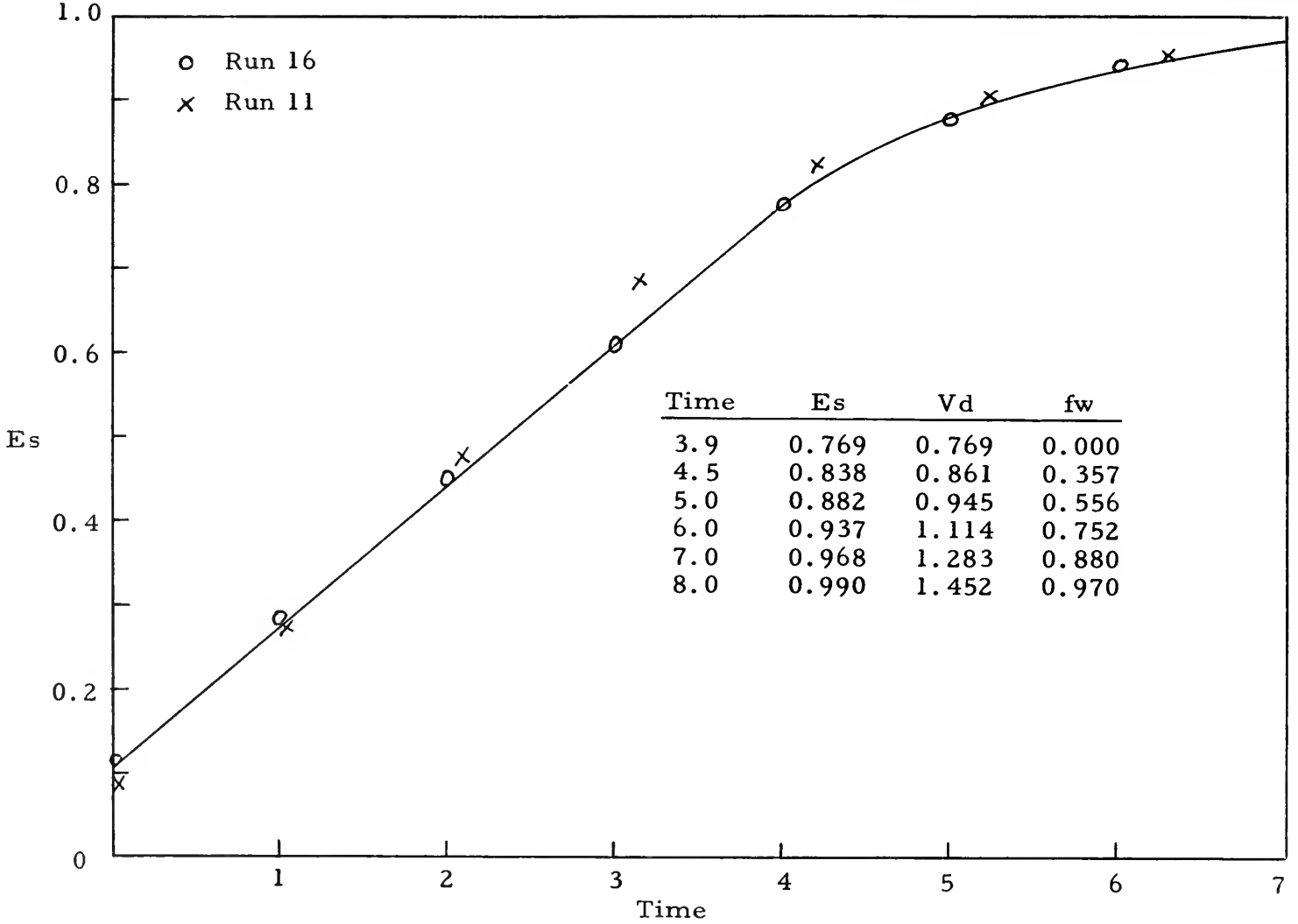

Time	Es	Vd	fw
3.9	0.769	0.769	0.000
4.5	0.838	0.861	0.357
5.0	0.882	0.945	0.556
6.0	0.937	1.114	0.752
7.0	0.968	1.283	0.880
8.0	0.990	1.452	0.970

FIGURE 29. STAGGERED LINE DRIVE -- AREA SWEPT versus ELAPSED TIME
M = 1

TABLE XIX

STAGGERED LINE DRIVE

Run	Initial Pressure	Mobility Ratio
13	14.7	3.13

Elapsed Time	Corrected Time	Fractional Area Swept	Pressure	Conductance Ratio
0	-	0.098	9.1	1.62
1.0	-	0.229	8.9	1.65
2.0	-	0.369	8.9	1.65
3.0	-	0.509	8.8	1.67
4.0	-	0.636	8.8	1.67
5.0	-	0.739	8.1	1.81
6.0	-	0.778	7.3	2.01
7.0	-	-	7.1	2.07
8.0	-	0.832	7.0	2.10
10.0	-	0.873	7.0	2.10
13.0	-	0.911	7.0	2.10
15.0	-	0.936	7.0	2.10
17.0	-	0.969	7.0	2.10
19.0	-	0.988	7.0	2.10

TABLE XX

STAGGERED LINE DRIVE

Run	Initial Pressure	Mobility Ratio
18	14.2	3.13

Elapsed Time	Corrected Time	Fractional Area Swept	Pressure	Conductance Ratio
0	0	0.098	-	-
1.0	0.728	0.191	-	-
2.0	1.46	0.287	-	-
3.0	2.19	0.377	-	-
4.0	2.92	0.465	-	-
5.0	3.64	0.553	10.5	1.35
6.0	4.37	0.632	10.5	1.35
7.0	5.10	0.694	10.4	1.37
8.0	5.83	0.759	10.1	1.41
9.0	6.56	0.802	9.9	1.43
10.0	7.28	-	9.5	1.49
11.0	8.02	0.837	9.2	1.54
12.0	8.75	-	9.1	1.56
13.0	9.48	0.866	9.0	1.58
15.0	10.92	0.895	9.0	1.58
18.0	13.10	0.920	9.0	1.58
20.0	14.60	0.956	9.0	1.58
23.0	16.80	1.973	9.0	1.58

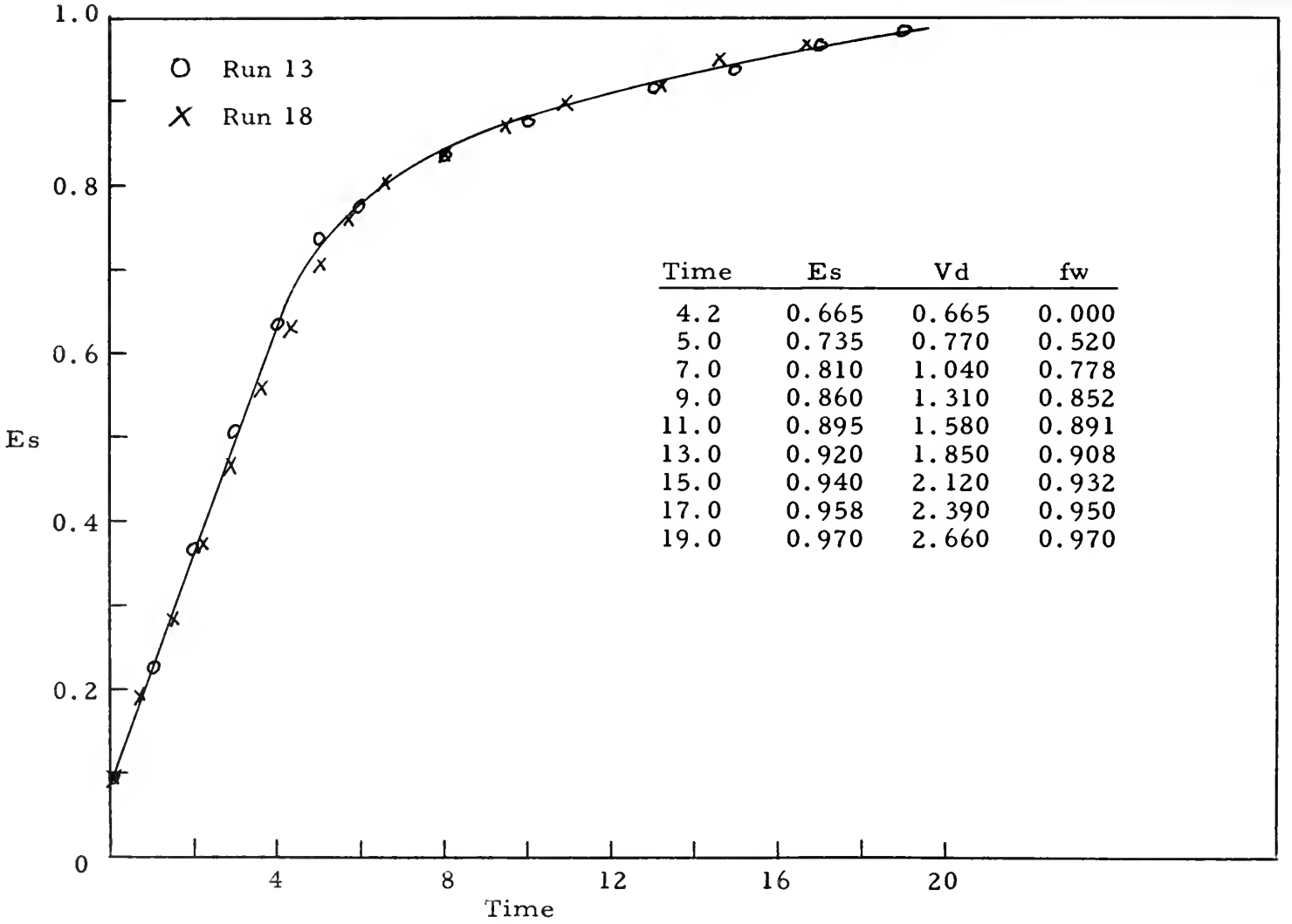

Time	Es	Vd	fw
4.2	0.665	0.665	0.000
5.0	0.735	0.770	0.520
7.0	0.810	1.040	0.778
9.0	0.860	1.310	0.852
11.0	0.895	1.580	0.891
13.0	0.920	1.850	0.908
15.0	0.940	2.120	0.932
17.0	0.958	2.390	0.950
19.0	0.970	2.660	0.970

FIGURE 30. STAGGERED LINE DRIVE -- AREA SWEPT versus ELAPSED TIME
M = 3.13

TABLE XXI

STAGGERED LINE DRIVE

Run	Initial Pressure	Mobility Ratio
15	16.0	12.1

Elapsed Time	Corrected Time	Fractional Area Swept	Pressure	Conductance Ratio
0	-	0.014	-	-
1.0	-	0.072	8.6	1.86
2.0	-	0.134	8.2	1.95
3.0	-	-	7.8	2.05
4.0	-	0.254	7.6	2.11
5.0	-	0.315	7.4	2.16
7.0	-	0.424	7.1	2.25
8.0	-	0.477	7.0	2.29
9.0	-	-	6.3	2.54
10.0	-	0.584	4.8	3.33
12.0	-	0.644	4.8	3.33
13.0	-	-	4.2	3.81
14.0	-	-	3.8	4.21
16.0	-	0.715	3.4	4.71
18.0	-	0.749	3.4	4.71
24.91	-	0.785	3.4	4.71
42.65	-	0.877	3.4	4.71
55.08	-	0.915	3.4	4.71

TABLE XXII

STAGGERED LINE DRIVE

Run	Initial Pressure	Mobility Ratio
20	16.5	12.1

Elapsed Time	Corrected Time	Fractional Area Swept	Pressure	Conductance Ratio
0	0	0.038	9.2	1.79
1.0	0.523	0.104	8.2	2.01
4.33	2.27	0.204	7.8	2.11
7.58	3.97	0.294	7.8	2.11
10.91	6.79	0.385	7.8	2.11
14.16	7.42	0.468	7.8	2.11
17.50	9.15	0.553	7.8	2.11
18.50	9.68	0.579	7.8	2.11
20.50	10.7	-	7.5	2.20
21.50	11.2	0.648	7.2	2.29
22.50	11.8	-	7.0	2.36
25.00	13.1	0.693	6.8	2.43
28.25	14.8	-	6.2	2.66
31.66	16.6	0.747	5.5	3.0
39.25	20.5	0.771	5.5	3.0
48.08	25.1	0.807	5.5	3.0
57.83	30.2	0.827	5.5	3.0
67.41	35.2	0.853	5.5	3.0
76.08	39.8	0.872	5.5	3.0

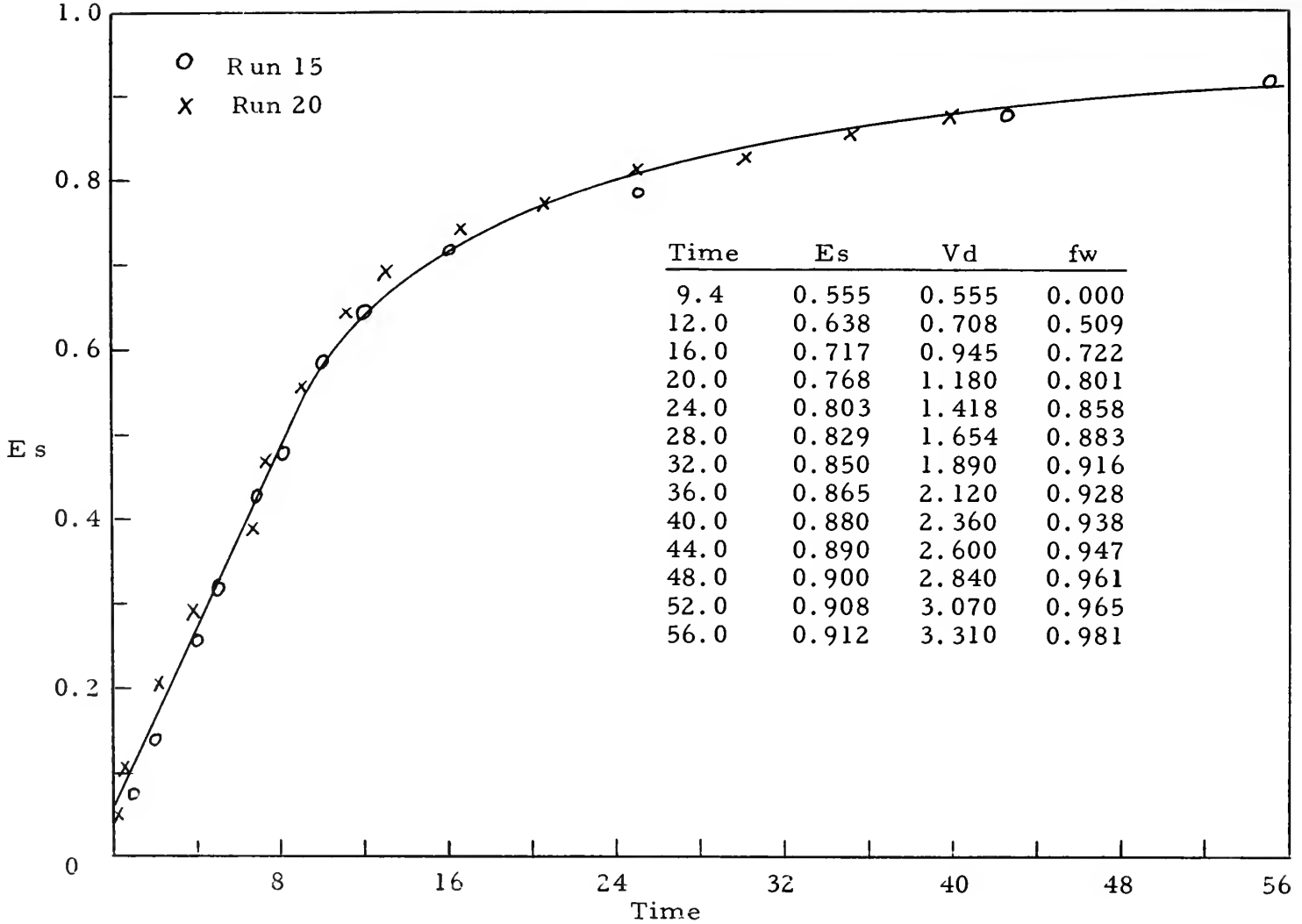

Time	Es	Vd	fw
9.4	0.555	0.555	0.000
12.0	0.638	0.708	0.509
16.0	0.717	0.945	0.722
20.0	0.768	1.180	0.801
24.0	0.803	1.418	0.858
28.0	0.829	1.654	0.883
32.0	0.850	1.890	0.916
36.0	0.865	2.120	0.928
40.0	0.880	2.360	0.938
44.0	0.890	2.600	0.947
48.0	0.900	2.840	0.961
52.0	0.908	3.070	0.965
56.0	0.912	3.310	0.981

FIGURE 31. STAGGERED LINE DRIVE -- AREA SWEPT versus ELAPSED TIME
M = 12.1

APPENDIX C

FIGURES OF INTERPRETED DATA

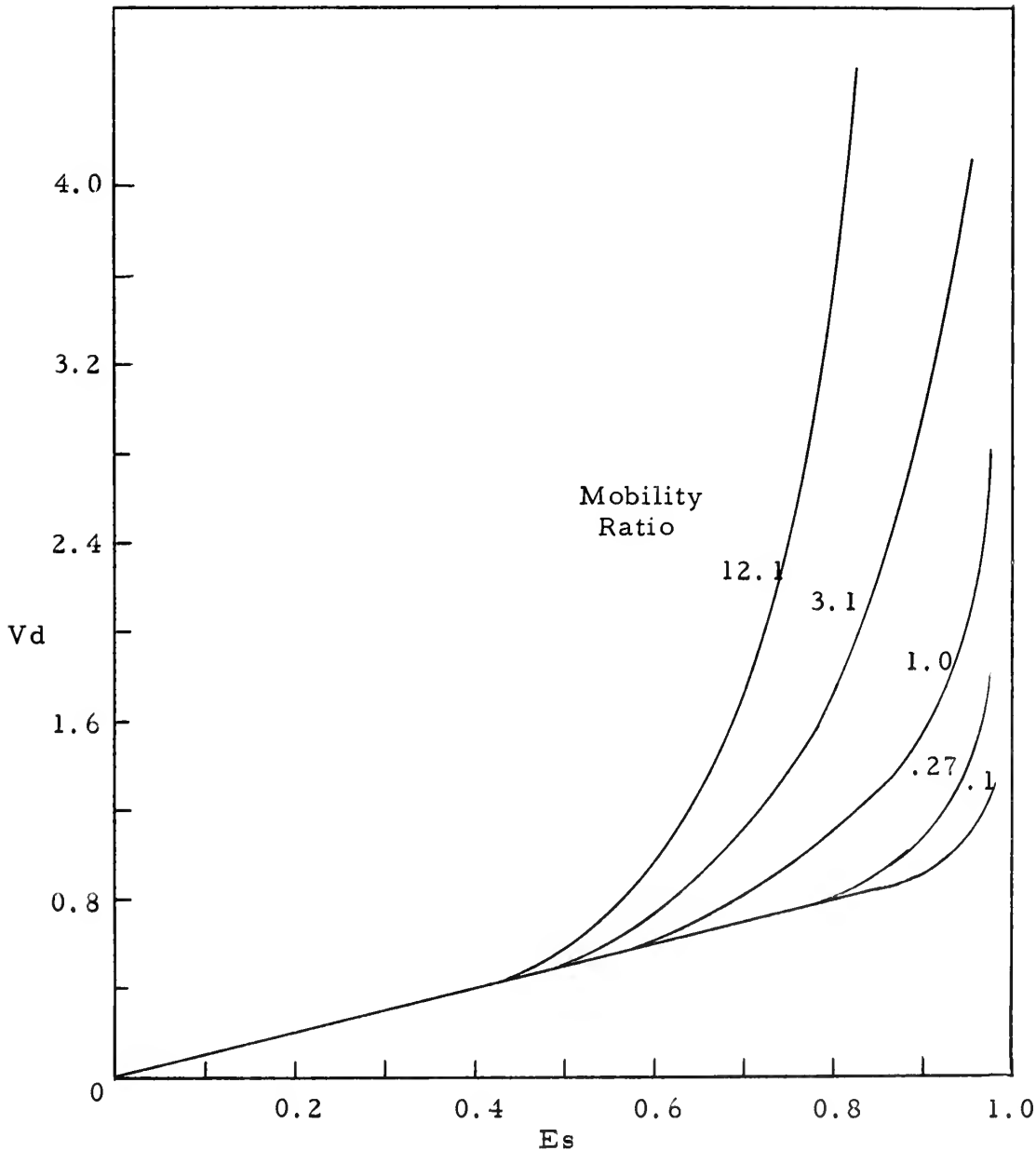

FIGURE 32. DIRECT LINE DRIVE -- MOBILITY RATIOS for DISPLACEABLE VOLUMES INJECTED versus AREA SWEPT

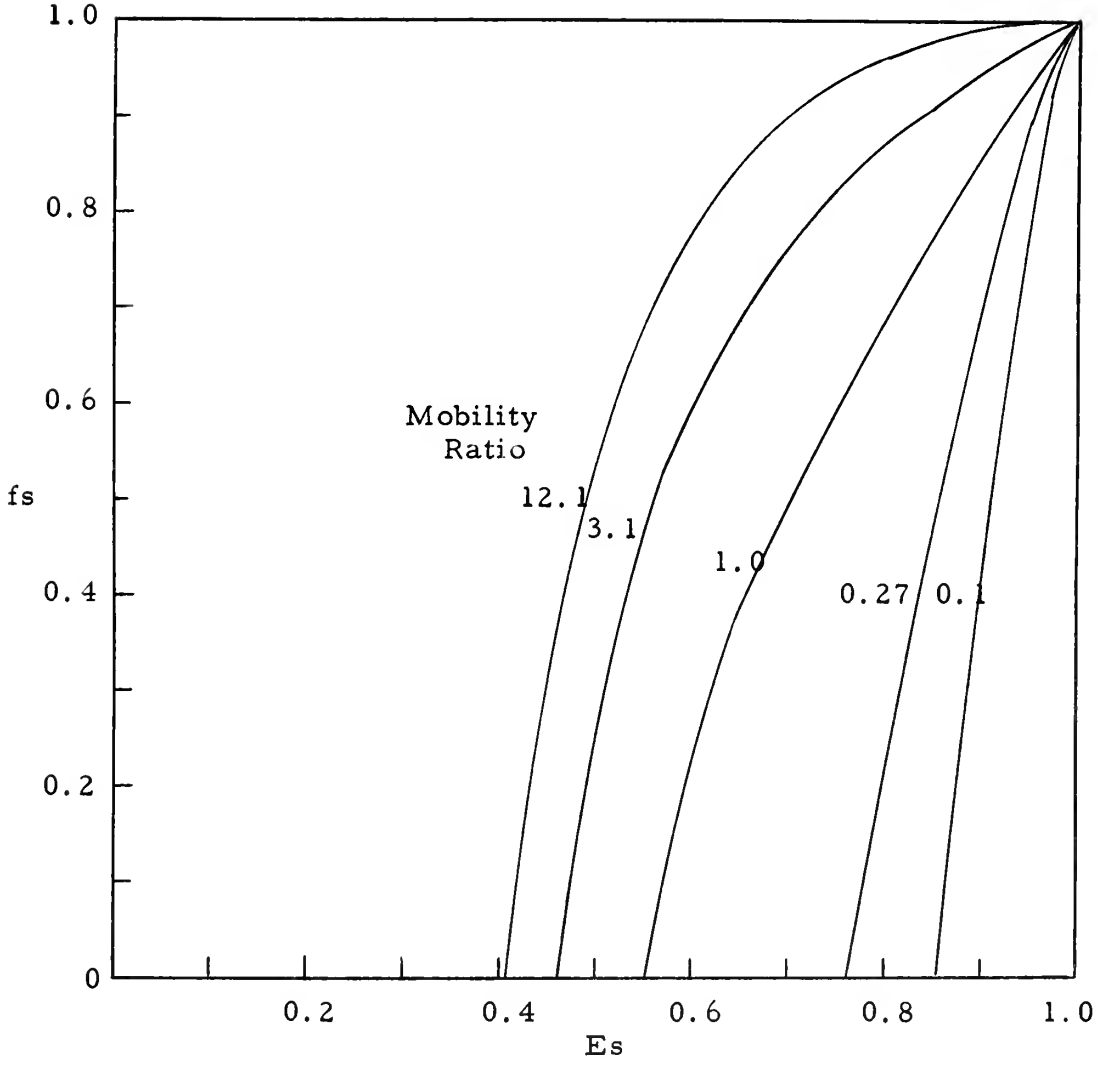

FIGURE 33. DIRECT LINE DRIVE -- MOBILITY RATIOS
for FRACTIONAL FLOW versus AREA SWEPT

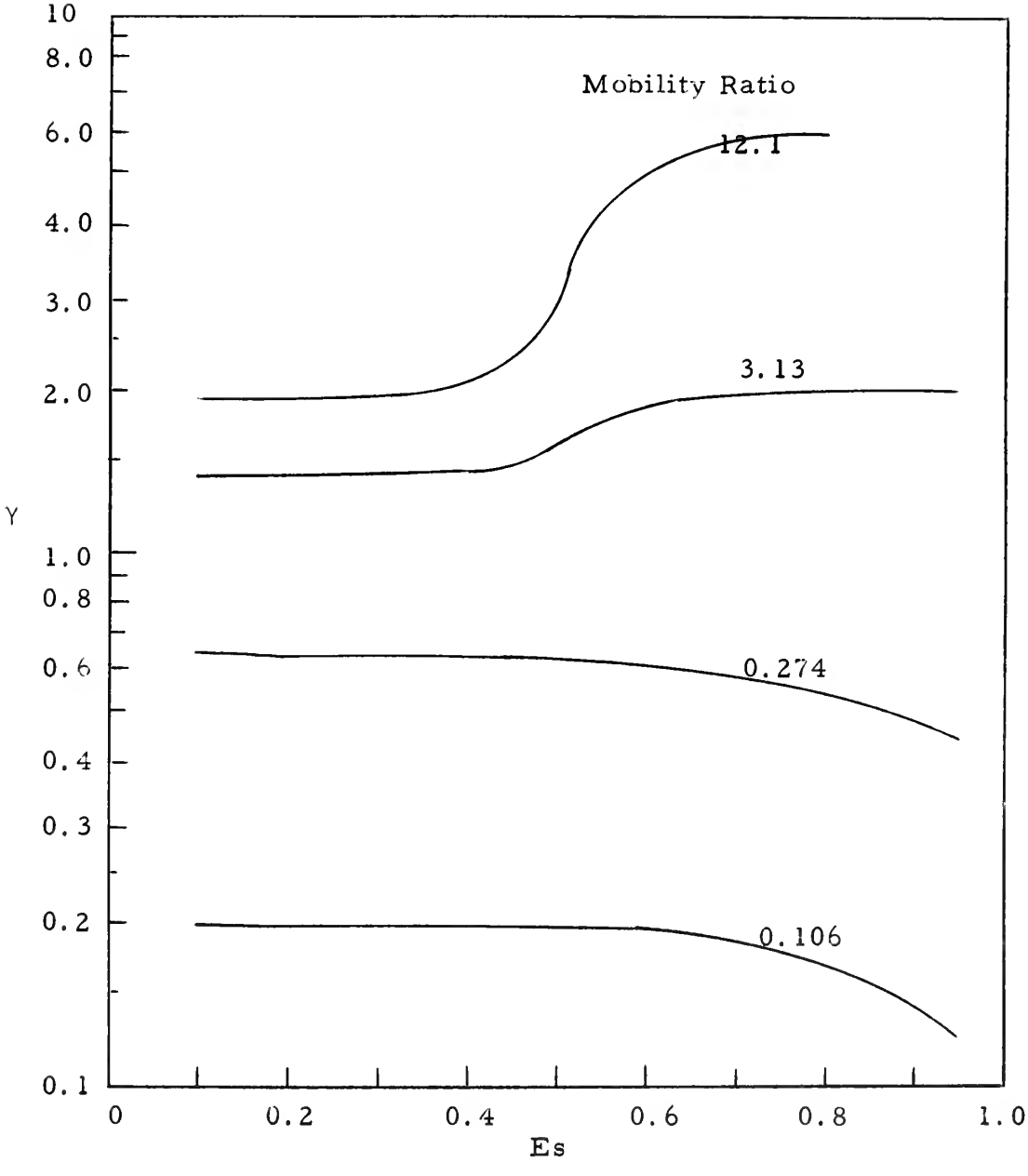

FIGURE 34. DIRECT LINE DRIVE -- MOBILITY RATIOS
for CONDUCTANCE RATIO versus AREA SWEPT

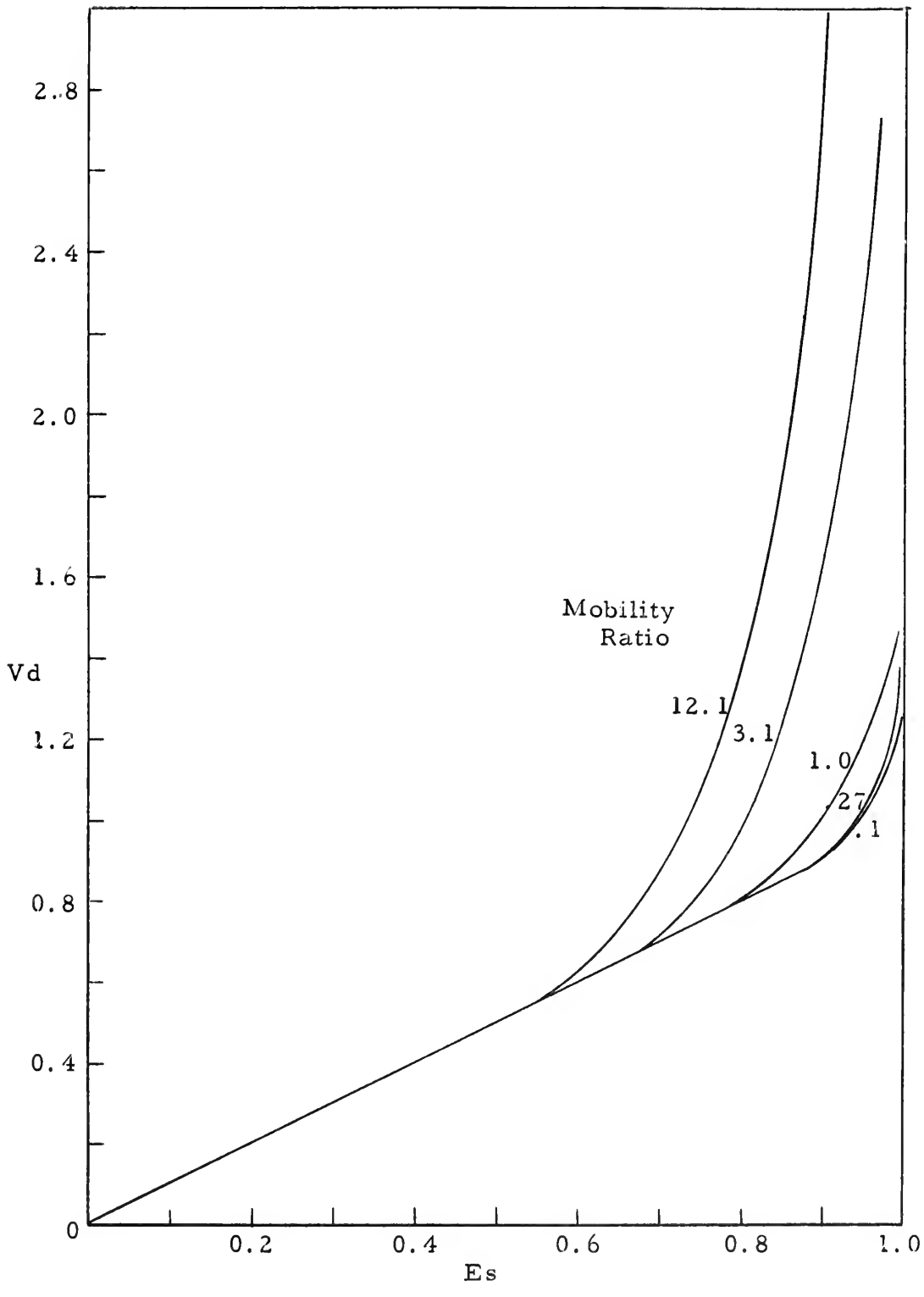

FIGURE 35. STAGGERED LINE DRIVE -- MOBILITY RATIOS for DISPLACEABLE VOLUME INJECTED versus AREA SWEPT

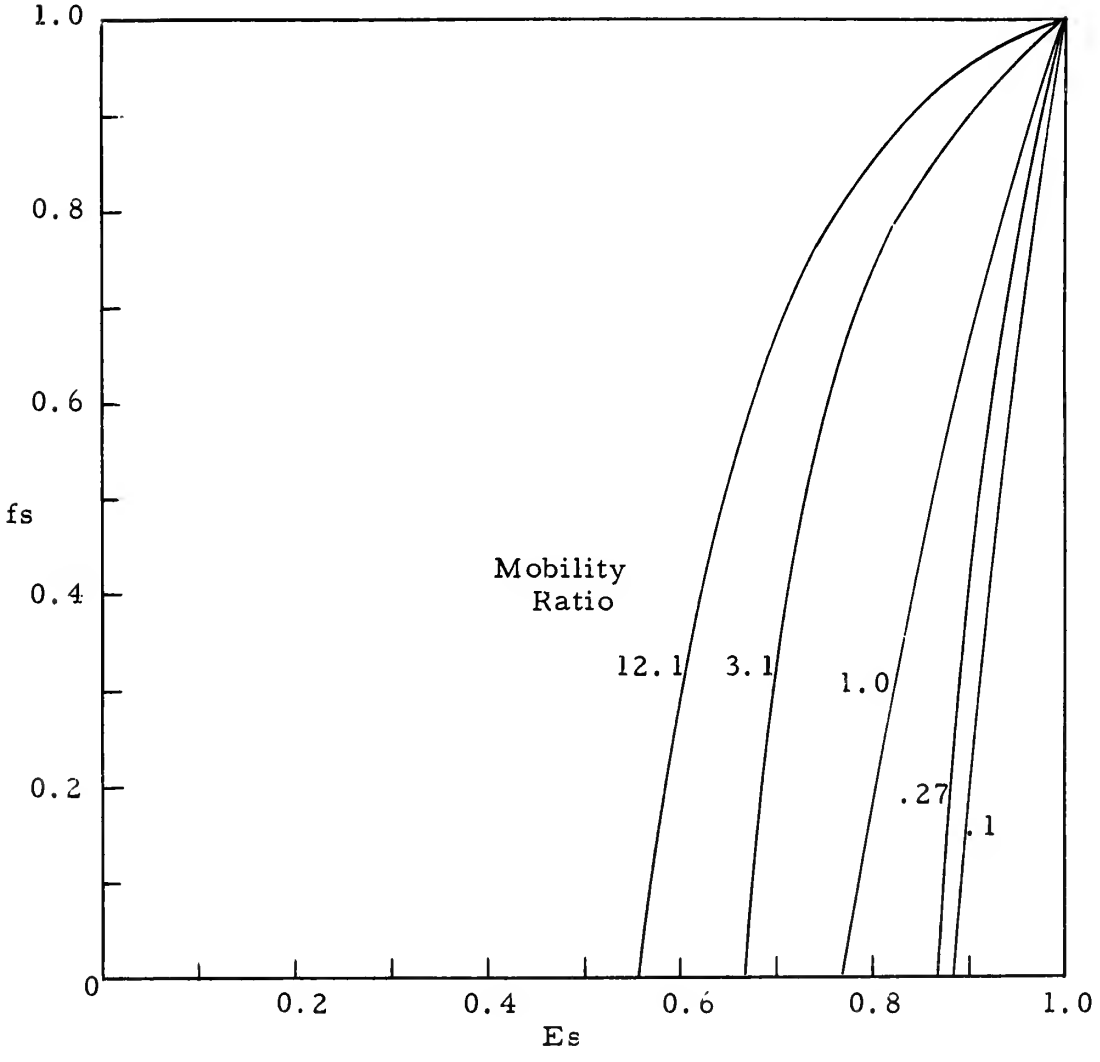

FIGURE 36. STAGGERED LINE DRIVE -- MOBILITY RATIOS for FRACTIONAL FLOW versus AREA SWEPT

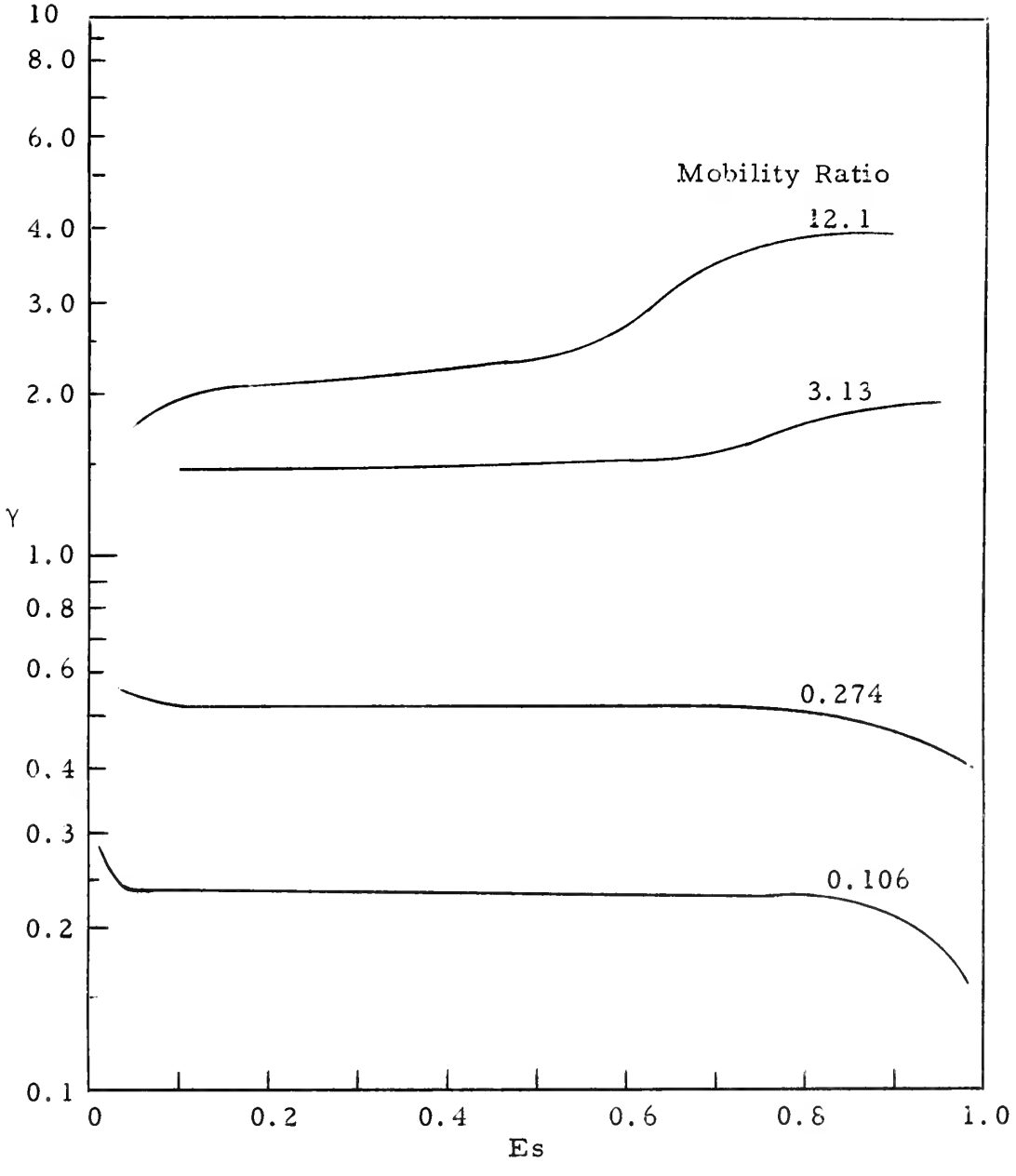

FIGURE 37. STAGGERED LINE DRIVE -- MOBILITY RATIOS for CONDUCTANCE RATIO versus AREA SWEPT

APPENDIX D

COMPUTED CONDUCTANCE RATIOS

```
      PROGRAM CONRA
      DIMENSION RM(10),DFS(20),ES(10,20)
      READ 1, JE,(RM(J), J=1,JE)
      READ 1, KE, (DFS(K), K=1,KE)
    1 FORMAT (I3,11F7.0)
      DO 10 J=1,JE
    2 FORMAT (11F7.0)
   10 READ 2, (ES(J,K), K=1,KE)
      RM IS THE MOBILITY RATIO AND JE IS THE NUMBER OF MOBILITY RATIOS
      WHICH ARE TO BE STUDIED.  DFS IS FRACTIONAL FLOW FROM THE SWEPT REGION
      AND KE IS THE NUMBER OF FRACTIONAL FLOW VALUES TO BE READ IN.
      ES VALUES ARE AREAL SWEEP EFFICIENCIES CORRESPONDING TO THE DFS VALUES.
      SET INITIAL VALUES
      D = 1.0
      A = D
      REI = 0.25*D
      RW = D/320.0
      RLW= 0.5*(D/A - 1.17 + 0.637*LOGF(A/REI))
      ESA = 3.1416*REI**2/(2.0*D*A)
      DO 70 J=1,JE
      PRINT 3,RM(J)
   30FORMAT (1H1,40X,16HMOBILITY RATIO =F5.2//10X,19H CONDUCTIVITY RATI
     1O,10X,14HFRACTION SWEPT,13X,2HFS//23X,7H1.00000,19X,1H0,19X,1H0)
      ESBT = ES(J,2)
      REP = SQRTF(2.0*D*A*(1.0-ESBT)/3.1416)
```

```
      DES = 0.01
      ES(J,1) = DES
      DO 70 K=1,KE
80    IF (ES(J,K) - ESA) 20,20,30
30    IF (ES(J,K) - ESBT) 40,50,50
20    DLW = 0.0
      RF = SQRTF(2.0*D*A*ES(J,K)/3.1416)
      GO TO 60
40    RF = REI
      DLW =RLW*(ES(J,K) - ESA)/(ESBT - ESA)
      DES = 0.05
      GO TO 60
50    RF = REI
      DLW = RLW
600CR = (LOGF(REI/RW) + 6.28*RLW+ LOGF(REP/RW))/(1./RM(J)*LOGF(RF/RW)
     1+ LOGF(REI/RF) + 6.28*(1./RM(J) - 1.0)*DLW + 6.28*RLW+ LOGF(REP/RW
     2)*(1.0 - DFS(K))/(1.0-DFS(K)/(RM(J)-DFS(K)*(RM(J)-1.0))))
      PRINT 4, CR,ES(J,K),DFS(K)
 4    FORMAT (10X,3F20.5)
      ES(J,K) = ES(J,K) + DES
      IF (ES(J,K) - ESBT) 80,70,70
70    CONTINUE
      END
```

Flow Diagram Program CONRA

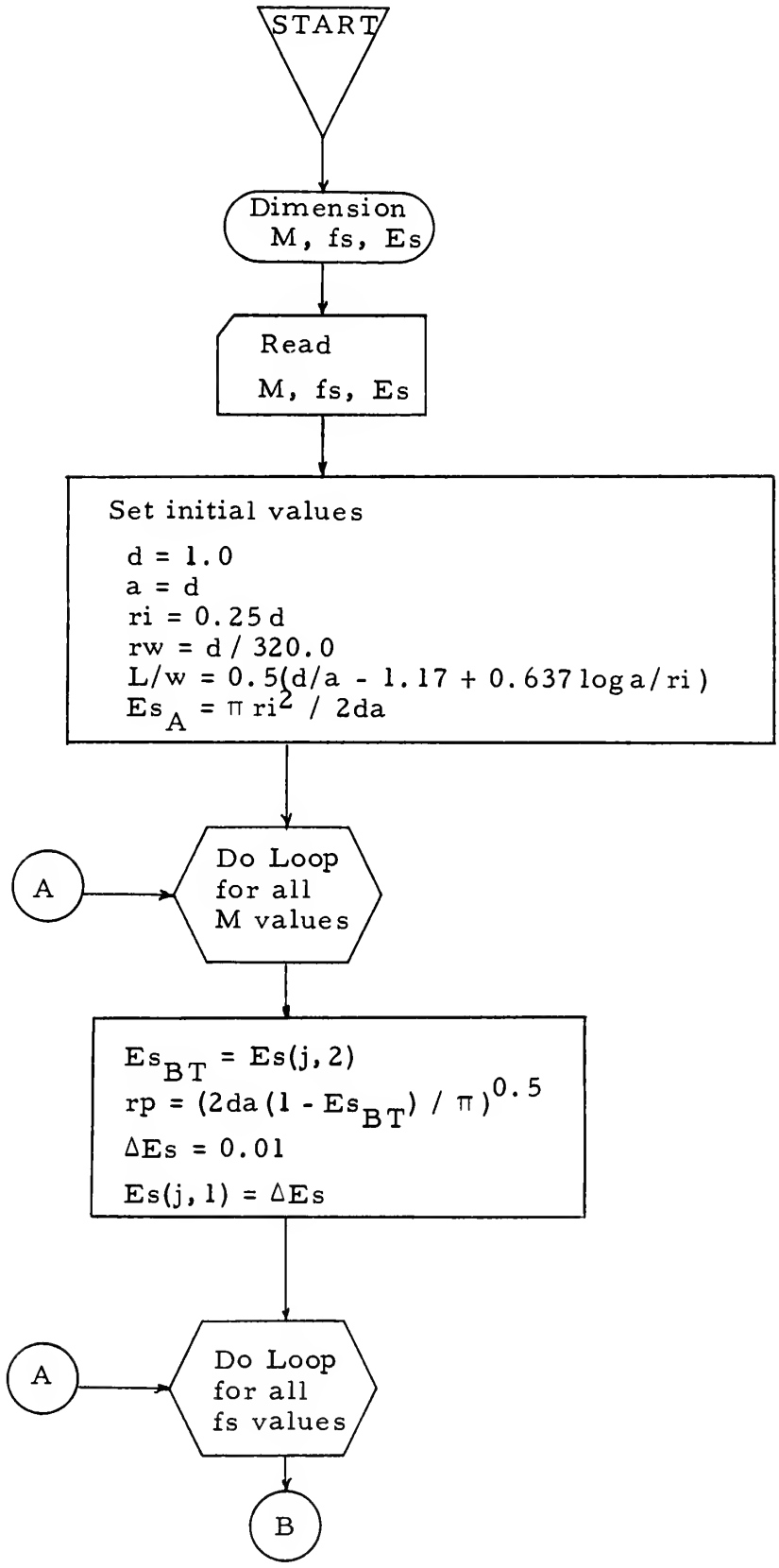

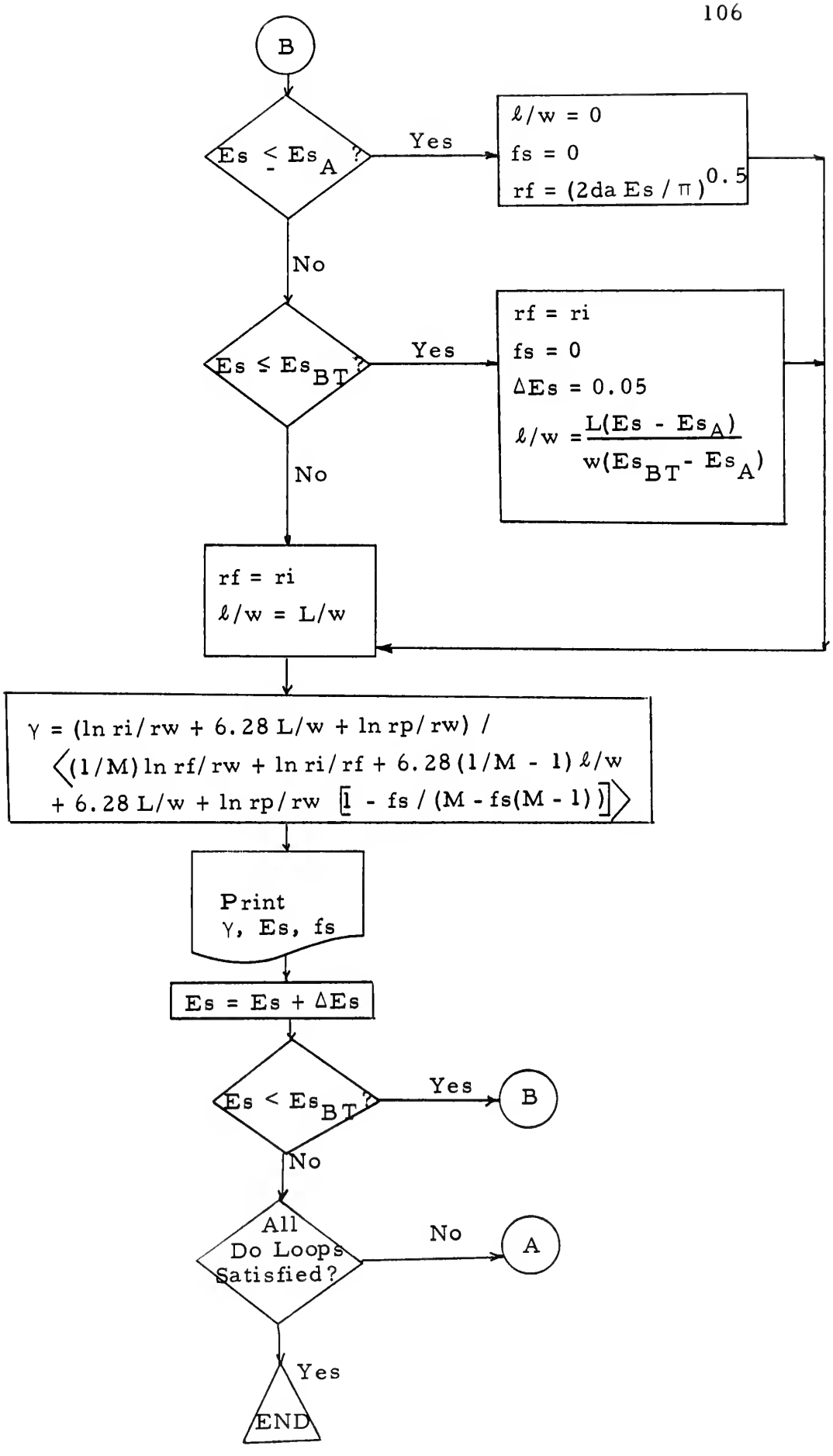
B
Es ≤ Es_A ?
Yes
ℓ/w = 0
fs = 0
rf = (2da Es / π)^0.5
No
Es ≤ Es_BT ?
Yes
rf = ri
fs = 0
ΔEs = 0.05
ℓ/w = L(Es - Es_A) / w(Es_BT - Es_A)
No
rf = ri
ℓ/w = L/w
γ = (ln ri/rw + 6.28 L/w + ln rp/rw) /
⟨(1/M) ln rf/rw + ln ri/rf + 6.28 (1/M - 1) ℓ/w
+ 6.28 L/w + ln rp/rw [1 - fs / (M - fs(M - 1))]⟩
Print
γ, Es, fs
Es = Es + ΔEs
Es < Es_BT ?
Yes
B
No
All
Do Loops
Satisfied?
No
A
Yes
END

FORTRAN SYMBOL CONVERSION CHART

FORTRAN	Nomenclature	Description
A	a	well spacing
CR	γ	conductance ratio
D	d	row spacing of wells
DES	ΔEs	increment of area swept
ES	Es	fractional area swept
ESA	Es_A	radial flow region around injection well
ESBT	Es_{BT}	area swept at breakthrough
DFS	fs	fractional flow from swept region
DLW	ℓ/w	partial length to width ratio
REI	ri	radius of radial flow region around injection well
REP	rp	radius of radial flow region around production well
RF	rf	frontal radius
RLW	L/w	length to width ratio
RM	M	mobility ratio
RW	rw	radius of wellbore

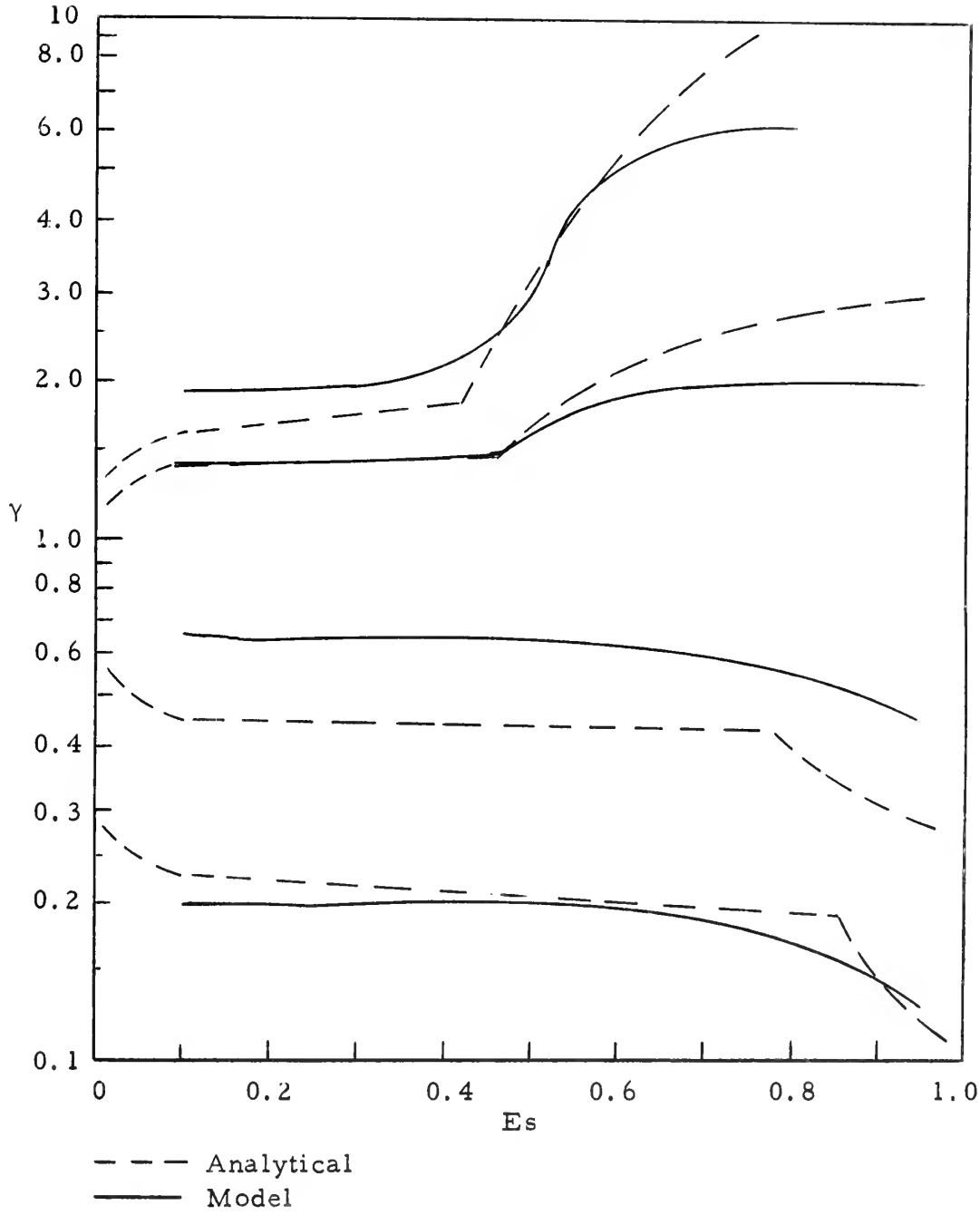

FIGURE 38. DIRECT LINE DRIVE -- COMPARISON OF ANALYTICAL and MODEL CONDUCTANCE RATIOS

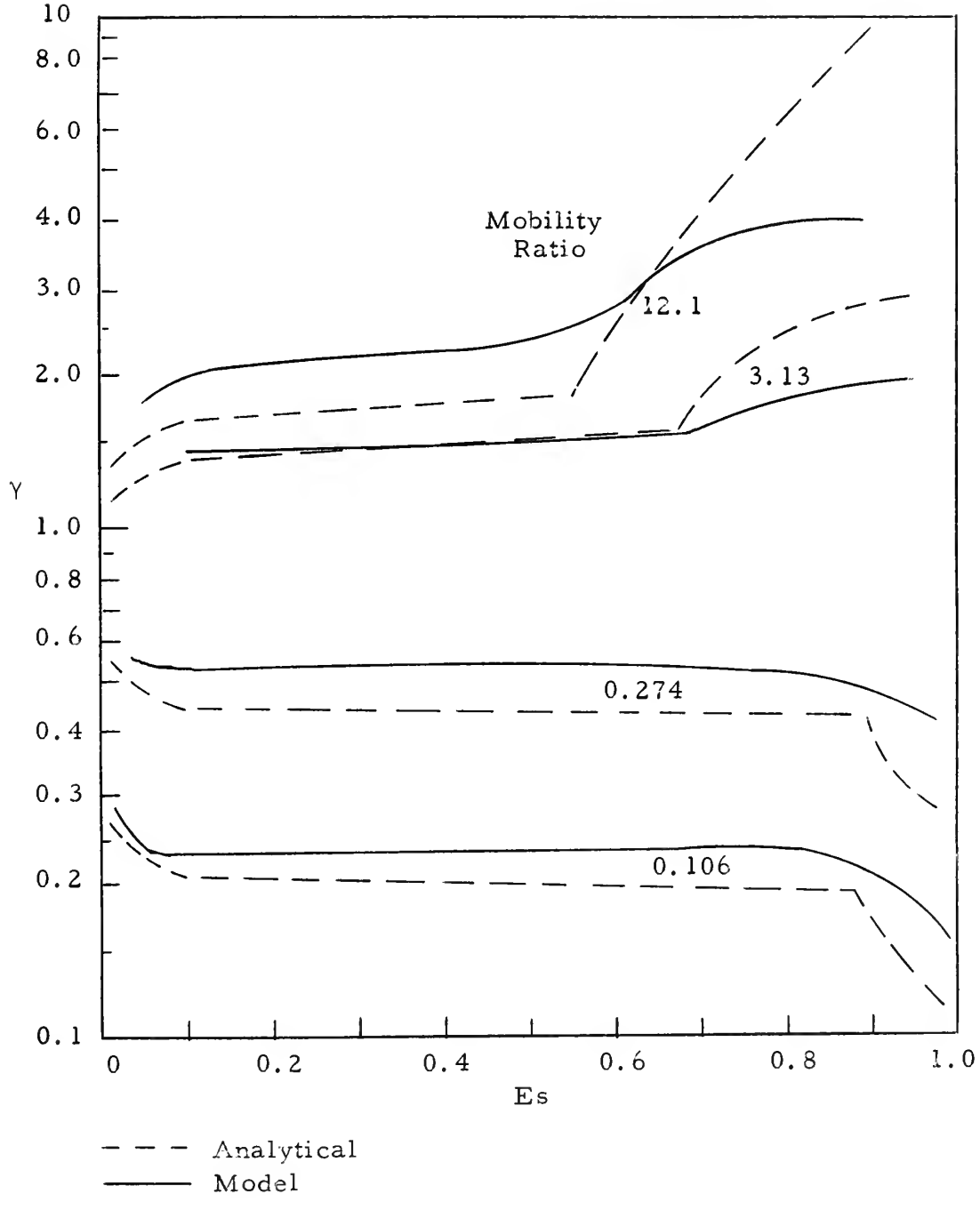

FIGURE 39. STAGGERED LINE DRIVE -- COMPARISON OF ANALYTICAL and MODEL CONDUCTANCE RATIOS

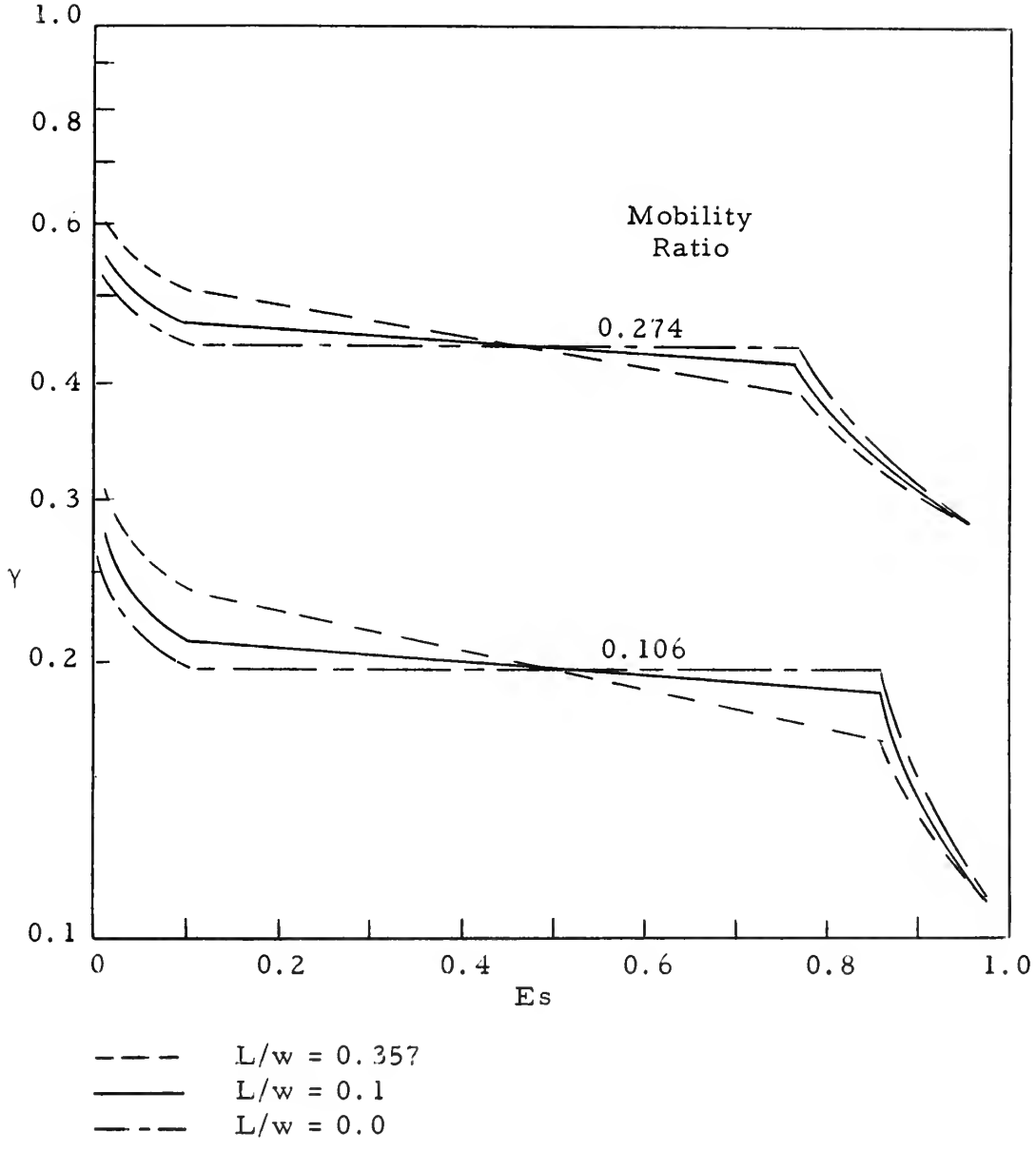

FIGURE 40. DIRECT LINE DRIVE -- EFFECT OF L/w RATIO ON CONDUCTANCE RATIO

APPENDIX E

EXAMPLE PREDICTION FOR STRATIFIED RESERVOIR

APPENDIX E

EXAMPLE PREDICTION FOR STRATIFIED RESERVOIR

To illustrate the procedure described for stratified reservoirs, assume a staggered line drive unit of 40 acres well spacing composed of 2 strata. Under reservoir conditions, the oil viscosity is 4 cp and the water viscosity is 0.4 cp. Assume that no gas saturation exists.

The reservoir properties are:

	Stratum 1	Stratum 2
Height	20 feet	20 feet
Porosity	0.30	0.25
Connate water (Scw)	0.30	0.25
Residual oil (Sro)	0.30	0.30
k_o (at Scw)	200 md	75 md
k_w (at Sro)	20 md	22 md

The bulk volume in each stratum will be the same or (20) (80) = 1600 acre ft.

$$Vd = Vb\,\phi\,(1-Scw-Sro)$$

$$Vd_1 = (1600)\,(0.30)\,(1-0.30-0.30) = 192 \text{ acre-ft}$$

$$Vd_2 = (1600)\,(0.25)\,(1-0.25-0.30) = 180 \text{ acre-ft}$$

The mobility ratios for each stratum are

$$M = (k_w/\mu_w)/(k_o/\mu_o)$$

$$M_1 = (20/0.4)/(200/4) = 1$$

$$M_2 = (22/0.4)/(75/4) = 3.13$$

and

$$\frac{k_1 Vd_1}{k_2 Vd_2} = \frac{(200)(192)}{(75)(180)} = 2.84$$

To obtain ct for each stratum from equation (25) the inverse of the conductance ratio is plotted versus displaceable volumes injected (from Figures 13 and 15). The resulting curves (Figure 41) are graphically integrated to obtain ct_1 and ct_2. (Note that the data for each Figure is in the preceding Table.)

Cumulative water injected and the corresponding oil produced are obtained from Figure 13 in dimensionless terms of displaceable volumes injected and fractional area swept. These are then converted to Wi and Np and plotted for each stratum versus ct in Figure 42. Total water injected and oil produced can be obtained from Figure 42 by summing the Wi and Np curves for each stratum and is plotted in Figure 43. This curve can be converted to an actual time relationship by knowing the maximum injection rate and well allowables. Fractional flow from the swept region is obtained as the slope of the Np versus Wi curve and the total conductance ratio is obtained from equation (31). Fractional flow is plotted on Figure 43 and conductance ratio versus water injected for the system is plotted on Figure 44.

The above example does not consider the presence of a free gas saturation at the start of the water flood. However, it will be within the realm of engineering accuracy to assume that oil bank fill up occurs simultaneously in all strata. This will be true except in the case of high gas saturations because of the unusually favorable mobility ratio during oil bank fill up. The volume occupied by free gas prior to oil

bank fill up can then be added to the cumulative water injected and volume swept to obtain satisfactory performance predictions when there is free gas present at the beginning of the flood.

TABLE XXIII

Wi/Vd fraction	Wi acre-ft	γ_2	$1/\gamma_2$
0	0	1.0	1.0
0.1	18.0	1.48	0.675
0.5	90.0	1.50	0.675
0.665	119.8	1.52	0.657
1.0	180.0	1.75	0.571
1.5	270.0	1.83	0.546
2.0	360.0	1.84	0.544
2.5	450.0	1.85	0.540

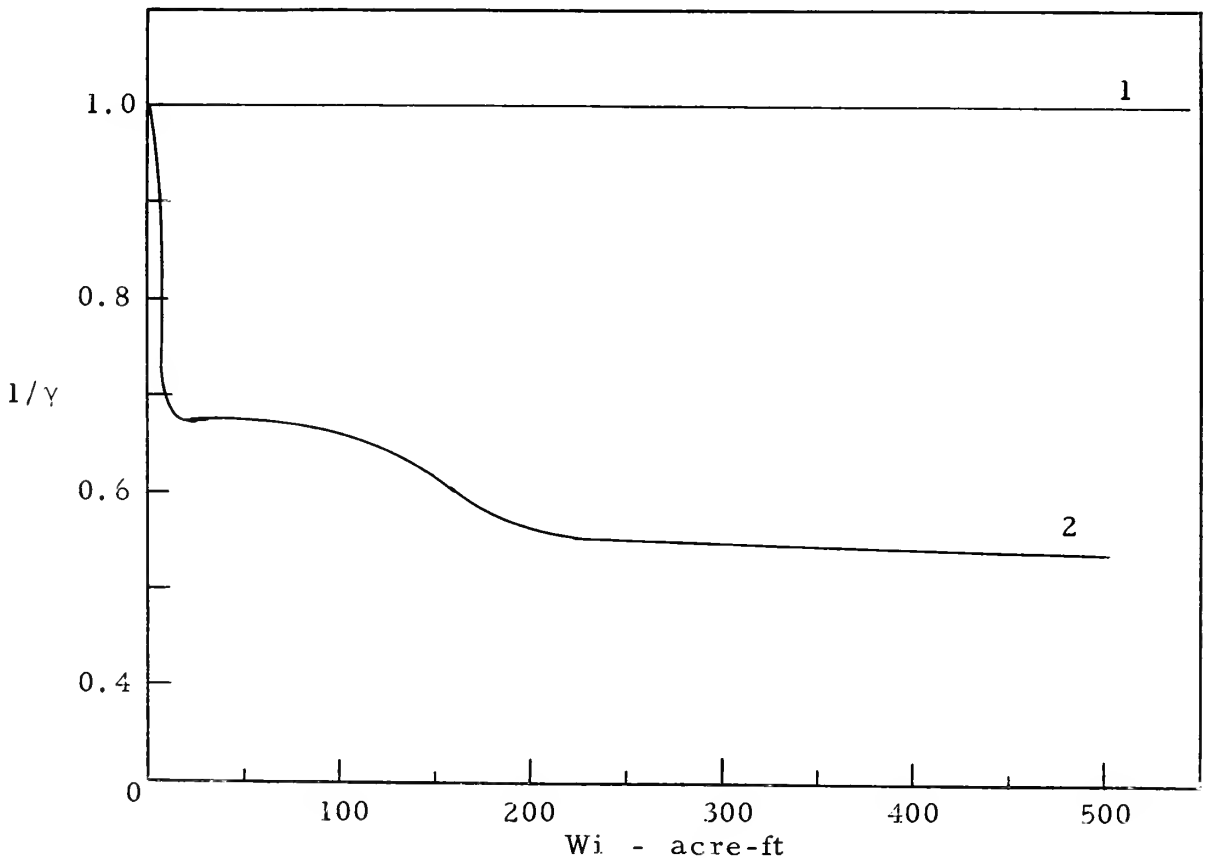

FIGURE 41. INVERSE CONDUCTANCE RATIO versus WATER INJECTED for STRATA 1 and 2

TABLE XXIV

Stratum one		Stratum two		
Wi	ct_1	Wi	$(1/\gamma)\,dWi$	$2.84\,(1/\gamma)\,dWi$
0.0	0.0	0.0	0.0	0.0
100.0	100.0	50.0	35.38	100.5
200.0	200.0	100.0	68.83	195.5
300.0	300.0	150.0	100.88	285.0
400.0	400.0	200.0	132.88	377.0
		300.0	188.18	535.0
		400.0	242.48	688.0
		500.0	296.38	843.0

Wi/Vd fraction	Np/Vd fraction	Wi acre-ft	Np acre-ft	Wi/Vd fraction	Np/Vd fraction	Wi acre-ft	Np acre-ft
0.769	0.769	147.5	147.5	0.665	0.665	119.5	119.5
0.80	0.795	153.5	152.5	0.80	0.743	143.8	133.5
1.0	0.90	192.0	173.0	1.0	0.803	180.0	144.2
1.2	0.952	230.0	182.8	1.5	0.883	269.0	158.7
1.4	0.985	269.0	189.0	2.0	0.930	359.0	167.0
				2.5	0.961	449.0	173.0

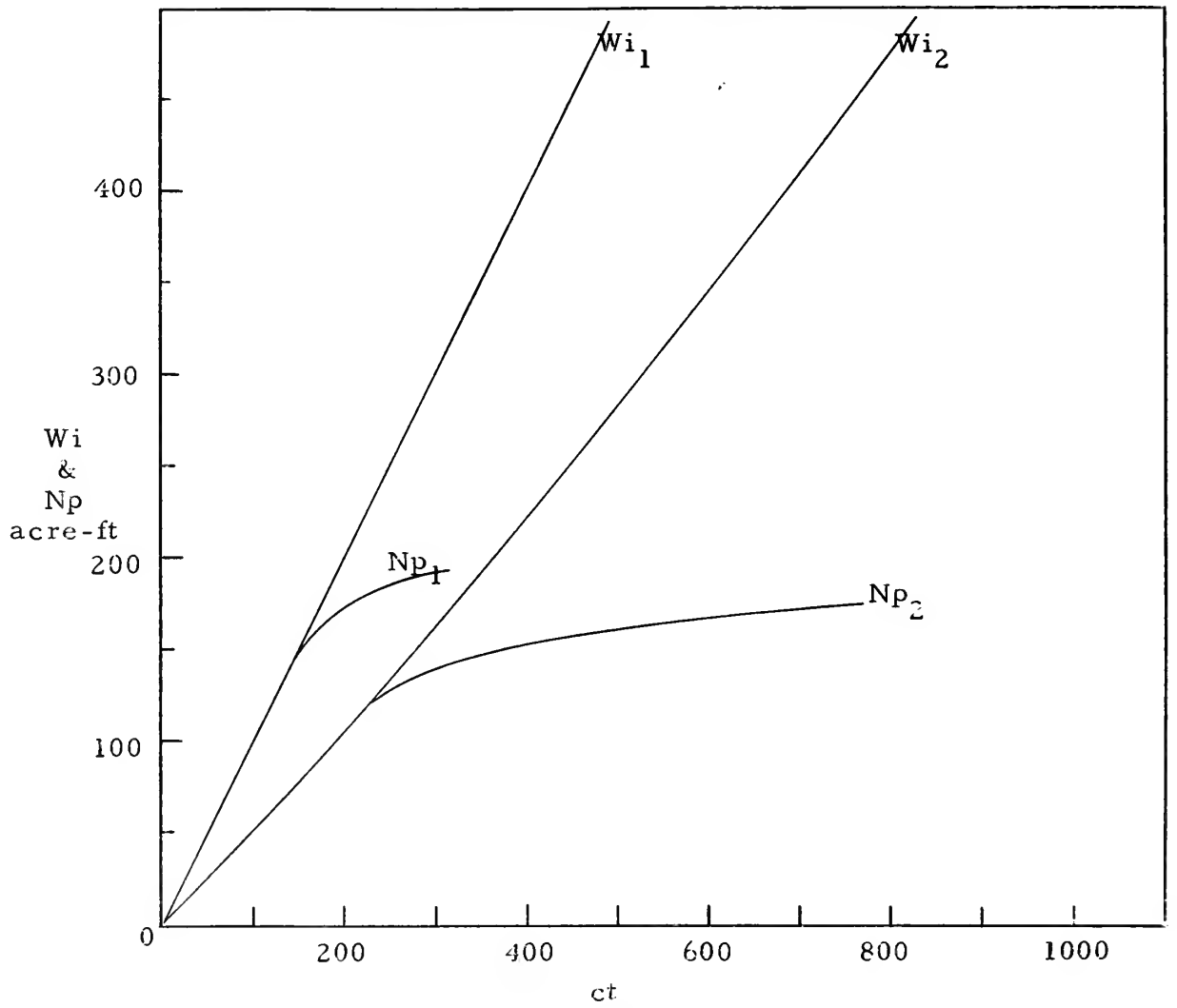

FIGURE 42. WATER INJECTED and OIL PRODUCED versus ct for STRATA 1 and 2

TABLE XXV

ct	Wi_1	Wi_2	Np_1	Np_2	Wi	Np
100	100	50	100	50	150	150
145	145	75	145	75	220	220
200	200	105	173	105	305	278
225	225	120	180	120	345	300
250	250	132	185	127	382	312
300	300	160	190	138	460	328
350	350	187	190	146	537	336
400	400	216	190	152	616	342
500	500	276	190	160	776	350
600	600	344	180	166	944	356
700	700	410	190	171	1110	361

Wi	fo	fw
220	1.000	0.000
300	0.590	0.410
340	0.550	0.450
350	0.400	0.600
400	0.245	0.755
500	0.127	0.873
600	0.054	0.946
800	0.038	0.962
1000	0.031	0.969

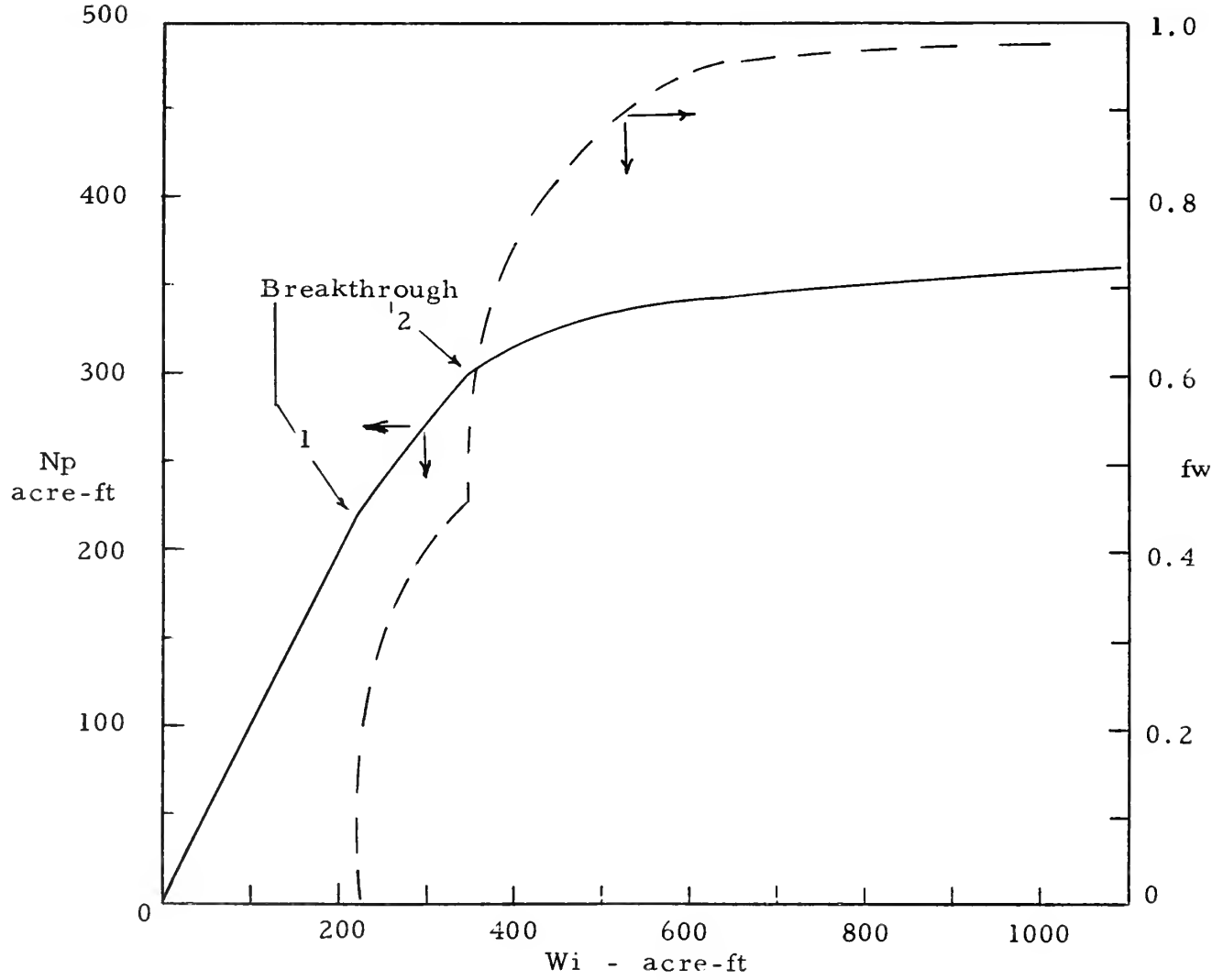

FIGURE 43. OIL PRODUCED and WATER CUT versus WATER INJECTED for STRATIFIED SYSTEM

TABLE XXVI

$$\gamma = \frac{\gamma_1 + \frac{k_2 Vd_2}{k_1 Vd_1}\gamma_2}{1 + \frac{k_2 Vd_2}{k_1 Vd_1}} = \frac{1 + 0.352\,\gamma_2}{1.352}$$

ct	Wi_2	$1/\gamma_2$	γ_2	Wi	γ
50	25	0.675	1.480	75	1.126
100	50	0.672	1.490	150	1.128
150	78	0.670	1.492	225	1.128
200	105	0.660	1.518	305	1.134
300	160	0.600	1.669	460	1.172
400	216	0.552	1.812	616	1.210
500	276	0.550	1.820	776	1.214
600	344	0.542	1.845	944	1.220
700	410	0.540	1.850	1110	1.221

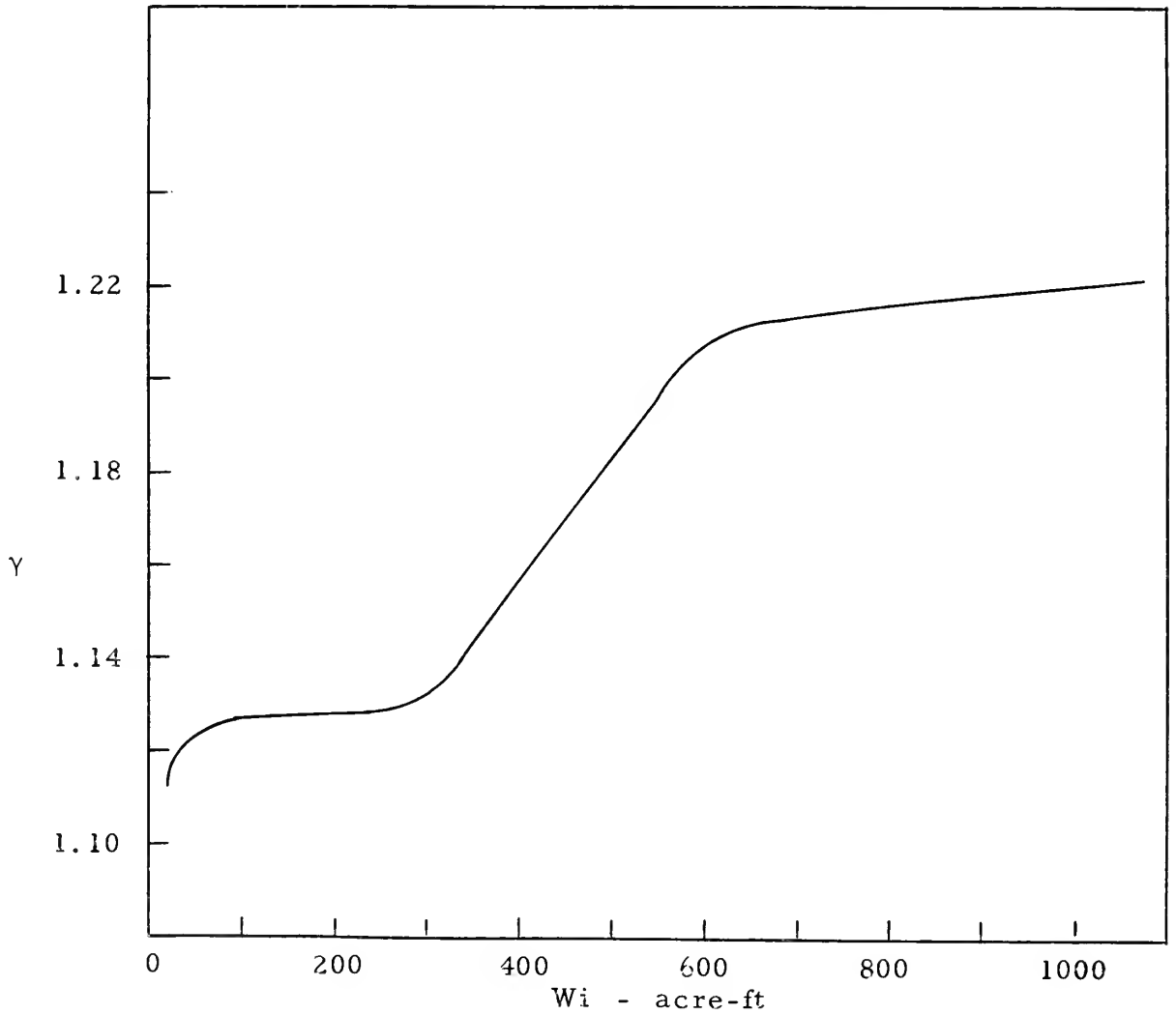

FIGURE 44. CONDUCTANCE RATIO versus WATER INJECTED for STRATIFIED SYSTEM

VITA

Robert Burns Wilson was born in Washington, D.C. on 12 April 1934, the son of Kenneth G. and Edna C. Wilson.

After completing his high school work at Gwynn Park High School, Brandywine, Maryland in June, 1952, he then attended Duke University, Durham, North Carolina, graduating with the degree of Bachelor of Science in Mechanical Engineering in June, 1956.

He has been on active duty with the U.S. Navy since being commissioned after graduation from Duke University and is presently a Lieutenant in the Civil Engineer Corps of the Navy. He has had duty at Newport, Rhode Island; Norfolk, Virginia; and in Puerto Rico. He was selected for postgraduate education in Petroleum Engineering and entered the Graduate School of The University of Texas in September, 1963.

He is married to the former Patricia A. Ingle, of Raleigh, North Carolina, and they have three children, Ellen Marie, Robert Eric, and Wendy Elizabeth.

Permanent address: Route 3, Box 209
Brandywine, Maryland

This thesis was typed by Dorothy S. Fuller.